

Assessing the Geological Sources of Manganese in the Roanoke River Watershed

Zachary A. Kiracofe

Thesis submitted to the faculty of the Virginia Polytechnic Institute and State University in
partial fulfillment of the requirements for the degree of

**Master of Science
in
Geosciences**

Madeline E. Schreiber

William S. Henika

J. Donald Rimstidt

James S. Beard

April 17, 2015

Blacksburg, VA

Keywords: manganese, ore deposits, groundwater, naturally-occurring contaminants

Assessing the Geologic Sources of Manganese in the Roanoke River Watershed

Zachary A. Kiracofe

Abstract

Elevated manganese (Mn) concentrations have been measured in groundwater within the Roanoke River watershed, Virginia. Concentrations of Mn often exceed the secondary drinking water standard. A historic belt of Mn ores, the James River-Roanoke River Manganese District (JRRRMD), occurs in the eastern part of the watershed. The project objectives were to 1) evaluate the formation of the JRRRMD ore deposits and 2) analyze existing groundwater chemistry data to evaluate sources and processes that control groundwater Mn.

Analysis of ore minerals, morphologies, and chemistry provides support that the ore deposits are supergene in origin, consistent with previous work. Spatial correlations between Mn ore locations and stream terrace deposits support a model of ore formation in which Mn-oxides were precipitated near discharge zones as anoxic groundwater mixed with oxic groundwater. Terrace deposits present at elevations higher than modern streams suggests that topography has been inverted, allowing ores to be found at higher elevations than what is typically associated with ores formed in discharge zones.

Analysis of groundwater chemistry data shows positive correlations between Mn, calcium and bicarbonate concentrations in groundwater, suggesting that carbonate-bearing lithologies are probable sources of Mn to groundwater. Regionally, groundwater flows toward the Roanoke River where the flowpath terminus is marked by elevated Mn. The inverse correlation of Mn with dissolved oxygen suggests that reducing conditions that develop along flowpaths allow for Mn to persist in groundwater. Overall, results suggest that the same processes that allowed for formation of the JRRRM ore deposits continue to occur today.

Acknowledgements

Dominion Power and the Geological Society of America for providing the funding necessary to complete this project.

The members of my committee who were always available and allowed me to draw upon their collected wealth of knowledge as I worked to complete my research objectives.

Joshua Rubinstein, William Lassetter, Bradley White, Neil Johnson, Luca Fedele, Andrew Muscente, Lowell Moore, and student members of the Virginia Tech Chemical Hydrogeology Research Group for assisting me in the field, in the lab, or with creative insight.

Friends and family for their love and support as I pursued my graduate degree in geosciences.

Table of Contents

Abstract.....	ii
Acknowledgements.....	iii
Table of Contents.....	iv
List of Figures.....	vi
List of Tables.....	viii
Chapter 1: Introduction.....	1
Study Area.....	1
Manganese in Aqueous Environments.....	3
Study Objectives.....	5
History of Mining in the James River-Roanoke River Manganese District.....	5
Geology of the Roanoke River Watershed.....	6
Mineralogy of the James River-Roanoke River Manganese District.....	8
Chapter 2: Methods.....	13
Sample Collection.....	13
XRD.....	14
SEM.....	15
Bulk Chemistry.....	16
LA-ICMPS.....	16
Statistical Analyses.....	19
Soil Map Analysis.....	18
Groundwater Data Collection.....	18
Statistical Analyses.....	19
Potentiometric Surface Map.....	20
Chapter 3: Results.....	21
XRD & SEM.....	21
Bulk Chemical Analysis.....	26
LA-ICPMS.....	29
Statistical Analyses of Groundwater Data.....	37
Potentiometric Surface Map of Study Area.....	47
Chapter 4: Discussion.....	48
Chapter 5: Conclusions.....	57
References.....	59
Appendix Tables.....	63
Appendix A.....	63
Appendix B.....	74

Appendix C.....	82
Appendix D.....	85
Appendix E.....	94
Appendix F.....	96
Appendix G.....	102
Appendix H.....	105
Appendix I.....	107

List of Figures

Figure 1: Map of the Roanoke River watershed.....	3
Figure 2: Eh-pH stability diagram for Mn-oxides.....	4
Figure 3: Generalized geologic map of the Roanoke River watershed in Virginia.....	9
Figure 4: Detailed explanation of lithologies present in the geologic regions depicted in Figure 2.....	10
Figure 5: Geologic map of a representative portion of the study area, predominantly located in southwestern Campbell County.....	11
Figure 6: Locations of ore samples collected in the field and from museum collections.....	14
Figure 7: Plots of (a) K vs Mn, (b) Ca vs Mn, (c) Ba vs Mn, (d) Co vs Mn from ore samples analyzed by acid digestion and ICPMS.....	27
Figure 8: Thick section of RBG01-BH.....	29
Figure 9: Thick section of LVL-100.....	29
Figure 10: Thick section of RBG-114A.....	29
Figure 11: Representative soil maps of Campbell County showing alluvial soils (terrace deposits) in both Piedmont Uplands and modern stream valleys.....	35
Figure 12: Boxplots of the distribution of elevations of A) Piedmont Upland alluvial soils, B) modern stream valley alluvial soils, and C) known Mn mining locations in Campbell County, VA.....	36
Figure 13: Boxplots showing the distribution of total Mn concentrations (ppb) in groundwater in all counties in which all or part of the Roanoke River watershed encompasses.....	38
Figure 14: Boxplots showing the distribution of total Mn concentrations (ppb) in groundwater from wells open to different geologic formations within the Roanoke River watershed..	39
Figure 15: Dissolved oxygen versus filtered Mn concentrations for all Virginia groundwater samples in the Piedmont and Blue Ridge crystalline aquifers from Chapman (2013).....	40
Figure 16: Boxplots of grouped samples and DO concentrations for all Virginia groundwater samples from the Piedmont and Blue Ridge crystalline aquifers (Chapman, 2013).....	41
Figure 17: Total Mn concentrations versus total Fe concentrations for wells within a selected portion of the study area.....	42
Figure 18: Boxplots of grouped samples and total Fe concentrations for wells within a selected portion of the study area.....	45
Figure 19: Boxplots of grouped samples and pH values for wells within a selected portion of the study area.....	47
Figure 20: Regional potentiometric surface map of study area.....	48

Figure 21: Conceptual alternate model for the formation of the ore deposits of the JRRRMD...51

Figure 22: Field site in Hurt, VA displaying an example of modern Mn-oxide deposition.....53

Figure 23: Conceptual diagram of topographic inversion in relation to the formation and occurrences of Mn-oxides in the Piedmont Uplands within the JRRRMD.....55

List of Tables

Table 1: Summary of XRD and SEM results for selected ore samples.....21

Table 2: Chemical analysis of ore samples by near-total digestion and ICPMS analysis,
conducted by Activation Labs, Inc.....26

Table 3: Pearson correlation matrix for selected chemical analytes in ore samples analyzed by
acid digestion and ICPMS by Activation Labs, Ltd.....28

Table 4: Summary of LA-ICPMS data for RBG01-BH.....30

Table 5: Summary of LA-ICMPS data for LVL-100.....31

Table 6: Summary of LA-ICPMS results for RBG-114A.....32

Table 7: Pearson correlation matrix for groundwater chemical data obtained from Chapman
(2013) for wells within the state of Virginia in the Blue Ridge and Piedmont crystalline
aquifers.....43

Table 8: Pearson correlation matrix for groundwater chemical data obtained from the STORET
dataset.....44

INTRODUCTION

Manganese (Mn) is a naturally-occurring metal with average concentrations of Mn in soil and rocks of 850 parts per million (ppm) and 650 ppm, respectively (Gilkes & McKenzie, 1988). The Environmental Protection Agency (EPA) has established 50 parts per billion (ppb) as the secondary drinking water standard (SDS) for total Mn for aesthetic reasons (taste, color, clogging potential) (Environmental Protection Agency, 2004). The EPA has also set 300 ppb for total Mn as the human health benchmark, as studies have linked chronic exposure of children to total Mn concentrations > 300 ppb in drinking water with learning impairments (Khan et al., 2012; Bouchard et al. 2007; 2011). Manganese is of particular concern in the Roanoke River watershed of Virginia, as Mn concentrations in both the Roanoke River and groundwater in the watershed routinely exceed 50 ppb (USEPA, 2014; USGS, 2004; Chapman, 2013; Nelms & Harlow, 2003).

In addition to naturally occurring sources, Mn can also be discharged into aquatic environments due to human activities. Manganese is commonly used in the manufacturing of steel and can be discharged into water sources from steel plants and other industrial facilities (Nadaska et al., 2010). Other means by which Mn can enter the environment due to human activities are municipal wastewater discharge, landfills, and mineral processing from mining activities (Nadaska et al., 2010). Because human sources of Mn are at discrete locations (i.e., point sources), examination of the spatial distribution of Mn concentrations can be helpful in evaluating if the Mn source is natural or related to human activity.

Study Area

The region of interest for this report is the Roanoke River watershed in Virginia. Spanning across 14 counties in southern Virginia, this watershed covers approximately 16% of Virginia

and is home to around 750,000 Virginians (Chesapeake Bay Foundation, 2005). **Figure 1** depicts the entirety of the Roanoke River watershed. This drainage basin includes the counties of Montgomery, Roanoke, Bedford, Franklin, Floyd, Patrick, Henry, Pittsylvania, Campbell, Appomattox, Charlotte, Halifax, Mecklenburg, and Brunswick. Multiple stretches of streams in this watershed are classified as impaired with respect to several water quality parameters, including Mn (Commonwealth of Virginia Department of Environmental Quality, 2014).

Shown in **Figure 1** are the locations of wells (circles) obtained from the National Uranium Resource Evaluation (NURE) dataset and USGS studies with the corresponding filtered Mn concentrations in groundwater (color-coded to represent different concentration ranges in ppb). The data from NURE and the two USGS studies used to prepare **Figure 1** are included in **Appendix A**. In the watershed, the median Mn concentration in groundwater samples in the NURE and other USGS datasets (Chapman, 2013; Nelms & Harlow, 2003) is approximately 27 ppb. As seen from **Figure 1**, most Mn concentrations in groundwater are below 50 ppb (blue dots). Approximately 30 percent of wells, however, show elevated Mn concentrations above 50 ppb. In addition to well locations, **Figure 1** shows the locations of mines (dark red circles) that have been historically known to mine Mn. The coordinates for these localities were extracted from the Mineral Resources of Virginia (MRV) database from the Virginia Department of Mines, Minerals, and Energy (DMME). Extending through Appomattox, Campbell, and Pittsylvania counties is a linear belt of significant Mn mineralization. This region is known as the James River-Roanoke River Manganese District, described in more detail below.

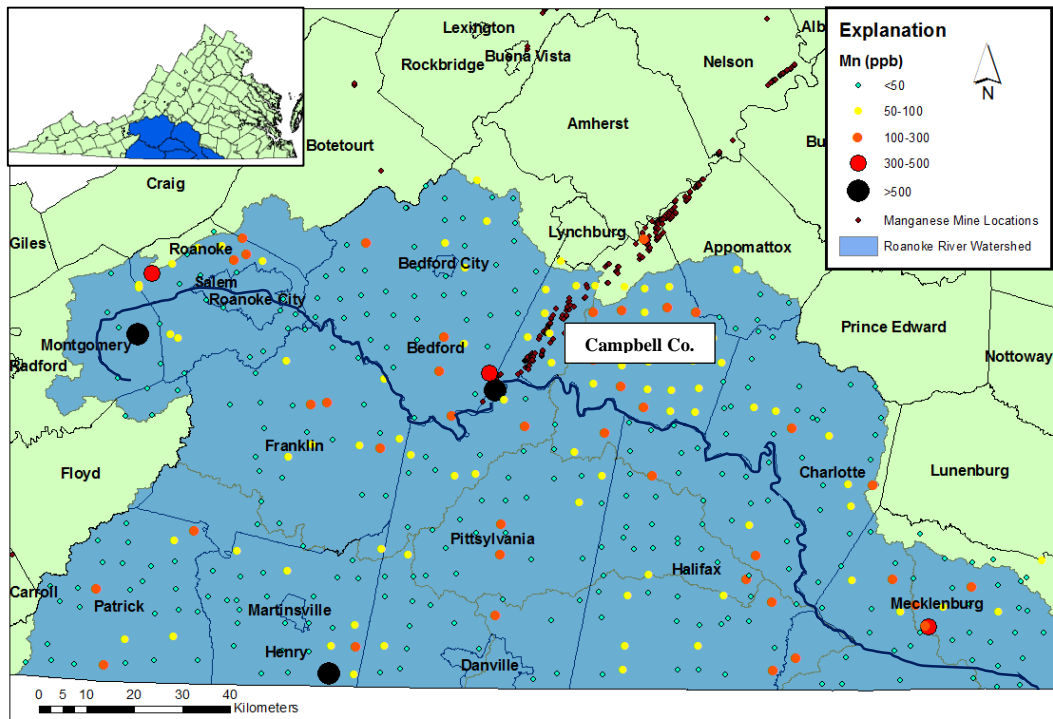
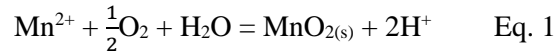


Figure 1: Map of the Roanoke River watershed (blue shaded area). The Roanoke River (blue line) lies in the center of the watershed. Circles represent well locations and colors correspond to filtered Mn concentrations (ppb). Red diamonds represent the locations of known Mn mines. Well data were obtained from the National Uranium Resource (NURE) dataset (USGS), and two USGS publications (Chapman, 2013; Nelms & Harlow, 2003). Manganese mine location information was retrieved from the Mineral Resources of Virginia (MRV) database (courtesy of the Virginia Department of Mines, Minerals and Energy). These ore deposits are referred to as the James River-Roanoke River Manganese District.

Manganese in Aqueous Environments

Manganese is a redox-sensitive element that occurs most commonly within the environment in three oxidation states: Mn^{2+} , Mn^{3+} , and Mn^{4+} . In aqueous systems, Mn occurs as dissolved Mn^{2+} and as colloidal Mn^{3+} and Mn^{4+} oxides and oxyhydroxides. **Figure 2** shows the relationship between Mn-oxides and redox conditions (pE) over a range of pH. The soluble 2+ oxidation state occurs in reducing aqueous environments (lower pE values). In oxidizing environments (greater pE values), the insoluble 3+ and 4+ oxidation states are favored. Mn can be transformed from one oxidation state to another via coupled oxidation-reduction reactions. For example, the

reaction below shows that electrons are transferred from Mn^{2+} to oxygen, (Eq. 1), resulting in oxidation of Mn^{2+} to Mn^{4+} .



The products of this reaction are a Mn-oxide solid (pyrolusite) and hydrogen ions. If other ions (e.g. potassium and barium) are present in water, other Mn-oxides (e.g. cryptomelane ($\text{KMn}_8\text{O}_{16}$)) and romanechite ($(\text{BaMn}_9\text{O}_{16}(\text{OH})_4$)) may precipitate either directly out of solution or by autocatalysis on previously-formed minerals. This process is often observed at the surface in streambeds, forming black coatings on sediments. In aquifers, oxidation of soluble Mn ions to insoluble Mn oxides can occur as coatings along rocks surfaces, mineralization in fractures and void spaces, as well as replacement of aquifer materials (massive replacement) (Kim, 1984). Mn oxides can also be present in water as particulates, often referred to as colloids.

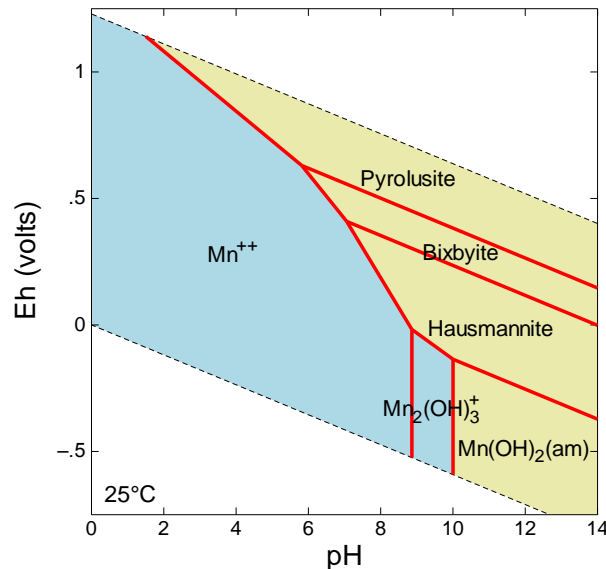


Figure 2: Eh-pH stability diagram for manganese. The water stability field is shown for $P_{\text{O}_2} = 1 \text{ atm}$ and $P_{\text{H}_2} = 1 \text{ atm}$. Figure was created using Geochemist's Workbench 10.0.

Equation 1 illustrates a general reaction for the formation of Mn-oxides in which soluble Mn^{2+} is oxidized to insoluble Mn^{4+} in the presence of DO. In the absence of DO, these minerals are thermodynamically unstable and may be reductively dissolved, a process that is often microbially-mediated.

Study Objectives

There are three main objectives of this thesis. The first two objectives are to evaluate the geological origins of the ore deposits within the James River-Roanoke River Manganese District and to examine other Mn-bearing rocks in the Roanoke River watershed. The third objective is to analyze groundwater geochemistry data from existing datasets in order to evaluate the probable geologic sources and processes that control both the release and persistence of Mn in groundwater within the Roanoke River watershed.

History of Mining in the James River-Roanoke River Manganese District

The James River-Roanoke River Manganese District (JRRRMD) is a historic belt of Mn mineralization with a NE-SW strike. This belt extends from the western boundaries of Appomattox and Campbell Counties and continues into northwestern Pittsylvania County (see **Figure 1**). In addition to Mn, this district was also mined for iron and barite from the mid-nineteenth century until the end of the Second World War (Gooch, 1954; Gooch, 1955; Edmundson, 1938). Peak production of Mn ore occurred between 1911 to 1919 when operations at the Piedmont mine—the most productive mine in the JRRRMD and one of the ore sampling locations in this report—were most active (Brown, 1958). A total of 26,107 long tons of washed ore is reported as the official amount of ore mined from the ore belt during its active years, but it is estimated that the actual amount of mined ore is twice as large as this sum (Espenshade, 1954).

Geology of the Roanoke River Watershed

The general geology of the Roanoke River watershed is displayed in **Figure 3**. Geologic formations were grouped into geologic regions by factors such as geographic location, structural relationships, and geologic terranes described by the USGS (2003). Detailed descriptions of the lithologies present in the various geologic regions are available in **Figure 4**. **Figure 5** focuses on the study area presented in this report and depicts the major geologic formations in a section of Campbell County. The majority of the known Mn mine locations are found within the Proterozoic Alligator Back Formation. This formation consists primarily of interlayered metamorphosed sedimentary rocks (e.g. quartzite, pelitic schists, metagraywacke, marble) and metamorphosed igneous rocks (e.g. amphibolite schist) (Berquist, 2003). These formations were consolidated into the Alligator Back Formation and its three main units by Henika (1992). The nomenclature from Espenshade (1954) refers to these rock units as members of the Evington Group—which included the Mount Athos Formation, Archer Creek Formation, and an unnamed greenstone. **Figure 5** depicts the lithologic members of the Alligator Back Formation which include 1) metagraywacke member (formerly Mount Athos Formation), 2) actinolite schist member (formerly unnamed greenstone), and 3) marble member (formerly Archer Creek Formation). It is worth noting that these are merely the major rock types of each lithologic member. Each formation member contains other rock types intermixed in less abundant spatial extents. For example, marbles can be found interlayered with the metagraywacke and actinolite schist lithologic members. To a lesser extent, some Mn deposits are also located in the Cambrian Candler Formation, composed of phyllite, metasilstone, and quartz mica schist with occurrences of marble (Berquist, 2003).

The lithologic members of the Alligator Back Formation—the upper unit of the Lynchburg Group (Berquist, 2003)—are believed to have been formed during the rifting of the supercontinent Rodinia, during which a rift basin was created (Conley, 1978). This restricted basin was believed to have contained abundant submarine volcanic vents responsible for expelling large quantities of metal-rich fluids from deep within the Earth’s crust (Henry, Craig, and Gilbert, 1973; Buhn and Stanistreet, 1993). Actinolite schists have been interpreted as metamorphosed basaltic lava flows which were originally extruded during the thinning and subsequent rifting of the Rodinian supercontinent by extensional tectonics (Conley, 1978); marbles (originally limestones) were likely deposited around volcanic vents as calcite precipitated directly from sea water. As continued rifting provided more accommodation space, clastic sediments became concentrated in deep water, forming interlayered sedimentary rocks (e.g. sandstone, greywacke, shale)(Conley, 1978). The Candler Formation represents an increase in water depth after subaerial flood basalts of the Alligator Back—equivalent to the flood basalts of the Precambrian Catoctin Formation—were extruded (Conley, 1978; Berquist, 2003). Subsequent regional metamorphism from the collision of land masses altered the original sedimentary and igneous rocks into the metamorphic rocks seen today. Furthermore, extensive folding and faulting of geologic formations in the study area has constrained the location of the majority of Mn mineralization in the study area to a NE-SW trending belt less than 10 kilometers wide. This narrow zone is bounded by two thrust faults—the Bowens Creek Fault on the west side and the Ridgeway Fault on the east side. Between the two faults, the lithologic units of the Alligator Back Formation—and to a lesser extent the Candler Formation—are highly folded with several anticlines and synclines that form a crenulated assemblage of geologic units.

Mineralogy of the James River-Roanoke River Manganese District (JRRRMD)

Previous work in the study area has separated the Mn oxide minerals into two main groups: “psilomelane type” and “wad” (Espenshade, 1954). As defined by Espenshade (1954), psilomelane refers to Mn-oxides with high specific gravity whereas “wad” is a poorly-defined term which essentially refers to soft, powdery weathering products of Mn-rich geologic materials. Manganese oxide minerals identified in the JRRRMD by Espenshade (1954) are cryptomelane, psilomelane, and pyrolusite. Psilomelane is a collective term for crystalline Mn-oxides with variable amounts of essential cations in their structures belonging to the Cryptomelane group (Williams, 1990). Specific examples of minerals in this group include potassium-bearing cryptomelane ($\text{KMn}_8\text{O}_{16}$), barium-bearing romanechite ($\text{BaMn}_9\text{O}_{16}(\text{OH})_4$), and aluminum and lithium-bearing lithiophorite ($(\text{Al,Li})\text{MnO}_2(\text{OH})_2$) (Williams, 1990).

Manganese oxides of the JRRRMD are predominantly concentrated in saprolite and fractured bedrock and occur in the following forms: 1) massive replacement, in which original rock material has been replaced by Mn-oxides, 2) void spaces and fractures filled in with Mn-oxides; 3) cementing material (matrix) of vein quartz and quartzite breccias; 4) nodular masses of Mn-oxides; and 5) wad. It is important to note that iron oxides are also abundant throughout the JRRRMD, often occurring as mixed mineral assemblages with the Mn-oxides.

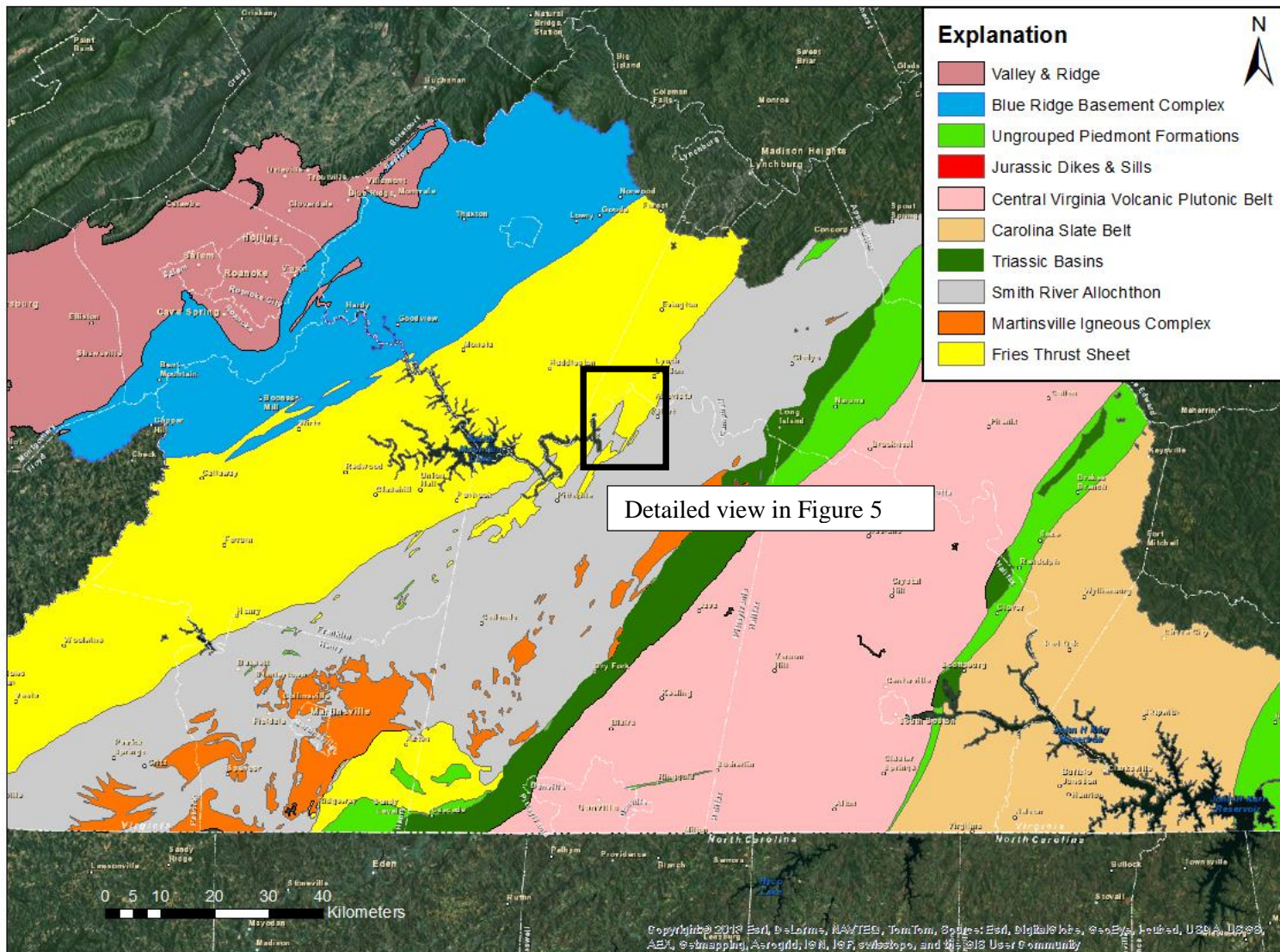


Figure 3: Generalized geologic map of the Roanoke River watershed in Virginia. Geologic data were obtained from the USGS (Dicken et al., 2005).

Explanation

-  **Valley & Ridge**—Lower topography (valleys) is underlain predominantly by carbonate rocks (e.g. limestone and dolomite). Geological formations in ridges of higher elevation consist of clastic sedimentary rocks (e.g. shale, siltstone, sandstone). Ages of formations range in age from Cambrian to Devonian. Clastic formations of Cambrian age are often metamorphosed from parent rocks (i.e. sandstone to quartzite, shale to phyllite, etc.).
-  **Blue Ridge Basement Complex**—High-grade (granulite facies) plutonic rocks which are dominated by gneiss with various forms defined by differences in mineralogy and texture. Some unmetamorphosed igneous rocks are present (e.g. granodiorite and granite). Rocks are of Middle Proterozoic age (Grenville Orogeny) and among the oldest rocks in the study area.
-  **Ungrouped Piedmont Formations**—Geologic formations not grouped into a specific geologic region based on geographic location or rock types. Rocks are typically of Proterozoic age and composed of high-grade metamorphic rocks. Gneissic rocks can be either orthogneiss (derived from an igneous parent rock) or paragneiss (derived from a sedimentary parent rock). Mylonitic rocks are formed in shear zones where rocks are highly deformed in or near fault zones.
-  **Jurassic Dikes & Sills**—vertical (dike) and horizontal (sill) igneous intrusions which cut across older pre-existing rocks. Diabase is the primary rock type. Dikes and sills are of Jurassic age.
-  **Central Virginia Volcanic Plutonic Belt**—Interlayered felsic and mafic metavolcanic rocks. Metamorphosed plutonic rocks (e.g. gneiss) are also common in this geologic region with smaller amounts of schist. Granite is also observed in spatially restricted areas. Rocks range in age from Proterozoic to Cambrian.
-  **Carolina Slate Belt**—Proterozoic rocks which include plutonic and volcanic igneous rocks. Metavolcanic (e.g. greenstone) and metasedimentary (e.g. slate and phyllite) are also present.
-  **Triassic Basins**—Mesozoic basins from the Upper Triassic Period. Basins contain interlayered siliciclastic sedimentary rocks which include sandstone, siltstone, and shale with minor beds of conglomerate.
-  **Smith River Allochthon**—Proterozoic-Cambrian assemblage of metamorphosed sedimentary and plutonic igneous rocks. Allochthon is composed predominantly of mica schist. Metamorphosed igneous rocks are less common and consist of biotite gneiss, granite gneiss, and amphibolite.
-  **Martinsville Igneous Complex**—Cambrian plutonic rocks (e.g. norite, gabbro, granite, diorite). Minor amounts of gabbroic lithologies have been metamorphosed.
-  **Fries Thrust Sheet**—Proterozoic and Proterozoic-Cambrian suite of metamorphic rocks similar to those found in the Smith River Allochthon, containing both metamorphosed igneous and sedimentary rocks. Metamorphic igneous rocks include plutonic (e.g. biotite gneiss) and volcanic (actinolite schist) lithologies. Metasedimentary rock types include phyllite, schist, metagraywacke, quartzite, and minor amounts of marble.

Figure 4: Detailed explanation of lithologies present in the geologic regions depicted in Figure 3. Descriptions of rock units were obtained from the Virginia Division of Geology and Mineral Resources (Berquist, 2003).

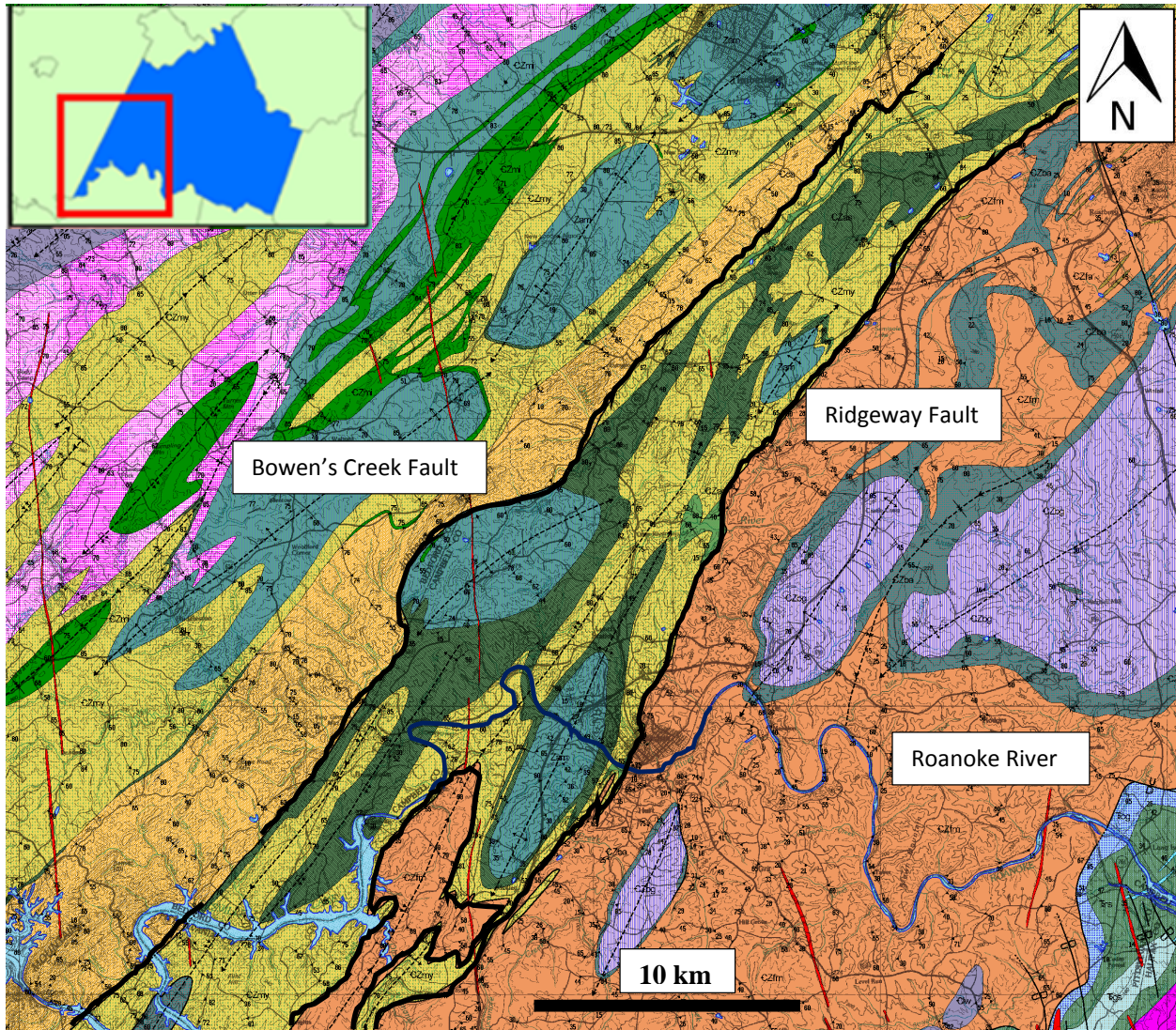






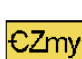



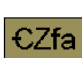

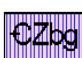
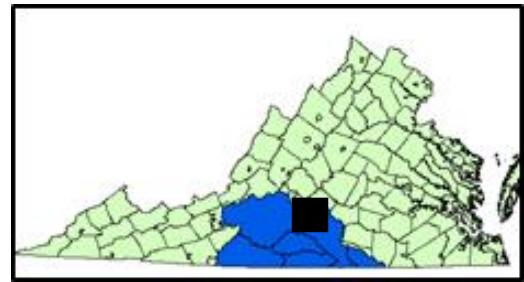
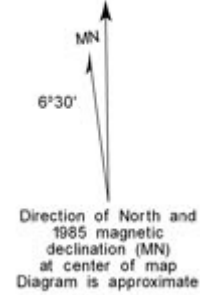


Figure 5: Geologic map of a representative portion of the study area, predominantly located in southwestern Campbell County. Geologic data were obtained and modified from Henika (1997). Explanation for Figure 5 is a limited edition digital draft of VDMR Publication 148, obtained through personal communication with Henika (2015) and modified.

EXPLANATION

	Igneous dikes and sills.
	Candler Formation- phyllite and schist.
	Candler Formation- dolomitic limestone.
	Amphibolite
	Schist
	Alligator Back Formation- actinolite schist.
	Alligator Back Formation- laminated mica gneiss.
	Alligator Back Formation- calcareous gneiss, and schist. marble.
	Ashe Formation- biotite gneiss and schist.
	Fork Mountain Formation- schist, gneiss, quartzite and granofels, marble.
	Fork Mountain Formation- amphibolite and gneiss.
	Bassett Formation- amphibolite and gneiss.
	Bassett Formation- gneiss and granofels.

DECLINATION DIAGRAM



METHODS

Rock Sample Collection

To conduct chemical and mineralogical analyses of the JRRMD ore deposits and other Mn-bearing rocks, we designed a solid sampling program using geologic maps and known localities of the ore deposits. Samples were collected on 11/19/13 from the Leesville Lake Quadrangle (LVL-100, LVL-101, LVL-102) and on 2/20/14 from the Rustburg Quadrangle (RBG01-BH, RBG-312, RBG-110, RBG-111, RBG-112A, RBG-113, RBG-114). The locality for samples from the Leesville Lake Quadrangle was an unnamed mine located approximately 0.8 km northwest of the Myers Hematite Mine in northern Pittsylvania County. Rustburg Quadrangle samples were collected from the Piedmont Mine in northern Campbell County, located approximately 10 km southeast of the city of Lynchburg, Virginia. The ore samples were targeted visually in the field based on the appearance of black-colored minerals (presumable Mn oxides) in hand sample. In almost all of the samples, the black minerals were intermixed with dark-brown iron oxides. Additional samples were obtained from museum collections. Five ore (both Mn and Fe) samples from the JRRMD were obtained from the DMME. Three Mn ore samples were collected from the Virginia Museum of Natural History. Locations of samples collected both in the field and from museum collections are shown in **Figure 6**.

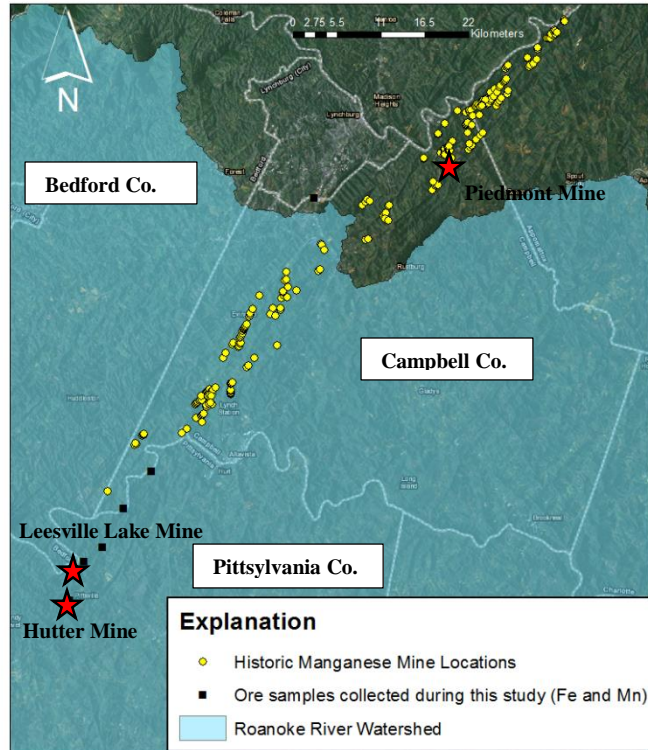


Figure 6: Locations of ore samples collected in the field and from museum collections (DMME and VMNH). Red stars represent localities of interest.

XRD

Powder x-ray diffraction (XRD) was used to determine minerals in bulk samples. Hand samples collected in the field or obtained from museum collections were first broken into smaller pieces using a rock hammer. The resulting fragments were inspected with the objective of separating “pure” Mn or iron oxides from gangue minerals (e.g. quartz) to increase the likelihood of identifying desired mineral species. For each sample investigated, these fragments were then powdered with the use of either a percussion mortar or a porcelain mortar and pestle. Powdered samples were then loaded into or onto XRD sample holders. Care was taken to ensure that the powdered sample was in line with the top of the sample holder to ensure accurate diffraction patterns. Excess powder was removed with a paint brush. For small amounts (452 mm^3) of

sample, the powder was mixed with methanol, pipetted onto the surface of a sample holder, and allowed to dry.

The X-ray diffraction analyses were conducted using a Rigaku MiniFlex II Desktop X-ray Diffractometer. Cu K α radiation was used with a fixed tube output voltage of 30kV and fixed tube output current of 15 mA. Unless noted otherwise, the sampling parameters for all samples are as follows: an x-ray scanning range of 5-85 degrees 2θ , step size of 0.020 degrees 2θ , and a scanning speed of 1 degree 2θ per minute.

The XRD patterns were analyzed using the PDXL software package provided by Rigaku to match the peaks from the diffraction patterns with known mineral species from the software database. Plausible mineral species were narrowed by including Mn as part of the mineral-matching criteria.

SEM

Ore textures and qualitative elemental abundances were observed using scanning electron microscopy (SEM). The instrument used for these microscopic visual inspections was a Hitachi TM3000 Tabletop Microscope with a Bruker silicon drift detector. Relative elemental abundances were determined through the use of energy dispersive spectroscopy (EDS) in the form of elemental maps. All samples were analyzed using back-scattered electrons (BSE) to collect Z-contrast images with an accelerating voltage of 15 kV. A working distance (space between the electron beam aperture and sample) of 12 mm was used. Elemental maps were generated using EDS; data were collected for approximately 400 seconds per sample image. The lower limits of EDS detection for individual point analysis are approximately 0.1 weight percent for any given element.

SEM analysis was used to verify mineral identification suggested by XRD. For ore samples in which Mn minerals were unable to be determined by XRD, elemental maps created by EDS allowed inferences to be made about plausible minerals. In samples where Mn mineralogy could not be inferred, SEM analysis was able to determine if the samples contained Mn.

Bulk chemistry

Seven ore samples (RBG01-BH, RBG-110, RBG-111, LVL-100, LVL-101, LVL-101A) were selected for bulk chemical analysis. Sample preparation began with crushing ore samples using a percussion mortar and sledge hammer. Samples were continuously pulverized using a percussion mortar until roughly powdered. All samples with the code “LVL” (Leesville Lake Quadrangle) were ores confined to quartz-rich lithologies (e.g. quartzite) with relatively fresh country rock commonly present. For these samples, oxide minerals were manually separated from the bulk sample mass after being roughly crushed with a percussion mortar before being powdered.

The powdered samples were shipped to Activation Laboratories Ltd. (Actlabs) in Ontario, Canada for chemical analysis. Samples were subject to a “near-total digestion” by four separate acids (hydrochloric, nitric, perchloric and hydrofluoric) and then analyzed by inductively-coupled plasma mass spectroscopy (ICP-MS). Data are provided in **Table 2**.

LA-ICPMS

Three samples (RBG01-BH, RBG-114, LVL-100) were selected for analysis by laser ablation inductively-coupled plasma mass spectroscopy (LA-ICPMS). This method allows highly sensitive analysis of major, minor, and trace elements on solid samples. Samples selected for LA-ICPMS analysis were cut by a rock saw to the dimensions of a standard thin section (27 x 46

mm). The blocks were then glued to a frosted glass slide using Crystalbond™ adhesive. Samples were trimmed to a ~1-mm thickness using a cut-off saw and grinder. Sample preparation was completed by controlled polishing by hand with a series of three polishing papers gradually decreasing in grit size (from coarse to fine).

LA-ICPMS analyses were performed at Virginia Tech using a methodology outlined by Severs et al. (2009). Samples were analyzed using an Agilent 7500ce quadrupole ICPMS and a Lambda Physik GeoLas 193 nm excimer laser ablation system coupled to an Olympus petrographic microscope equipped with a 25x UV and visible Schwarzschild objective for analysis. Both a 5x and 10x objective were used to view samples. Before and after each analysis, a standard reference material (NIST 610 glass) was analyzed twice. To cover a larger area of sample, a beam diameter of 90 μm was used instead of the 24 μm diameter used in Severs et al. (2009). For each analysis, a baseline signal was collected for ~40-60 seconds with the laser shutter closed. Once opened, the laser shutter was allowed to ablate the sample for ~40-60 seconds. After data collection, AMS analytical software was used to reduce the data signals and obtain concentrations for major, minor, and trace elements.

For quantitative interpretations, values both above and below detection limits had to be addressed for bulk chemical data. For further analyses of the data, values below detection are substituted with a value one-half that of the detection limit. For concentrations above the detection limit, the upper detection limit value is used. The exception is Zn in RBG01-BH. For this sample, the average concentration for Zn in RBG01-BH from LA-ICPMS analysis is the substituted value (see **Table 3**).

Soil Mapping

Soil types, specifically soils derived from alluvial processes, were examined to evaluate models of ore formation. First, alluvial soils in Campbell County were examined using descriptions from Bullard (1977). Alluvial soils were then identified in the county using the Gridded Soil Survey Geographic Database (Soil Survey Staff, 2014) obtained online from the United States Department of Agriculture Natural Resources Conservation Service (NRCS) Geospatial Data Gateway at <https://gdg.sc.egov.usda.gov/>. Alluvial soils were separated into two categories: Piedmont Upland terrace soils (greater elevations) and Modern Stream Valley soils (lower elevations), which were overlaid with the known locations of Mn ore deposits using ArcGIS 10.2 (ESRI, 2013). Spatial relationships in the xy-plane between alluvial soils and Mn mine locations were examined visually. In the z-direction (vertical), spatial relationships were evaluated by extracting the elevations of Mn mining locations from digital elevation maps for Campbell County also obtained online from the NRCS Geospatial Data Gateway. Elevations of soil horizons and Mn mines were modeled using ArcGIS.

Groundwater Data Collection

Groundwater geochemistry data in the Roanoke River watershed were gathered from the National Uranium Resources Evaluation (NURE) dataset (USGS, 2004) (419 samples), the Storage and Retrieval (STORET) data warehouse (USEPA, 2014) (175 samples), and published studies conducted by the USGS (Chapman, 2013; Nelms & Harlow, 2003) (91 and 9 samples, respectively). For the NURE and STORET datasets, it is reported that water samples were filtered (0.8 micron) for the NURE samples and unfiltered for STORET data. Data from Chapman (2013) were obtained from the U.S. Geological Survey (USGS) National Water-Quality Assessment (NAWQA) Program from 1994 through 2008. Analyses for most

constituents were conducted on filtered samples. Manganese analyses reported in Nelms & Harlow (2003) were also conducted on filtered samples (0.45 micron).

Statistical Analyses

Ore samples. Statistical analyses conducted on ore samples collected from the JRRRMD included calculating Pearson correlation coefficients and preparing scatter plots for analytes of interest. Correlation coefficients were calculated using JMP (SAS, 2013) to evaluate positive or negative associations between chemical constituents. Scatter plots were created using Microsoft Excel. All data analyzed were log transformed from original concentrations.

Groundwater samples. To investigate correlations between Mn and other measured parameters in groundwater, several statistical methods were used. Statistical analyses were conducted using JMP (SAS, 2013) or R (R Core Team, 2012). For statistical analysis, concentration data were log transformed, as the data do not follow a normal distribution, allowing data to be strongly influenced by outliers. Using log-transformed data minimizes the influence of outliers and converts the main body of data into a more symmetric distribution (Reimann, et al., 2008). Data from Chapman (2013) were used to examine dissolved oxygen (DO) in groundwater throughout Blue Ridge and Piedmont crystalline aquifers due to sparse data available specifically for the Roanoke River watershed. For other statistical tests on groundwater chemistry, STORET data were used to give a higher degree of resolution in a selected portion of the study area. In particular, the counties of Appomattox, Bedford, Campbell, Franklin, Henry, Patrick, and Pittsylvania were selected because they consist primarily of Neoproterozoic age rocks which are continuous along a northeast-southeast trend throughout the Roanoke River watershed.

Pearson correlation coefficients were calculated for all measured analytes. Scatter plots were prepared to look for visually distinct trends between Mn and analytes of interest. Total Mn concentrations were then categorized into three different groups. Group 1 contained samples with Mn concentrations <50 ppb; Group 2 contained samples with Mn concentrations >50 ppb and <300 ppb; and Group 3 contained samples with Mn concentrations >300 ppb. Boxplots were created to examine how the variation and median values for the three groups differed with respect to other chemical parameters (e.g. DO, Fe, pH). Because data are not normally distributed, a non-parametric Kruskal-Wallis test was used to see if at least two of the groups were statistically different from one another (i.e. greater or less). A 95 percent significance level was used with a confidence interval of 0.05. To compare individual groups for statistical differences, a Wilcoxon signed rank test was conducted. A 95 percent significance level was used with a confidence interval of 0.05 was also used.

Potentiometric Surface Map


A potentiometric surface map of the crystalline aquifer in a portion of the study area was created to establish generalized groundwater flow paths. Well data available from STORET (2014) were used to calculate hydraulic head at individual wells. Specifically, hydraulic head was determined by subtracting the static water level (feet below land surface) from the well elevation (feet above mean sea level). Potentiometric surfaces were interpolated from well points using ArcGIS 10.2 (ESRI, 2013). Data are available in **Appendix I**.


RESULTS


XRD & SEM


Table 1 summarizes the results of XRD and SEM analyses of selected ore samples. Selected SEM photomicrographs are included in **Appendix B**. It is worth noting that samples with the code “RBG” (Rustburg Quadrangle) come from a location near Lynchburg, Virginia and is technically located in the James River watershed. Because the geology of the James River-Roanoke River Manganese District is continuous in both the James River and Roanoke River watersheds, results obtained from any “RBG” samples can be applied to the Roanoke River watershed.


Table 1: Summary of XRD and SEM results for selected ore samples. In each picture, the hand lens shown for scale is ~30 mm across (long end).


Sample Number: LVL-100	Location: N 37.37099, W 79.03850
	Description: Quartzite impregnated by Mn and Fe oxides. Quartzite is relatively fresh without extensive weathering visible.
	XRD: No conclusive Mn-oxide minerals can be identified in this sample. Abundance of quartz masks Mn-oxides from identification.
	SEM: Fe and Mn oxides are abundant throughout sample. No associations between Mn and any other elements are observed; mineralogy cannot be constrained. Oxides commonly occur as fracture fillings.


Sample Number: LVL-101	Location: N 37.00641, W 79.46206
	<p>Description: Mn and possibly Fe ore. Appears to have replaced mica-schist country rock with mild to abundant Fe oxidation visible.</p>
	<p>XRD: No conclusive Mn-oxide phases can be identified in this sample. Relict quartz and mica in sample as well as Fe-oxides mask potential Mn-oxides from identification.</p>
	<p>SEM: Mn and Fe-oxides are abundant throughout sample. Associations between Mn, Al, and Na may suggest Mn-oxide mixture of lithiophorite and birnessite.</p>

Sample Number: LVL-102	Location: N 37.00642, W 79.46207
	<p>Description: Brecciated quartzite cemented by a Mn-oxide matrix.</p>
	<p>XRD: No conclusive Mn-oxide phases can be identified in this sample. Quartz and Fe-oxides mask potential Mn-oxides from identification.</p>
	<p>SEM: Mn and Fe-oxides are present throughout sample. Association between Mn, Al, and K may suggest mixtures of lithiophorite and cryptomelane.</p>

Sample Number: RBG01-BH	Location: N 37.37183, W 79.03732
	<p>Description: Nodular mass of Fe oxides with Mn-oxides present in lesser quantities. Nodule is moderately porous.</p>
	<p>XRD: Nodule composed mainly of goethite (Fe-oxide); Cryptomelane was identified as a Mn-oxide phases.</p>
	<p>SEM: Nodule composed predominantly of Fe-oxides (e.g. goethite). Manganese chiefly occurs in smaller concentrated areas.</p>

Sample Number: RBG-110	Location: N 37.37072, W 79.03861
	<p>Description: Massive (not visibly crystalline) Fe/Mn ore deposit. Country rock being replaced not easily distinguishable. Some quartz visible in hand samples. Surfaces appear more Mn-rich than sample interior of samples (Fe-oxides). Some soft (easily scratched by fingernail) Mn-oxide coatings appear on freshly-broken surfaces.</p>
	<p>XRD: No discernable Mn-oxides can be distinguished from sample due to abundance of Fe-oxides in sample.</p>
	<p>SEM: Mn-oxide coating intermixed with relatively smaller amounts of Fe-oxides. Mn association with Al may suggest the coating is composed of lithiophorite.</p>

Sample Number: RBG-111	Location: N 37.37073, W 79.03862
	<p>Description: Brecciated vein quartz cemented by Mn-oxides. Fe oxidation abundant on sample surfaces.</p>
	<p>XRD: Cryptomelane was identified as the main mineral in the oxide matrix.</p>
	<p>SEM: Sample is dominated by Mn and associated with K, confirming the plausibility of cryptomelane as the major Mn-oxide mineral. Smaller amounts of Al associated with Mn may suggest a less significant amount of lithiophorite is intermixed with cryptomelane.</p>

Sample Number: RBG-112A	Location: N 37.37071, W 79.03860
	<p>Description: Brecciated quartzite with what appear to be Mn-oxides filling fracture spaces. Botryoidal mineralization visible. Crystalline habit from surficial coating similar to manganite (MnOOH).</p>
	<p>XRD: Goethite was identified as the major oxide in this sample. No Mn-oxides were able to be detected.</p>
	<p>SEM: Oxide mineralization is dominated by Fe oxides. Considerably smaller amounts of Mn-oxides are disseminated throughout the sample. Fe abundance may completely mask Mn-oxides from identification.</p>

Sample Number: **RBG-114**

Location: **N 37.37355, W 79.03713**



Description: Weathered mica schist with Mn and Fe-oxide replacement along foliation planes. Some botryoidal growths visible on rock surface.

XRD: Lithiophorite was identified as the dominant Mn-oxide phases.

SEM: Within the weathered schist, Mn is both disseminated throughout sample and concentrated in tabular masses parallel to relict foliation planes. Botryoidal growth composed predominantly of Mn with some Fe. Mn and Al association provide support for lithiophorite as the dominant Mn-oxide mineral.

Bulk Chemical Analysis

Table 2: Chemical analysis of ore samples by near-total digestion and ICPMS analysis, conducted by Activation Labs, Inc. Na, Mg, Al, K, Ca, Fe are measured in weight percent. All other elements are measured in ppm.

	RBG-111	RBG-110	RBG01-BH	LVL-100	LVL-101	LVL-101A	LVL-102
B	< 1	< 1	< 1	< 1	3	< 1	5
Li	82.2	8.9	4.7	1.6	30	1	21.6
Na	0.22	0.04	0.04	0.21	0.05	0.03	0.04
Mg	0.03	0.05	0.18	0.01	0.15	0.01	0.15
Al	0.92	1.41	0.88	0.91	2.91	1.16	2.81
K	0.9	0.13	0.06	0.88	1	0.07	1.3
Ca	0.58	0.06	0.05	0.05	0.08	0.01	0.02
Cd	139	2.3	19	0.7	6.9	0.5	0.4
V	14	17	24	1	58	300	40
Cr	15.2	19.4	18.1	12.1	37	136	48.8
Mn	> 10000	4490	1780	2870	> 10000	354	7940
Fe	0.85	38	43.2	7.75	21.4	38.2	31.7
Hf	< 0.1	0.1	0.2	< 0.1	< 0.1	0.3	0.4
Ni	471	104	599	30.2	285	61.1	116
Er	13.8	7.5	7.2	0.4	7.8	2.4	2
Be	3.6	3.8	9.6	1.6	5.2	5.9	4.9
Ho	5.2	2.5	2.4	0.1	3	0.8	0.7
Hg	230	< 10	< 10	< 10	80	< 10	< 10
Ag	3.09	0.3	0.36	0.11	0.79	0.17	0.24
Cs	1.08	0.24	0.21	0.2	4.96	0.08	8.62
Co	> 500	337	297	20.5	447	6.9	52.9
Eu	6.41	2.95	2.15	0.2	4.55	0.96	1.22
Bi	0.03	0.15	0.07	0.02	0.11	0.03	0.03
Se	4.8	2.5	4.6	0.9	2.7	2.6	0.6
Zn	4030	1100	> 10000	256	784	164	671
Ga	147	2	4	0.5	< 0.1	4.3	9.5
As	5.2	38.7	64.2	3	9.2	94.3	2.1
Rb	26.8	5.8	4.3	16.8	230	2.8	121
Y	119	56.4	84.3	4.6	56.6	11	22
Zr	9	10	8	4	19	8	25
Nb	1.2	3.6	1.2	0.5	7.2	1.1	7.1
Mo	14.2	1.52	9.07	1.22	11.8	40	1.67
In	< 0.1	< 0.1	< 0.1	< 0.1	< 0.1	0.2	< 0.1
Sn	< 1	< 1	< 1	< 1	1	< 1	< 1
Sb	0.5	0.4	14.6	0.8	2.3	4	0.4
Te	0.2	0.3	0.3	0.3	0.4	0.5	0.2
Ba	> 5000	635	48	453	2640	35	469
La	39	38.7	94.3	4.7	51.9	4.8	23.7
Ce	172	94.5	150	7	124	16.6	32.5
Pr	16.4	13.8	19.8	0.9	19.9	2.4	5.3
Nd	79	57.9	59.3	3.2	84.9	11.4	22
Sm	25.8	13.4	8.7	0.6	19.3	3.8	4.6
Gd	30.2	12.8	10.6	0.6	18.8	3.7	4.7
Tb	4.7	2	1.6	< 0.1	2.9	0.7	0.6
Dy	27.5	12.7	10.4	0.6	16.7	4.1	3.7
Cu	839	117	1540	28.1	382	344	57.8

Table 2 continued

	RBG-111	RBG-110	RBG01-BH	LVL-100	LVL-101	LVL-101A	LVL-102
Ge	0.3	0.4	0.6	< 0.1	0.4	0.7	0.3
Tm	2	1.1	1	< 0.1	1.1	0.4	0.3
Yb	9.5	6.3	5.4	0.3	6	2.3	1.4
Lu	1.2	0.9	0.8	< 0.1	0.9	0.3	0.2
Ta	< 0.1	< 0.1	< 0.1	< 0.1	0.3	< 0.1	0.2
Sr	694	6	6.5	10	104	3.6	17.2
W	0.2	0.4	0.6	0.2	1.1	0.5	0.8
Re	0.024	0.018	0.019	0.023	0.021	0.015	0.015
Tl	2.07	0.38	0.14	0.36	3.02	0.16	0.92
Pb	128	24.8	777	12.3	10.9	32.9	6.8
Th	1	4.7	3.1	0.8	5.2	2.6	6.4
U	0.9	6.5	7.6	0.4	3.3	22.1	1.3

Note: Values preceded by “<” were below detection limits. Values preceded by “>” were above detection limits.

Figure 7 displays plots of Mn versus selected major and trace elements using the bulk chemical data for the seven ore samples.

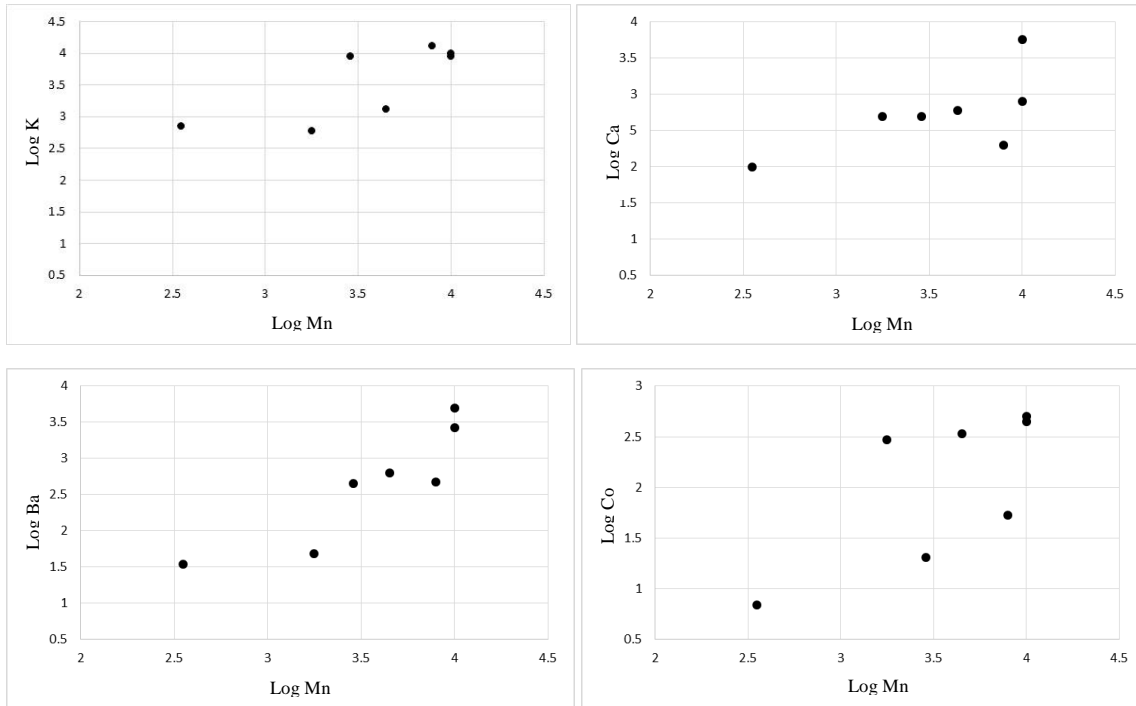


Figure 7: Plots of (a) K vs Mn, (b) Ca vs Mn, (c) Ba vs Mn, (d) Co vs Mn from ore samples analyzed by acid digestion and ICPMS. Concentrations are log-transformed from ppm concentrations.

The plots show that Mn has a clear positive correlation with Ca and Ba, with positive, but less significant, correlation with K and Co. Other scatter plots are shown in **Appendix C**.

Table 3 presents the correlation matrix for the ore concentration data. The correlation matrix shows a very strong positive ($r = +0.80$ or greater) relationship between Mn and Ba; strong positive ($r = +0.60$ to $+0.79$) relationships between Mn, K, Ca, and Co; moderately positive ($r = +0.40$ to $+0.59$) relationships between Mn, Mg, and Al; and weak positive ($r = +0.20$ to $+0.39$) relationships between Mn, Na, and Ni. The matrix shows a strong negative ($r = -0.60$ to -0.79) relationship between Mn and As; moderately negative ($r = -0.40$ to -0.59) relationships between Mn, Fe, and Mo; a weak negative ($r = -0.20$ to -0.39) relationship between Mn and Pb; and a very weak negative ($r = 0$ to -0.19) relationship between Mn and Cu.

Table 3: Pearson correlation matrix for selected chemical analytes in ore samples analyzed by acid digestion and ICPMS by Activation Labs, Ltd.

	Mn	Na	Mg	Al	K	Ca	Fe	Ba	Ni	Co	Cu	As	Mo	Pb
Mn	1.000	0.388	0.513	0.460	0.771	0.661	-0.440	0.888	0.381	0.709	-0.115	-0.712	-0.418	-0.253
Na	0.388	1.000	-0.428	-0.449	0.565	0.700	-0.893	0.573	-0.059	0.113	-0.173	-0.608	-0.202	0.020
Mg	0.513	-0.428	1.000	0.555	0.093	0.091	0.336	0.142	0.682	0.651	0.326	-0.060	-0.105	0.161
Al	0.460	-0.449	0.555	1.000	0.467	-0.256	0.362	0.316	0.007	0.125	-0.264	-0.336	-0.150	-0.677
K	0.771	0.565	0.093	0.467	1.000	0.387	-0.534	0.783	-0.077	0.141	-0.450	-0.958	-0.364	-0.597
Ca	0.661	0.700	0.091	-0.256	0.387	1.000	-0.824	0.773	0.566	0.747	0.356	-0.321	0.032	0.329
Fe	-0.440	-0.893	0.336	0.362	-0.534	-0.824	1.000	-0.674	-0.204	-0.258	-0.115	0.508	-0.102	-0.125
Ba	0.888	0.573	0.142	0.316	0.783	0.773	-0.674	1.000	0.241	0.596	-0.098	-0.655	-0.203	-0.320
Ni	0.380	-0.059	0.682	0.007	-0.077	0.566	-0.204	0.241	1.000	0.798	0.848	0.157	0.413	0.669
Co	0.709	0.113	0.651	0.125	0.141	0.747	-0.258	0.596	0.798	1.000	0.489	-0.048	-0.038	0.361
Cu	-0.115	-0.173	0.326	-0.264	-0.450	0.356	-0.115	-0.098	0.848	0.489	1.000	0.553	0.772	0.810
As	-0.710	-0.608	-0.060	-0.336	-0.958	-0.321	0.508	-0.655	0.157	-0.048	0.553	1.000	0.528	0.536
Mo	-0.418	-0.202	-0.105	-0.150	-0.364	0.032	-0.102	-0.203	0.413	-0.038	0.772	0.528	1.000	0.425
Pb	-0.253	0.020	0.161	-0.677	-0.597	0.329	-0.125	-0.320	0.669	0.361	0.810	0.536	0.425	1.000

Note: Correlation values are between -1 and +1. A value of -1 represents a perfect negative correlation while a value of +1 represents a perfect positive correlation. A value of 0 indicates that no correlation is present between two variables. Values ≥ 0.500 are bolded.

LA-ICPMS

Tables 4-6 include the data from LA-ICPMS analysis for samples RBG01-BH, LVL-100, and RBG-114. Thick sections are shown in **Figures 8-10**. Note that slide dimensions are 46 mm x 26 mm.



Figure 8: Thick section of RBG01-BH. Numbered red dots represent the sampling points analyzed on the LA-ICPMS.

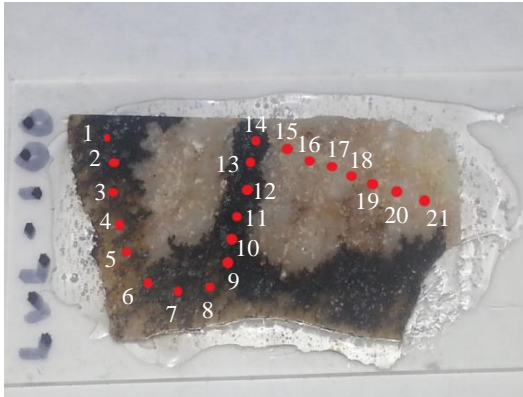


Figure 9: Thick section of LVL-100. Numbered red dots represent the sampling points analyzed on the LA-ICPMS.

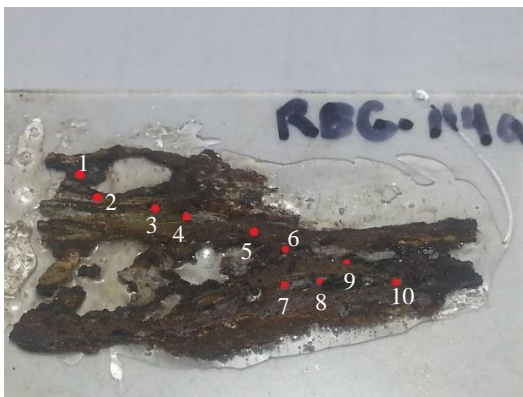


Figure 10: Thick section of RBG-114A. Numbered red dots represent the sampling points analyzed on the LA-ICPMS.

Table 4: Summary of LA-ICPMS data for RBG01-BH (see **Figure 8**)

Sample Number:	RBG01-BH									
Element	1	2	3	4	5	6	7	8	9	Average
Na	23.8	95.0	33.2	20.2	18.2	44.2	55.7	8.2	46.7	38.3
Mg	123.1	56.3	92.5	108	114	311	285	102	246	160
Al	2200	246	668	966	2480	4550	4778	1091	6369	2594
Si	8910	13841	10897	10056	9401	34195	20030	26448	17330	16790
K	19.9	11.5	21.4	21.7	13.9	1198	1284	12.6	581	352
Ca	223	157	216	260	165	203	196	163	241	203
Ti	0.7	0.6	1.4	0.5	0.5	36.6	47.9	3.2	339	47.8
Mn	933	1018	892	727	816	1201	1259	552	1604	1000
Fe	731920	732481	733858	734116	736195	690328	712489	666085	712821	716699
Co	535	429	395	326	645	461	485	176	403	428
Ni	1710	1164	1329	1232	2048	1375	1381	369	1256	1318
Cu	2188	2101	3402	4458	3671	1996	1933	1012	2550	2590
Zn	21574	16191	17954	17862	14514	16840	17810	65197	19134	23008
As	155	348	202	225	93.8	87.5	113	23.4	138	154
Mo	20.8	23.6	21.5	24.8	24.6	16.2	15.6	3.8	18.0	18.8
Pb	634	419	473	483	291	265	263	142	332	367

Note: Element concentrations are measured in parts per million (ppm). Numbers 1-9 represent analysis points on sample (see Figure 8). The column labeled Average is the arithmetic mean (average) of concentration in ppm.

The LA-ICPMS analysis of RBG01-BH shows that Fe dominates the sample with an averaged value of 716,699 ppm (approximately 72 weight %). RBG01-BH also contains Si (~1.7 avg. wt. %) and Zn (~2.3 avg. wt. %). Mn is present in all sampling points with an average value of 1000 ppm (~0.1 avg. wt. %). Trace elements, including Co, Ni, Cu, Zn, As, Mo, and Pb, are also measured in the sample.

Table 5: Summary of LA-ICMPS data for LVL-100 (see Figure 9)

Sample Number:	LVL-100																					Average †	Average *	Average ‡
Element	1	2	3	4	5	6	7	8	9	10	11	12	13	14	15	16	17	18	19	20	21	Average †	Average *	Average ‡
Na	9.6	-	9.5	4.8	10.2	96.2	2.2	-	89.7	30.0	8.4	163	44.5	25.9	5.1	8.9	10.2	8.8	18.0	4.2	25.2	22.1	60.2	11.5
Mg	-	-	2.4	-	-	2.8	36.3	-	96.6	14.2	2.1	19.2	48.9	5.7	-	4.0	7.8	-	3.5	-	1.3	34.5	31.1	4.2
Al	7.3	27.9	109	84.5	43.7	8241	14.7	18.0	546	261.1	8.5	1595	439	252	9.5	8.6	12.7	35.2	9.8	10.1	32.9	1010	517	17.0
Si	467414	466788	463373	466249	466682	348279	467298	466762	445110	457632	467395	420790	452620	459221	467397	467382	467389	467368	467390	467410	467354	450884	450461	467384
K	4.6	26.8	23.8	3.7	7.7	2770.0	-	-	1529	744.0	4.7	4797	1134	589	10.7	5.0	7.6	29.6	11.3	3.6	31.0	623.7	1466	14.1
Ca	-	-	3.5	2.2	4.4	12.3	8.2	-	21.7	10.8	-	62.7	27.0	14.1	-	10.5	2.5	1.4	2.1	-	12.7	8.7	27.2	5.8
Ti	5.1	10.4	2.3	12.0	6.8	3.0	4.0	10.9	4.9	9.7	9.4	5.7	13.0	5.2	8.6	8.6	9.5	9.9	10.0	11.2	2.1	6.6	8.0	8.6
Mn	-	973.0	42.3	6.0	9.8	694.4	97.8	-	25148	14637	19.5	69711	22186	12455	0.7	0.4	0.4	-	0.6	0.3	0.4	3853	24026	0.5
Fe	0.2	5.9	6471	1805	1135	181909	11.0	1068	9239	371	0.9	60.0	349	82.9	15.6	3.6	2.0	4.7	4.3	1.3	10.9	22405	1684	6.1
Co	-	1.3	0.7	-	-	18.8	-	-	32.1	35.8	-	86.7	45.3	29.0	-	-	-	-	-	-	-	13.2	45.8	-
Ni	0.7	2.1	2.2	-	1.7	37.8	-	-	7.6	9.2	1.6	78.7	21.3	9.6	-	-	-	-	1.7	-	1.3	8.7	21.3	1.5
Cu	-	1.0	2.3	4.7	1.0	79.4	-	2.3	35.4	2.9	-	7.5	4.9	17.8	-	0.9	-	-	-	1.2	0.4	18.0	13.7	0.8
Zn	7.6	14.6	40.3	10.6	11.1	609	37.2	5.6	96.6	43.6	9.0	277.8	93.1	46.7	8.9	33.6	17.1	7.7	10.2	6.9	6.0	92.5	94.5	12.9
As	1.3	1.5	1.2	1.3	2.6	1.5	0.9	2.6	2.3	1.8	1.4	1.7	2.0	2.4	0.9	1.6	1.7	1.4	1.2	1.2	1.7	1.7	1.9	1.4
Mo	-	-	0.0	-	-	0.2	0.1	-	0.1	0.0	-	-	-	-	-	-	-	-	-	-	-	0.1	0.1	-
Pb	0.1	0.1	0.5	0.1	0.1	4.4	0.4	0.2	1.1	0.3	-	0.0	0.2	1.0	0.1	0.2	0.1	0.0	0.3	0.1	0.1	0.8	0.5	0.1

Note: Elemental concentrations are measured in parts per million (ppm). A value of “-” is below detection. The column labeled Average † represents the arithmetic average concentrations of analyzed elements from points 1-8; Average * represents the arithmetic averages of analyzed elements from points 9-14; Average ‡ represents the arithmetic averages of analyzed elements from points 15-21.

Sample LVL-100 was divided into three separate zones of analysis due to heterogeneities within the quartzite sample (see **Figure 9**). Points 1-8 include portions of sample with visible impregnations of Mn and Fe oxides that grade into relatively fresh quartzite. Points 9-14 analyzed a fracture less than 0.5 mm thick filled in by Mn and Fe oxides. Fresh quartzite without any visible oxide impregnations was analyzed in points 15-21. In all sample point ranges, Si was the dominant chemical constituent; approximately 45 percent of the sample by weight in Si (oxygen is not included in analyses but we can infer that the combined weight percents of Si and O would sum to 90 - 100 percent). Averaged values of analytes show an increase in concentrations of Na, K, Ca, Mn, Co, and Ni from points 1-8 and points 9-14. Average Fe and Al concentrations decreased between the two sample zones. All other analytes maintained similar concentrations. Average concentrations of elements from points 15-21 in raw quartzite were all below 20 ppm for all elements except Si.

Table 6: Summary of LA-ICPMS results for RBG-114A (see **Figure 10**)

Sample Number:	RBG-114A										
Element	1	2	3	4	5	6	7	8	9	10	Average
Na	188	113	717	1093	65.7	253	180	727	331	123	379
Mg	586	1084	2678	4705	325	1066	536	2408	1976	616	1598
Al	3928	143075	41066	74865	6108	32069	16452	61212	31962	21712	43245
Si	42892	144052	51616	93602	18100	9187	27119	54827	32280	16332	49001
K	755	6590	15252	30629	102	4056	3537	16872	9395	1523	8871
Ca	561	202	278	324	404	723	385	343	520	267	401
Ti	12.7	80.3	566	894	318	98.4	723	715	218994	47138	26954
Mn	43740	2177	11876	2485	3359	171607	3238	77256	49240	18397	38338
Fe	648424	315471	594849	468963	727427	520405	692912	485304	327076	628942	540977
Co	602	52.5	214	94.3	62.8	2695	104	1929	283	125	616
Ni	496	111	328	182	162	3454	212	3113	306	272	864
Cu	21.0	32.9	10.6	10.4	9.2	48.2	46.0	31.4	98.4	37.6	34.6
Zn	4594	1824	4443	2642	5963	10041	6164	7441	3382	6879	5337
As	1.9	1.5	1.5	1.4	1.1	2.3	2.6	2.0	1.7	4.1	2.0
Mo	23.1	1.4	11.3	2.1	0.7	70.0	5.4	177	11.3	3.0	30.5
Pb	31.6	4.2	17.8	6.5	8.1	22.8	14.8	30.4	33.9	9.3	17.9

Note: Elemental concentrations are measured in parts per million (ppm). Numbers 1-10 represent analysis points on sample. The column labeled Average is the arithmetic mean (average) concentration of analyzed elements.

Sample RBG-114 is a weathered mica schist with Mn and Fe oxides that permeate the relict foliation planes of the schist, as seen in both hand sample and in the SEM (see **Figure 10**). Points selected for analysis visually displayed strong signs of oxidation (red from Fe and black from Mn). Fe concentrations averaged 540,977 ppm (54 wt. %). Mn concentrations vary greatly (2,177 – 171,606 ppm) with an average concentration of 38,338 ppm. Average concentrations of Si and Al are fairly similar and are likely due to residual mica and quartz minerals in the sample or—in the case of Al—from Mn-oxide minerals containing Al (e.g. lithiophorite). The trace elements present in highest concentrations in the sample are Co, Ni, and Zn. Cu, As, Mo, Pb are all present in the sample but at concentrations considerably lower than Co, Ni, and Zn.

Analysis by LA-ICPMS has several advantages for bulk analysis of samples compared to other analytical methods. It allows highly sensitive elemental analyses to be conducted on solid samples with little to no sample preparation required. Furthermore, results are available almost instantly. In the case of this study, the largest disadvantage to LA-ICPMS analysis becomes apparent when interpreting results. After samples are ablated with a laser and element signals are collected, results are calculated by normalizing all analytes to 100 percent in relation to each other. Only 16 elements were analyzed in the three samples. The samples are most likely composed predominantly of the elements selected for analysis, ensuring the collection of reasonably accurate data. A larger suite of analytes, however, may result in more accurate elemental concentrations. For this reason, specific comparisons between elements in samples will be performed using data from bulk chemical analysis from near-total acid digestions.

Soil Mapping

Soil maps were compiled to examine the spatial correlations between the known locations of Mn mines in Campbell County (ore deposits) and alluvial soils (derived from fluvial activity). The resulting map compilations are shown in **Figure 11**, which shows a representative portion of the study area in southwest Campbell County. Soils are separated into two groups: Piedmont Upland terrace deposits (red) which are found at higher elevations in the Piedmont and modern stream valley soils (blue) occurring in or near present day streams. Locations of known Mn mining localities generally cluster either within or near alluvial soils. Henika (personal communication, 2015) suggests the existence of a relict meander belt in the region north of the Roanoke River (see **Figure 11**), based on presence of the Piedmont Upland terrace deposits and other geomorphologic features.

Elevation data for the alluvial soil deposits and Mn mining locations modeled using ArcGIS are shown in **Figure 12**. From these figures we can see that the distribution of elevations is most similar between Piedmont Upland terrace deposits and Mn mining locations. The overall implications of these statistical observations are that ore deposits are spatially correlated with alluvial soils in three dimensions, suggesting that the ore deposits were at the same relative locations of discharge zones (streams) during their time of formation.

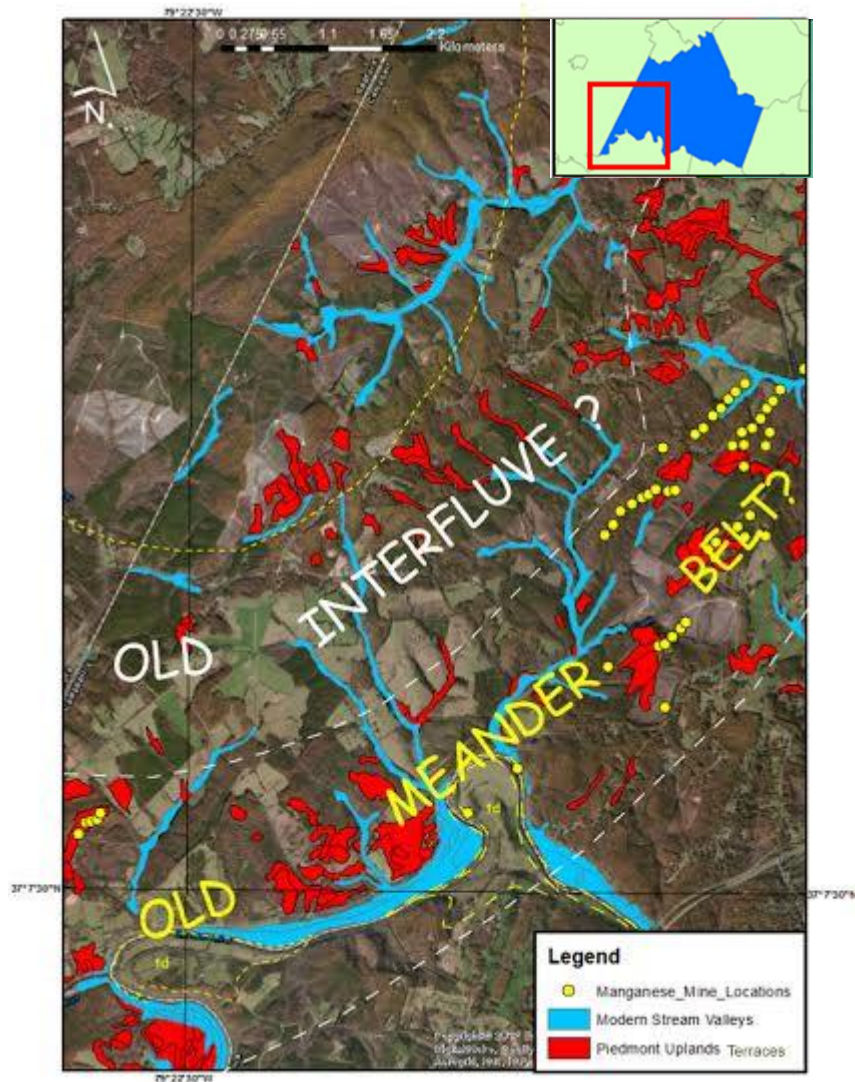


Figure 11: Representative soil maps of Campbell County showing alluvial soils (terrace deposits) in both Piedmont Uplands and modern stream valleys. Soil data from SSURGO database (Soil Survey Staff, 2014). Possible geomorphic interpretations have been annotated. “td” represents terrace deposits in Pittsylvania County, mapped by Henika (2015).

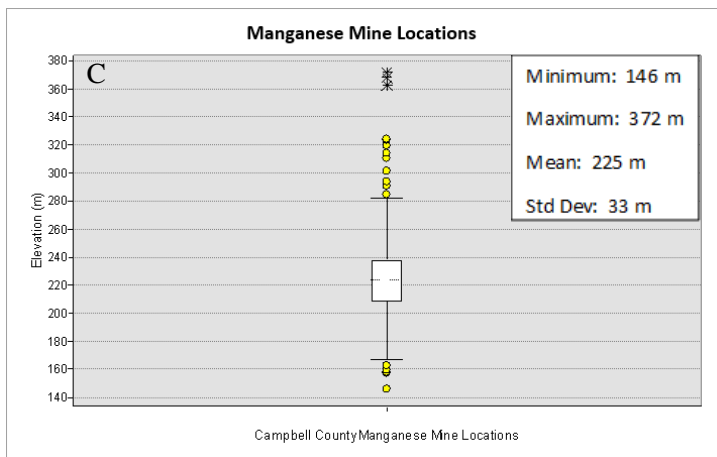
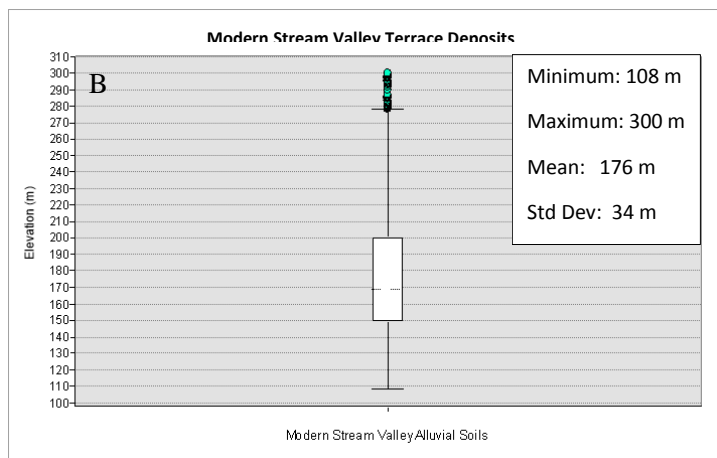
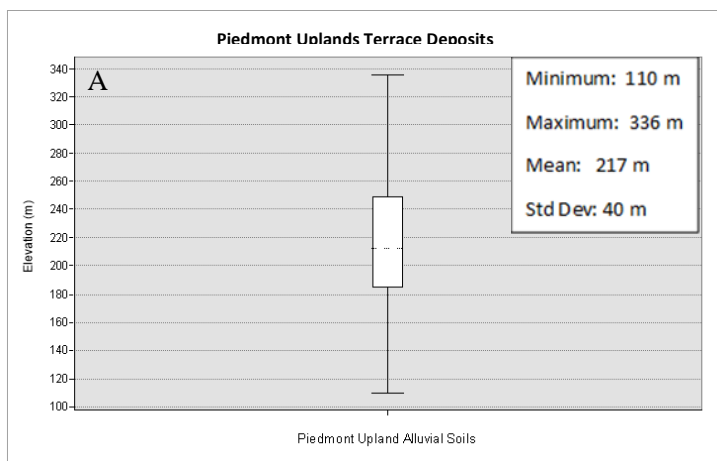


Figure 12: Boxplots of the distribution of elevations of A) Piedmont Upland alluvial soils, B) modern stream valley alluvial soils, and C) known Mn mining locations in Campbell County, VA. Yellow and blue circles represent outliers of the elevation data; Asterisks represent extreme outliers of the data. Plots were created using ArcGIS 10.2 (ESRI, 2013).

Statistical Analyses of Groundwater Data

Figure 13 shows how total Mn concentrations in groundwater are distributed throughout the counties within the Roanoke River watershed. Data are provided in **Appendix D**. As shown in the figure, total Mn concentrations in groundwater vary over three orders of magnitude across the different counties within the watershed. Excluding outliers, the total Mn in Campbell County has the greatest amount of variance in the upper 25th percentile. Most groundwater samples in Campbell County have total Mn concentrations than 50 ppb, with ~25% of concentrations exceeding 50 ppb and ~9 percent of concentrations exceeding 300 ppb. In **Figure 13** we can also see that for several counties the 25th quartile is the same as the minimum value (lower limit of range). This is because of several entries of total Mn concentrations in the STORET database were listed as 10 ppb.

Figure 14 shows the distribution of total Mn concentrations in geologic formations in the proximity of the JRRRMD (see **Figure 5**). These formations are continuous in a NE-SW trend throughout the Roanoke River watershed. Due to this continuity, water samples from multiple counties that contain these geologic units—not just those near the JRRRMD—were analyzed to show how total Mn varies in groundwater from formation to formation. Data are available in **Appendix E**. The Candler Formation, Bassett Formation, and Alligator Back Formation are the three formations which have the greatest 50th percentile for total Mn concentrations in groundwater. The Candler Formation only has three samples but all are greater than 50 ppb and one exceeds 300 ppb. The Alligator Back Formation has ~32% of its total Mn concentrations exceeding 50 ppb and ~11% exceeding 300 ppb; the Bassett Formation has 50% exceeding 50 ppb and ~7% exceeding 300 ppb. The Alligator Back Formation has the greatest amount of

variance in the upper 25th percentile of the data, also having the greatest observed total Mn concentration in groundwater of 1,300 ppb.

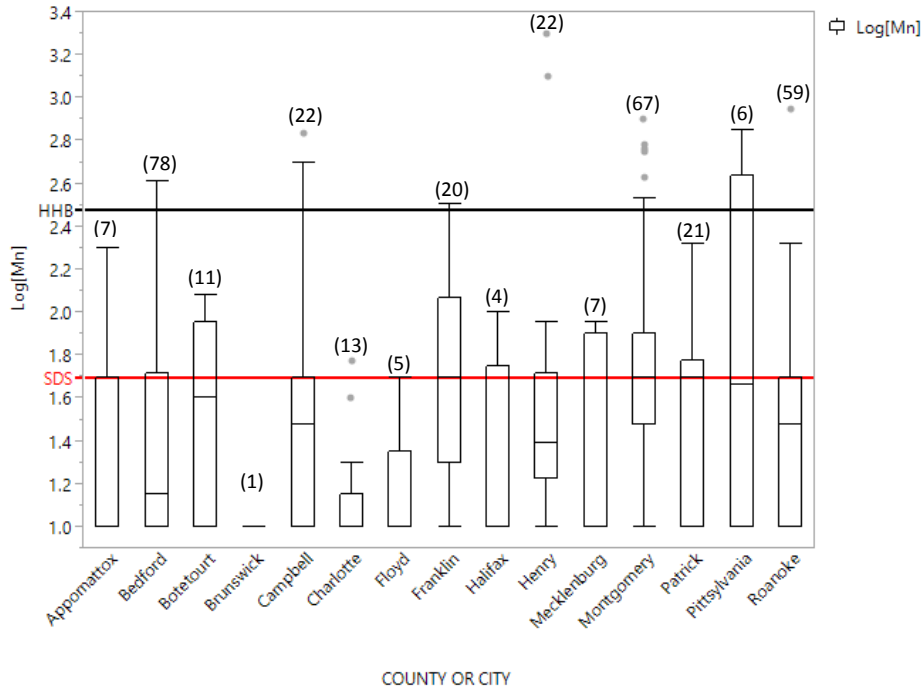


Figure 13: Boxplots showing the distribution of total Mn concentrations (ppb) in groundwater in all counties encompassed in the Roanoke River watershed. Data from STORET (2014) are used to create the figure. The red reference line represents the secondary drinking standard (SDS) for Mn (50 ppb). The black reference line represents the human health benchmark (HHB) for Mn (300 ppb). Sample numbers for each county are shown above each county's boxplot inside parentheses.

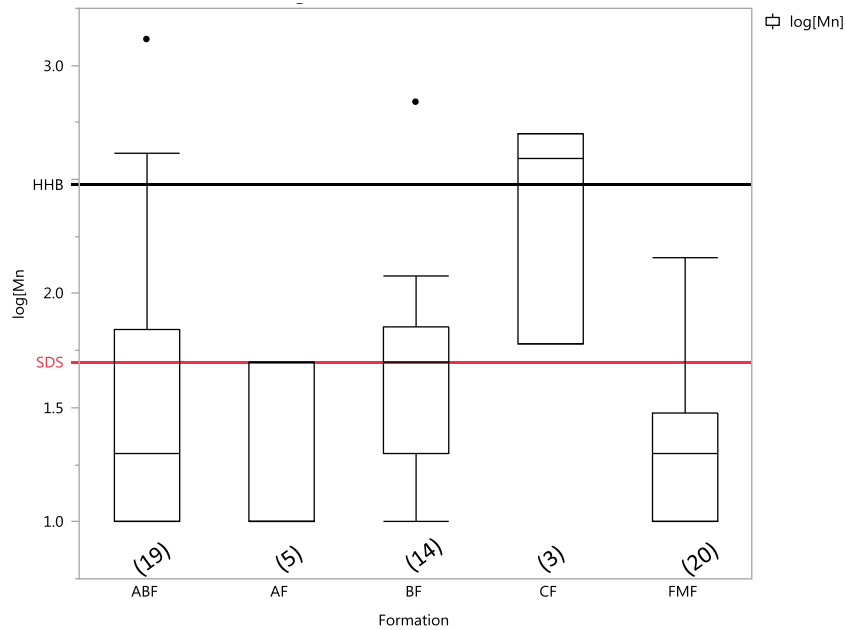


Figure 14: Boxplots showing the distribution of total Mn concentrations (ppb) in groundwater from wells open to different geologic formations within the Roanoke River watershed. ABF=Alligator Back Formation, AF=Ashe Formation, BF=Bassett Formation, CF=Candler Formation, FMF=Fork Mountain Formation. Red reference line represents the secondary drinking standard (SDS) for Mn (50 ppb). The black reference line represents the human health benchmark (HHB) for Mn (300 ppb). Sample numbers are shown above formation abbreviations inside parentheses. Data are from STORET (2014).

Statistical evaluation of the relationship of Mn with other chemical analytes is useful for examining possible geochemical processes influencing Mn concentrations. Dissolved oxygen (DO) will be evaluated first, because Mn is an element sensitive to redox (reducing-oxidizing) conditions in aqueous environments. A complete list of chemical data used in these tests is included in **Appendix F**. Statistical tests on additional chemical parameters are included in **Appendix G**. Because DO data are sparse in the study area, we used the Chapman (2013) dataset, which includes wells located within the entirety of the Piedmont and Blue Ridge Crystalline Aquifers in Virginia (**Appendix H**).

Figure 15 displays filtered Mn concentrations plotted against DO concentrations in the Piedmont/Blue Ridge aquifers (data from Chapman, 2013). In general, filtered Mn concentrations are inversely correlated with DO concentrations. The relationship between the

two variables is not perfectly linear, but DO is a notoriously difficult parameter to measure in the field, commonly being overestimated. Because of this, it is likely that the true DO values where several the data points show high Mn concentrations at high DO concentrations may be lower, falling closer to the line of regression drawn on the plot.

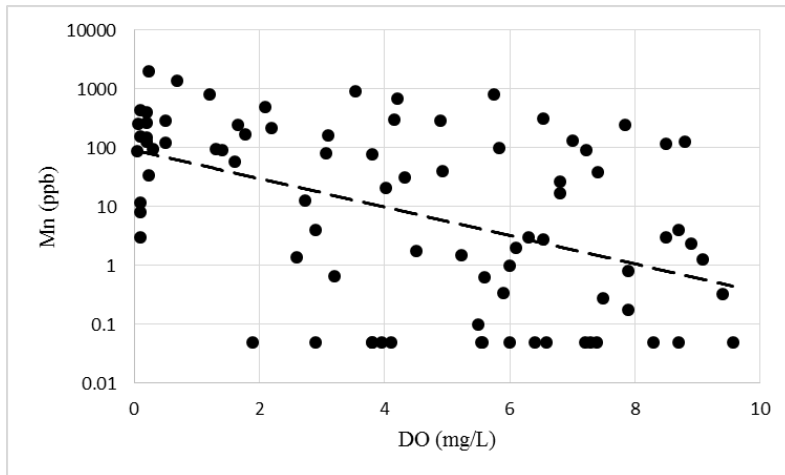


Figure 15: Dissolved oxygen versus filtered Mn concentrations for all Virginia groundwater samples in the Piedmont and Blue Ridge crystalline aquifers from Chapman (2013).

To examine the significance of the association between DO and filtered Mn in groundwater, samples were divided into three groups. Group 1 included samples where filtered Mn was below 50 ppb; Group 2 included samples where filtered Mn was between 50 and 300 ppb; Group 3 included samples where filtered Mn exceeded 300 ppb. **Figure 16** show these grouped data represented as boxplots. The boxplots show that median DO values for both Groups 2 and 3 are less than the median value in Group 1. This suggests that Mn concentrations >50 ppb are associated with low DO concentrations. To evaluate the strength of this assumption, a Kruskal-Wallis test was employed to test if a significant difference exists between the central values of at least two groups (Reimann et al., 2008). The test was conducted for 95 percent significance and a 5 percent confidence interval (p -value = 0.05). The results of the Kruskal-

Wallis test showed a p-value of 0.016, indicating that the median values of at least one of the three groups is statistically different than the other two groups. To evaluate which groups differ, a Wilcoxon signed rank test was used to test the statistical significance between the median values of paired groups. As with the Kruskal-Wallis test, the groups were tested using the Wilcoxon signed rank test for 95% significance and a 5% confidence interval. The p-values for the comparison between Groups 1 and 2 and Groups 1 and 3 were 0.060 and 0.016, respectively. This shows that there is a statistical difference in the medians of groundwater samples in > 300 ppb and those with concentrations < 300 ppb, but no difference between samples with < 50 ppb and those with Mn between 50 and 300 ppb.

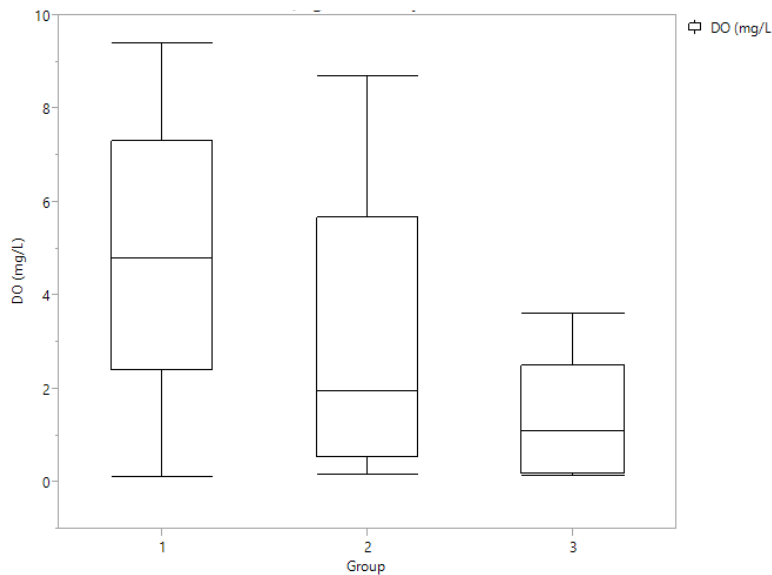


Figure 16: Boxplots of grouped samples and DO concentrations for all Virginia groundwater samples from the Piedmont and Blue Ridge crystalline aquifers (Chapman, 2013). Group 1 (n=48) represents samples where filtered Mn concentrations were <50 ppb. Group 2 (n=26) represents samples where Mn concentrations were >50 ppb and <300 ppb. Group 3 (n=10) represents samples where Mn concentrations were >300 ppb.

We used two datasets to assess relationships between Mn and Fe concentrations in groundwater. In samples from the Virginia Piedmont/Blue Ridge aquifers (Chapman, 2013), filtered Fe was positively correlated with filtered Mn ($r = 0.814$). Using the STORET dataset,

total Fe and Mn were also positively correlated ($r = 0.50$) (**Table 8** and **Figure 17**). The significance of the Mn-Fe associations (see **Figure 17**) were evaluated in the same way DO was analyzed above.

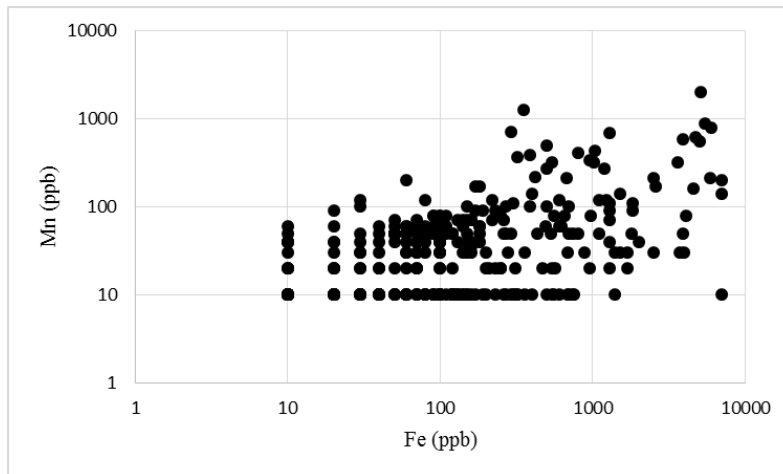


Figure 17: Total Mn concentrations versus total Fe concentrations for wells within a selected portion of the study area. Data from the STORET database (2014). Although many concentrations were listed in the STORET database as 10 ppb and are thus presented as 10 ppb, it is likely that they were intended to be listed as <10 ppb.

Table 7: Pearson correlation matrix for groundwater chemical data obtained from Chapman (2013) for wells within the state of Virginia in the Blue Ridge and Piedmont crystalline aquifers.

	Mn	DO	pH	Alk	As	Ba	Co	Cu	Fe	Pb	Mo	Ni	Zn	Al	Ca	Mg	Na	K	Cl	SO4	F	SiO2	TDS
Mn	1.000	-0.476	-0.142	-0.008	-0.059	0.393	0.382	-0.493	0.814	-0.559	0.033	0.417	-0.404	-0.291	0.020	0.102	0.126	0.160	0.283	0.127	0.061	0.065	0.104
DO	-0.476	1.000	-0.443	-0.449	-0.016	-0.118	-0.089	0.341	-0.431	0.302	-0.006	0.049	0.491	0.289	-0.461	-0.398	-0.311	-0.275	-0.243	-0.532	-0.403	-0.198	-0.454
pH	-0.142	-0.443	1.000	0.758	-0.014	-0.192	-0.333	-0.442	-0.094	-0.214	0.306	-0.479	-0.407	-0.236	0.684	0.445	0.255	0.138	0.012	0.472	0.406	0.221	0.541
Alk	-0.008	-0.449	0.758	1.000	-0.157	0.000	-0.222	-0.410	0.017	-0.279	0.173	-0.301	-0.421	-0.523	0.816	0.609	0.409	0.113	0.212	0.547	0.333	0.339	0.693
As	-0.059	-0.016	-0.014	-0.157	1.000	0.132	0.562	0.030	-0.178	0.407	0.131	0.307	0.164	0.395	-0.002	-0.111	-0.427	-0.166	0.048	-0.094	-0.182	-0.561	-0.117
Ba	0.393	-0.118	-0.192	0.000	0.132	1.000	0.243	-0.089	0.193	-0.091	-0.314	0.440	-0.010	0.181	0.198	0.284	0.283	0.418	0.474	-0.035	-0.330	-0.051	0.374
Co	0.382	-0.089	-0.333	-0.222	0.562	0.243	1.000	-0.178	0.366	0.021	-0.136	0.724	0.015	0.125	-0.194	-0.102	-0.246	-0.399	0.254	-0.162	-0.324	-0.515	-0.142
Cu	-0.493	0.341	-0.442	-0.410	0.030	-0.089	-0.178	1.000	-0.664	0.598	-0.119	-0.037	0.485	0.289	-0.272	-0.257	-0.136	-0.037	-0.075	-0.140	-0.216	-0.126	-0.248
Fe	0.814	-0.431	-0.094	0.017	-0.178	0.193	0.366	-0.664	1.000	-0.638	-0.076	0.250	-0.458	-0.429	-0.068	0.066	0.069	0.091	0.148	0.068	0.105	0.168	0.021
Pb	-0.559	0.302	-0.214	-0.279	0.407	-0.091	0.021	0.598	-0.638	1.000	0.143	-0.155	0.527	0.508	-0.245	-0.341	-0.489	-0.026	-0.364	-0.233	-0.159	-0.358	-0.353
Mo	0.033	-0.006	0.306	0.173	0.131	-0.314	-0.136	-0.119	-0.076	0.143	1.000	-0.259	0.074	0.136	0.186	-0.066	-0.072	0.027	-0.191	0.173	0.397	-0.025	-0.010
Ni	0.417	0.049	-0.479	-0.301	0.307	0.440	0.724	-0.037	0.250	-0.155	-0.259	1.000	0.045	0.126	-0.085	0.124	0.068	-0.305	0.485	-0.162	-0.436	-0.373	0.063
Zn	-0.404	0.491	-0.407	-0.421	0.164	-0.010	0.015	0.485	-0.458	0.527	0.074	0.045	1.000	0.422	-0.328	-0.269	-0.275	-0.071	-0.141	-0.375	-0.219	-0.371	-0.272
Al	-0.291	0.289	-0.236	-0.523	0.395	0.181	0.125	0.289	-0.429	0.508	0.136	0.126	0.422	1.000	-0.216	-0.158	-0.208	0.138	-0.056	-0.252	-0.036	-0.607	-0.165
Ca	0.020	-0.461	0.684	0.816	-0.002	0.198	-0.194	-0.272	-0.068	-0.245	0.186	-0.085	-0.328	-0.216	1.000	0.735	0.563	0.208	0.492	0.638	0.268	0.273	0.905
Mg	0.102	-0.398	0.445	0.609	-0.111	0.284	-0.102	-0.257	0.066	-0.341	-0.066	0.124	-0.269	-0.158	0.735	1.000	0.585	0.219	0.585	0.600	0.223	0.200	0.870
Na	0.126	-0.311	0.255	0.409	-0.427	0.283	-0.246	-0.136	0.069	-0.489	-0.072	0.068	-0.275	-0.208	0.563	0.585	1.000	0.239	0.598	0.404	0.328	0.429	0.754
K	0.160	-0.275	0.138	0.113	-0.166	0.418	-0.399	-0.037	0.091	-0.026	0.027	-0.305	-0.071	0.138	0.208	0.219	0.239	1.000	0.198	0.220	0.286	0.196	0.297
Cl	0.283	-0.243	0.012	0.212	0.048	0.474	0.254	-0.075	0.148	-0.364	-0.191	0.485	-0.141	-0.056	0.492	0.585	0.598	0.198	1.000	0.255	-0.013	-0.001	0.667
SO4	0.127	-0.532	0.472	0.547	-0.094	-0.035	-0.162	-0.140	0.068	-0.233	0.173	-0.162	-0.375	-0.252	0.638	0.600	0.404	0.220	0.255	1.000	0.383	0.273	0.628
F	0.061	-0.403	0.406	0.333	-0.182	-0.330	-0.324	-0.216	0.105	-0.159	0.397	-0.436	-0.219	-0.036	0.268	0.223	0.328	0.286	-0.013	0.383	1.000	0.330	0.282
SiO2	0.065	-0.198	0.221	0.339	-0.561	-0.051	-0.515	-0.126	0.168	-0.358	-0.025	-0.373	-0.371	-0.607	0.273	0.200	0.429	0.196	-0.001	0.273	0.330	1.000	0.317
TDS	0.104	-0.454	0.541	0.693	-0.117	0.374	-0.142	-0.248	0.021	-0.353	-0.010	0.063	-0.272	-0.165	0.905	0.870	0.754	0.297	0.667	0.628	0.282	0.317	1.000

Note: Concentration data were log transformed prior to analyses. Concentrations analyzed on filtered samples. Analytes measured in mg/L were DO, Ca, Mg, Na, K, Cl, SO₄, F, SiO₂, and TDS. Alkalinity (Alk) was measured in mg/L as CaCO₃. All other analytes were measured in units of µg/L (ppb). Correlation values are between -1 and +1. A value of -1 represents a perfect negative correlation while a value of +1 represents a perfect positive correlation. A value of 0 indicates that no correlation is present between two variables. Values ≥0.500 are bolded.

Table 8: Pearson correlation matrix for groundwater chemical data obtained from the STORET dataset. Samples were unfiltered.

	Mn	pH	Ca	Mg	K	Na	HCO3-	SO42-	F-	As	Cu	Fe	Pb	Ni	Zn	TDS
Mn	1.000	0.357	0.433	0.247	0.187	0.218	0.377	0.402	0.173	0.021	-0.207	0.500	0.033	0.306	0.131	0.399
pH	0.357	1.000	0.690	0.517	0.285	0.418	0.690	0.542	0.215	0.032	-0.253	0.313	0.001	0.131	-0.132	0.730
Ca	0.433	0.690	1.000	0.655	0.500	0.656	0.769	0.524	0.280	0.016	-0.215	0.307	0.121	0.006	-0.117	0.890
Mg	0.247	0.517	0.655	1.000	0.271	0.459	0.594	0.416	0.062	-0.021	-0.138	0.285	0.055	-0.011	-0.159	0.690
K	0.187	0.285	0.500	0.271	1.000	0.413	0.373	0.359	0.217	0.024	-0.088	0.150	-0.106	-0.168	-0.031	0.492
Na	0.218	0.418	0.656	0.459	0.413	1.000	0.644	0.412	0.239	0.066	-0.193	0.206	0.088	-0.074	-0.123	0.722
HCO3-	0.377	0.690	0.769	0.594	0.373	0.644	1.000	0.442	0.178	0.008	-0.256	0.238	-0.022	0.070	-0.130	0.903
SO42-	0.402	0.542	0.524	0.416	0.359	0.412	0.442	1.000	0.101	-0.115	-0.135	0.424	-0.043	-0.112	-0.108	0.611
F-	0.173	0.215	0.280	0.062	0.217	0.239	0.178	0.101	1.000	0.362	-0.302	-0.008	-0.305	-0.047	-0.134	0.237
As	0.021	0.032	0.016	-0.021	0.024	0.066	0.008	-0.115	0.362	1.000	-0.082	-0.026	-0.021	0.228	0.040	0.005
Cu	-0.207	-0.253	-0.215	-0.138	-0.088	-0.193	-0.256	-0.135	-0.302	-0.082	1.000	-0.214	0.453	0.087	0.079	-0.236
Fe	0.500	0.313	0.307	0.285	0.150	0.206	0.238	0.424	-0.008	-0.026	-0.214	1.000	0.208	0.000	0.170	0.327
Pb	0.033	0.001	0.121	0.055	-0.106	0.088	-0.022	-0.043	-0.305	-0.021	0.453	0.208	1.000	0.467	0.315	0.057
Ni	0.306	0.131	0.006	-0.011	-0.168	-0.074	0.070	-0.112	-0.047	0.228	0.087	0.000	0.467	1.000	0.037	-0.009
Zn	0.131	-0.132	-0.117	-0.159	-0.031	-0.123	-0.130	-0.108	-0.134	0.040	0.079	0.170	0.315	0.037	1.000	-0.105
TDS	0.399	0.730	0.890	0.690	0.492	0.722	0.903	0.611	0.237	0.005	-0.236	0.327	0.057	-0.009	-0.105	1.000

Note: Wells selected from the STORET dataset for statistical analysis were from the counties of greatest interest due to proximity to the James River-Roanoke River Manganese District or the continuity of geology formations encompassing or adjacent to the James River-Roanoke River Manganese District. Correlation values are between -1 and +1. A value of -1 represents a perfect negative correlation while a value of +1 represents a perfect positive correlation. A value of 0 indicates that no correlation is present between two variables. Values ≥ 0.500 are bolded.

Figure 18 shows the boxplots of Fe concentrations for the three groups of Mn concentrations (<50 ppb, >50 ppb and <300 ppb, >300 ppb). Excluding the outliers in Groups 1 and 2, the boxplots show that the variability in the Fe concentrations of Group 3 is greater than the other two groups. This is especially noticeable in the upper 75 percent of the data. Using a Kruskal-Wallis test yields a p-value of 6×10^{-6} , indicating a difference in the median values between at least two groups. Results of individual Wilcoxon signed rank tests show that all groups are statistically different from one another (all p-values <0.05). This implies that increases in Fe concentrations correspond significantly to Mn concentrations in groundwater. Both Fe and Mn are metals whose solubility in aqueous environments is controlled by the redox conditions of groundwater. As both Fe and Mn are negatively correlated with DO (see **Table 7**), median values of Fe increase among the groups (Group 3 > Group 2 > Group 1) because higher concentration of Mn in solution are indicative of increasingly reducing groundwater, which will also lead to an increase in Fe concentrations.

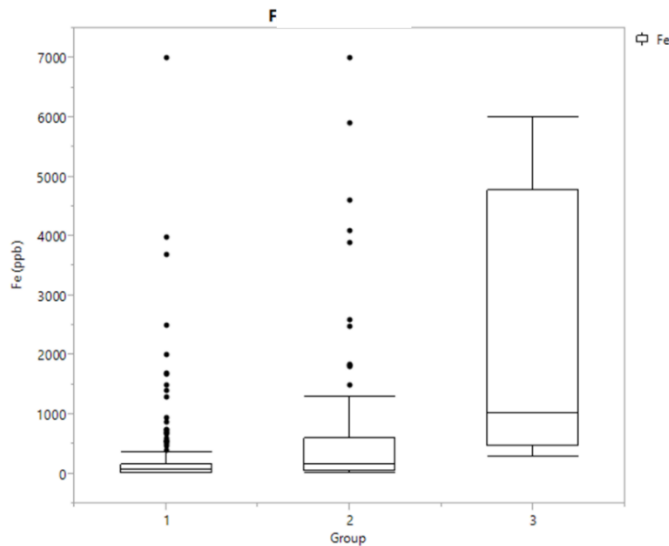


Figure 18: Boxplots of grouped samples and total Fe concentrations for wells within a selected portion of the study area. Data collected from STORET (2014). Group 1 (n=104) represents samples where total Mn concentrations were <50 ppb. Group 2 (n=59) represents samples where Mn concentrations were >50 ppb and <300 ppb. Group 3 (n=11) represents samples where total Mn concentrations were >300 ppb.

A third parameter assessed is pH. The stability of Mn oxides, such as the ore deposits from the James River-Roanoke River Manganese District, is sensitive to pH (see **Figure 2**). From a kinetics perspective, the dissolution rate of Mn-oxides increases with decreasing pH (Green, 2003; Chapman, 2013; Martin, 2003). However, it is also the case that the oxidation rate of Mn increases with increasing pH (Hem, 1972). Thus, the relationship between Mn oxides, soluble Mn species, and pH is complicated. In the study area, the highest Mn concentrations in groundwater occur at intermediate pH values (~6.5-8). Boxplots in **Figure 19** show that the median values of pH for each group increases with increasing Mn concentration (Group 3 > Group 2 > Group 1). Results of a Kruskal-Wallis test on these groups yield a p-value of 6×10^{-5} (at least two groups are statistically different from one another). When Wilcoxon signed rank tests are conducted on the different groups, the results show the pH values for Group 1 (Mn < 50 ppb) are statistically different than Group 2 and Group 3).

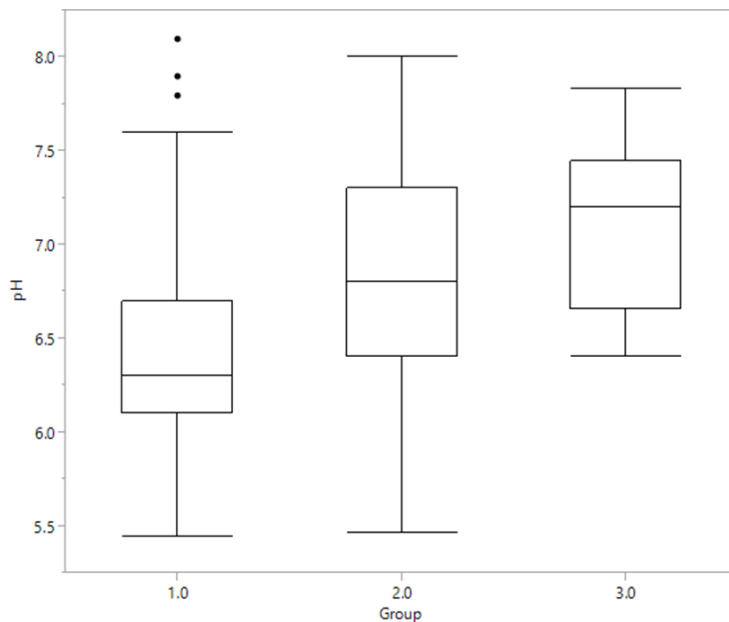


Figure 19: Boxplots of grouped samples and pH values for wells within a selected portion of the study area. Data collected from STORET (2014). Group 1 (n=102) represents samples where Mn concentrations were <50 ppb. Group 2 (n=55) represents

samples where Mn concentrations were >50 ppb and <300 ppb. Group 3 (n=9) represents samples where Mn concentrations were >300 ppb.

Potentiometric Surface Map of Study Area

Figure 20 shows a regional potentiometric map of the study area modeled from well data using ArcGIS. Groundwater flow patterns are complex because flow through fractured bedrock and saprolite is the dominant mechanism controlling direction, velocity, and quantity of groundwater flowing through the Blue Ridge and Piedmont crystalline aquifers (Chapman, 2013). Assuming groundwater flow is isotropic, the general flow direction of groundwater—shown with red arrows—in the southern portions of Bedford County and Campbell County as well as northern Pittsylvania County is toward the Roanoke River (presumed discharge zone for groundwater), which forms the southern border with Bedford County and Campbell County and the northern boundary of Pittsylvania County. The highest Mn concentrations (both total and filtered) occur near the Roanoke River which is a likely discharge zone for groundwater

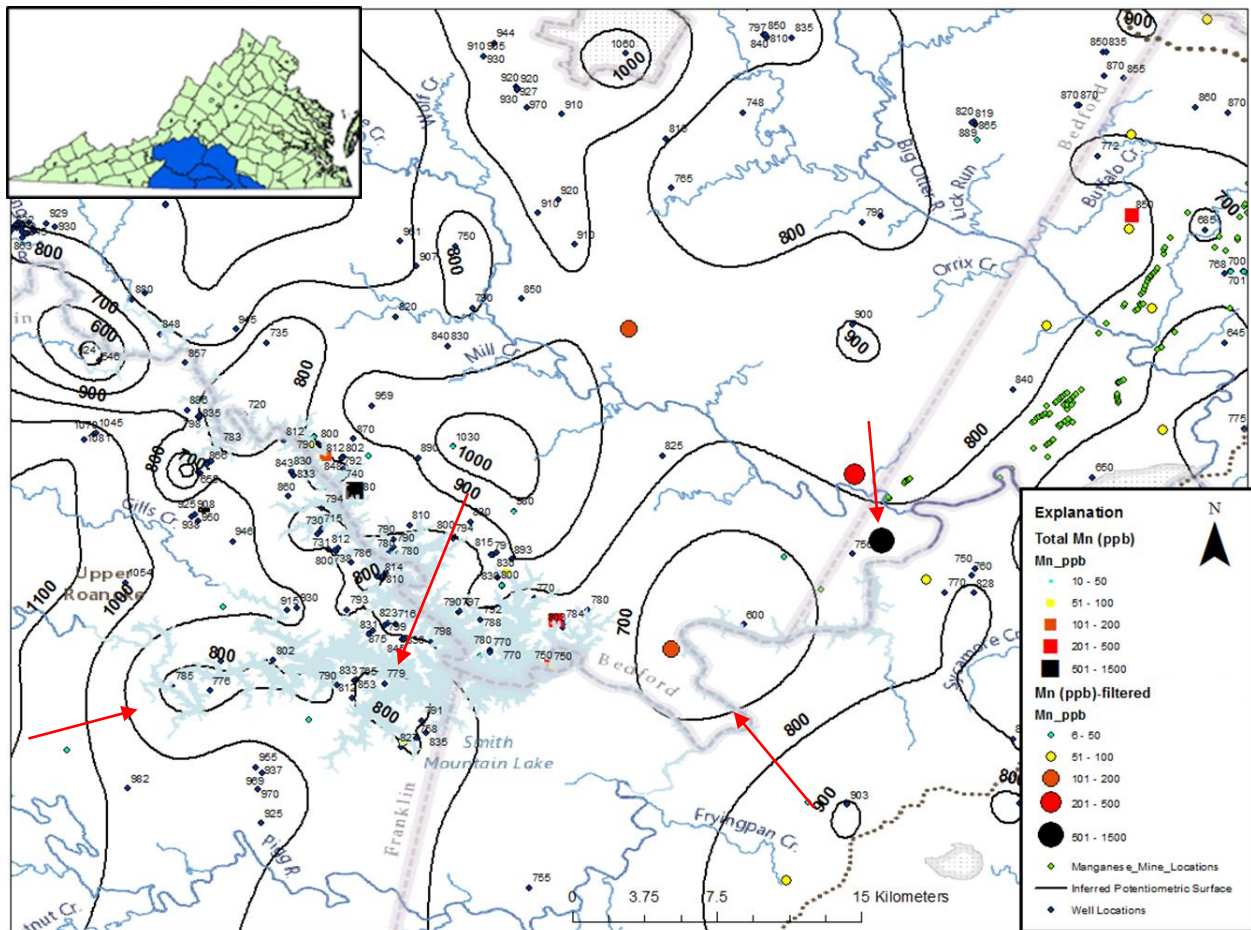


Figure 20: Regional potentiometric surface map of the crystalline aquifer in the study area. Surface was generated using well data and additional modeling in ArcGIS. Groundwater Mn data from NURE (filtered) and STORET (total). Potentiometric surface contours are in units of feet. Red arrows show inferred direction of groundwater flow from local recharge areas to the recharge area, the Roanoke River.

DISCUSSION

Origin of the James River-Roanoke River Manganese District ore deposits

Results from XRD, SEM, and ore chemical analysis suggest the ore deposits of the JRRRMD are supergene (formed at or near the Earth’s surface at low temperatures) in origin (Nicholson, 1992; Kim, 1984). XRD results show secondary Mn and Fe-oxide minerals (e.g. cryptomelane,

lithiophorite, goethite) that are commonly found in supergene ore deposits (Nicholson, 1992). Goethite (FeOOH) is not thermodynamically stable at temperatures that exceed 130 degrees Celsius (Schmaltz, 1959). This implies the fluids that formed the ore deposits of the JRRRMD never exceeded a temperature of 130 degrees Celsius. Further evidence of a supergene origin is provided by ore morphologies as observed using SEM. These morphologies, including fracture fillings by Mn and Fe-oxides, botryoidal Fe-oxides, botryoidal Mn-oxides and massive replacement of pre-existing material by Mn-oxides, are typical of supergene ore deposits (Kim, 1984). Lastly, bulk chemical analysis showed chemical associations between Mn and trace metals (e.g Ba and Co) that are also consistent with supergene ore deposits (Nicholson, 1992). By comparison, the Hutter Mine (see **Figure 6**) is a known hydrothermal deposit and contains an abundant array of Mn-bearing minerals formed at high temperatures. A few examples of these include manganosite (MnO), galaxite (MnAl_2O_4), and jacobsonite (MnFe_2O_4) (Beard, et al., 2002).

These interpretations are consistent with Espenshade (1954), who also proposed a supergene origin of the Mn-oxides of the JRRRMD. Espenshade's model of ore formation invokes dissolution of Mn from soluble mineral phases in the country rock by downward circulating groundwater. The model implies that the Mn-oxides were precipitated at depth as groundwater flowed downward through fractures and along planes of weakness (e.g. relict bedding planes) in weathered rock formations. This concept is problematic because it does not take into account how Mn-oxides form from a redox perspective. At shallow aquifer depths, DO in groundwater is replenished by recharge, resulting in oxidizing conditions under which Mn^{4+} is stable as insoluble Mn oxides. With increasing depth in aquifers, DO becomes more depleted as it is consumed by microbes and is not replenished by recharge. As a result, aquifers generally become more reducing with depth, favoring the soluble Mn^{2+} as the stable Mn species. Thus, in

typical aquifers, downward groundwater flow would not promote oxidation of Mn^{2+} to Mn^{4+} and subsequent precipitation of Mn oxides, as Espenshade's model assumes.

We propose an alternate model that like Espenshade, first invokes downward groundwater circulation. As groundwater flows downward through pore spaces and fractures, it can dissolve Mn from country rock through chemical weathering. During the diagenesis and subsequent metamorphism of sedimentary and igneous rocks, Mn^{2+} is the dominant oxidation state of Mn incorporated into mineral structures (McKenzie, 1980; Muller, 1971; Dromgoole & Walter, 1990) and is the most probable source of Mn released into solution by weathering reactions. At depth, as the aquifer becomes increasingly reducing, more Mn^{2+} is able to persist in solution. This reduced, Mn-bearing groundwater then upwells towards discharge zones where reduced groundwater containing Mn^{2+} can mix with shallow, oxic groundwater and promote the precipitation of Mn-oxides, likely mediated by bacteria. The alternate model described above is shown in **Figure 21**. The dashed line in **Figure 21** represents the redox boundary between alluvial sediments (alluvium) where oxic groundwater dominates and fractured saprolite and bedrock where reducing groundwater occurs. This redox interface is where shallow, oxic groundwater and deep, reducing groundwater can mix together, altering the redox chemistry to favor the precipitation of Mn-oxides in close proximity to streams.

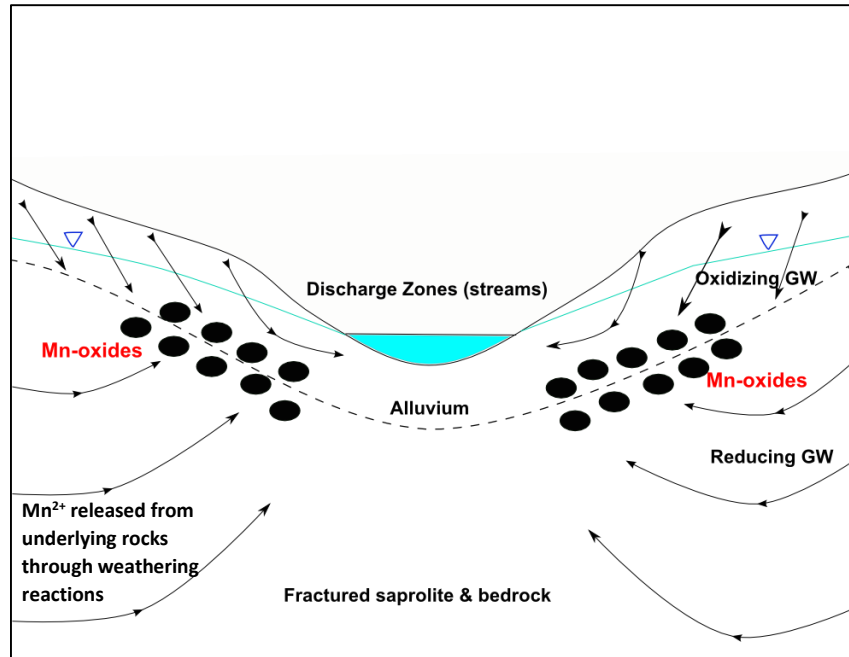


Figure 21: Conceptual alternate upwelling model for the formation of the ore deposits of the JRRRMD.

Evidence to support this upwelling model includes 1) spatial associations of ancient alluvial soils with Mn ores; 2) spatial associations of modern alluvial soils with Mn ores; and 3) support from the literature on similar interpretations of the origins of other Mn and Fe ores.

Spatial associations of ancient alluvial soils with Mn ore locations

Analysis of soil maps in the study area shows spatial associations between the location of known Mn mining localities, representing outcrop locations of Mn ore deposits, and ancient alluvial soils, which serve as relicts of previous discharge zones (streams) (see **Figure 21**). Statistical analysis of the elevations of alluvial soil deposits in the Piedmont Upland terrace deposits and locations of Mn mines show that the majority of mines occur within the elevation ranges of the Piedmont Upland terrace deposits (see **Figure 12**). Field observations show that most mining locations are located on hilltops well above the elevations of nearby streams. Together, these

results suggest that the majority of Mn ore deposits in the JRRRMD were likely formed in groundwater discharge zones in ancient stream valleys.

Why are the Piedmont Upland terrace deposits found at current day high elevations (ridges and hilltops)? The results gathered in this study, combined with results from other work, suggest that the topography of the study area (and the Piedmont in general) has been inverted throughout geologic time. Throughout the study area, alluvium is found at greater elevations than and often considerable distances from active streams (Henika, 2015). Alluvium is originally deposited in stream valleys (e.g. flood plain and terrace deposits). However, over time, terrace dissection and stream migration can result in a lowering of topography relative to relict alluvial deposits, resulting in stream valleys that later become ridges. Others have suggested that topographic inversion occurs in other regions of the Piedmont (Markewich et al., 1990) where differential weathering rates of geologic materials in this erosional terrain can promote such landscape evolution. The East Coast of the United States is, furthermore, considered a dynamic uplift zone which could promote such weathering processes (Rowley et al., 2013). Additionally, previous work by Prince et al. (2010) suggests that stream migration and capture also play a vital role in isolating relict terrace deposits (alluvial soils) at relatively higher elevations in both the Blue Ridge and Piedmont physiographic provinces.

Spatial associations of modern alluvial soils with Mn ore locations

Although the majority of Mn mines are spatially correlated with alluvium in the Piedmont Uplands, several mines do occur at lower elevations either within or proximally close to alluvium in modern stream valleys. The occurrence of Mn-oxides in modern alluvium and field observations of Mn-coated sediment in active streams near historic Mn mining locations suggests that the same hydrogeochemical processes that formed the JRRRMD ores in the past are still

occurring in the present day. An example of Mn-oxides forming in the present where observed in the field at a locality in Hurt, Virginia, located approximately 1 km south of the town of Altavista (see **Figure 22**). At this site, construction work has exhumed a mottled clay containing abundant Mn and Fe-oxides underlying a terrace deposit. These field observations of oxide minerals forming beneath a river terrace support both the theory that Mn-oxides such as those formed in the JRRRMD are continuing to be precipitated in the present day and that our conceptual model introduced earlier (see **Figure 21**) is plausible.



Figure 22: Field site in Hurt, VA displaying an example of modern Mn-oxide deposition. A) Aerial view of field site in Hurt, VA near the town of Altavista captured using Google Earth (Google, 2015). Location is designated with a yellow dot. Terrace deposits are shaded in blue. Soil data were obtained from the SSURGO database (Soil Survey Staff, 2014). B) Mottled clay underlying terrace deposits displaying abundant occurrences of both Mn and Fe-oxides. C) Blocks of marble within the Alligator Back Formation from which the mottled clay was derived.

Other examples of ore formation from upwelling

Examples of this upwelling model of ore formation are found in other regions. For example, in the Shenandoah Valley of Virginia, Hack (1965) associated the occurrence of secondary Mn-oxides derived from a dolomitic protore with overlying alluvial soil deposits. An additional

example of secondary oxides precipitating from upwelling reduced groundwater encountering oxic groundwater is described in Chan et al. (2001). Both Mn and Fe oxides were deposited as Mn and Fe was released from Jurassic sandstone and flowed upward to mix with shallow, oxygen-rich waters, causing the precipitation of Mn and Fe-oxides. In both Australia and Africa, upwelling groundwaters have also been responsible for the deposition of other redox-sensitive metal ore deposits, such as uranium and vanadium, precipitating within calcretes, hardened calcium-rich layers in certain soil profiles (Carlisle, 1983).

Figure 23 shows a conceptual model of the geomorphological evolution involved with topographic inversion as it relates to the proposed upwelling ore formation model. As section **A** of this model suggests, Mn-oxides were originally deposited by upward circulating groundwater that carried soluble Mn^{2+} from a reducing groundwater zone into an oxic groundwater zone which promoted the oxidation and subsequent precipitation of Mn-oxides. At some point after deposition, extensive weathering processes (e.g. stream migration, terrace dissection, preferential weathering) have caused the topography around the ore deposits in the Piedmont Uplands to become lowered. These weathering processes effectively cause topographic inversion, isolating the Mn-oxides of the JRRRMD in the Piedmont Uplands on hilltops and ridges where stream valleys were once present (see **B** in **Figure 23**).

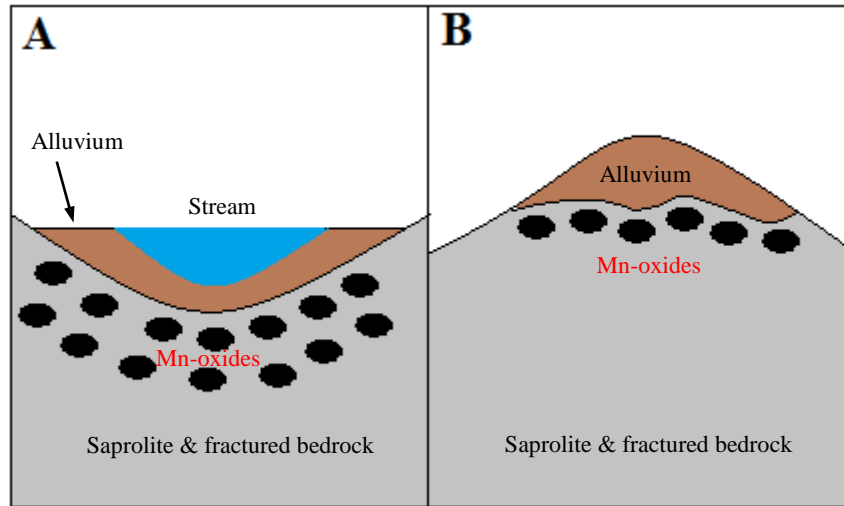


Figure 23: Conceptual diagram of topographic inversion in relation to the formation and occurrences of Mn-oxides in the Piedmont Uplands within the JRRRMD. A) Original formation model of ore deposits in stream valleys (discharge zones) as proposed in this study; possibly how ores are being deposited in the present day. B) Inverted topography caused by extensive weathering, causing ancient stream valleys to become ridges.

Geologic sources and controls on Mn concentrations in groundwater

The widespread regional distribution of Mn in groundwater within the Roanoke River watershed, across many land use types including forested, agricultural, residential and industrial, strongly suggests that the dominant source of Mn to groundwater across the watershed is naturally-occurring and not related to human activities. The spatial distribution of Mn concentrations was statistically evaluated by both county and geologic formation using boxplots. Across the watershed, Campbell County was found to contain the greatest variance of elevated total Mn concentrations in the upper 25th percentile (~25% exceeding 50 ppb and ~5% exceeding 300 ppb). With respect to geologic units, the Candler Formation, Alligator Back Formation, and Bassett Formation have the highest median values for total Mn in groundwater among the studied formations.

Analysis of the available chemical data for the area of interest in the Roanoke River watershed suggests that there is not one single geologic source that is responsible for elevated Mn concentrations in groundwater. Because the majority of the JRRRMD ore deposits are located at high elevations in the Piedmont Uplands, they are isolated from active groundwater systems, making the ores unlikely to contribute Mn to groundwater unless they persist at a great enough depth to interact with groundwater. Instead, the release of Mn into groundwater is most likely influenced by more diffuse weathering of Mn-bearing rocks in the watershed. For example, the sediments and volcanic materials in the study area—the Alligator Back Formation in particular—were deposited in a rift basin. These tectonic settings are associated with both Mn and Fe formations resulting from metal-rich fluids being exhaled from oceanic crustal venting (Buhn and Stanistreet, 1993) which could become entrained within sediments during the diagenesis of the protoliths for the metasedimentary rocks within the Alligator Back Formation. The correlation with Ca and bicarbonate may be indicative of the dissolution of carbonate rocks or carbonate-rich lithologies (e.g. marble, calcareous quartzite, calcareous schist) as a likely source of Mn. In addition to carbonate rocks, Ca may also be introduced into solution from minerals within metavolcanic rocks in the study area (e.g. amphiboles) as well as other Ca-bearing minerals.

The inverse relationship between Mn and DO in groundwater of the Piedmont and Blue Ridge crystalline aquifers shows that higher Mn concentrations are measured in groundwater with low DO concentrations. The reducing conditions that are widespread in these crystalline aquifers allow for soluble Mn (Mn^{2+}) to persist in groundwater. The association of elevated Mn concentrations with the terminus of groundwater flowpath inferred by potentiometric contours in the watershed suggests that once soluble Mn is released to groundwater, it can be transported

along the flowpath to the regional discharge zone, the Roanoke River. Because DO becomes depleted along flowpaths due to microbial consumption and lack of replenishment from recharge, as groundwater flows for extended periods of time (years, decades, centuries), it is reasonable to assume that reducing conditions will develop with depth, distance and time in an aquifer, promoting elevated Mn concentrations in groundwater.

CONCLUSIONS

The Mn-oxide minerals of the JRRRMD contain secondary minerals and morphologies which are consistent with deposition near the Earth's surface by circulating groundwater. The redox environment necessary for the formation of Mn-oxides suggests the ore deposits were formed from upwelling reduced groundwater—carrying soluble Mn^{2+} dissolved from the country rock—that mixes with oxic groundwater in ancient and modern discharge zones, promoting the oxidation of Mn^{2+} to insoluble Mn^{4+} and the precipitation of Mn-oxides. This interpretation is supported by the spatial associations between the locations of known Mn ore deposits and both relict and modern alluvial soil deposits, presumed to represent discharge zones. The presence of relict alluvial deposits on hilltops and ridges suggests that the topography in the JRRRMD has been inverted since the deposition of Mn ores in the Piedmont Upland terraces. This weathering process may explain why the majority of the ore deposits in the JRRRMD are located at elevations above modern streams and rivers.

Analysis of groundwater chemistry data in the Roanoke River watershed shows chemical associations between Mn, Ca, and HCO_3^- . These associations suggest that Mn-bearing carbonate rocks and carbonate-rich lithologies, likely from the Candler and Alligator Back Formations, are

likely sources of Mn to groundwater in the Roanoke River watershed. Groundwater chemistry analysis also shows that Mn concentrations are 1) inversely correlated with DO concentrations and 2) generally increase with distance along the flowpath. These patterns suggest that after Mn is released to groundwater through chemical weathering of Mn-bearing rocks, it persists in groundwater under reducing conditions and can be transported along flowpaths to the modern regional discharge area, the Roanoke River.

It is interesting to note that the interpreted mechanism of Mn release to and transport within groundwater in the Roanoke River watershed is the same interpreted mechanism of formation of the JRRRMD ores: 1) release of Mn to groundwater through chemical weathering of Mn-bearing rocks, 2) transport of soluble Mn under reducing conditions along the groundwater flowpath, and 3) discharge of the Mn-bearing groundwater to streams, allowing for mixing with oxygen and precipitation of Mn oxides. Field observations of Mn-staining on rocks and sediments near and within the Roanoke River suggest that Mn oxides are currently precipitating as groundwater discharges to the river; these oxides may in the future, become concentrated enough to be considered ores.

REFERENCES

- Beard, J. S., R.J. Tracy, and W.S. Henika, 2002, "Minerals of the Hutter Mine: A new manganese-barium mineral locality in northern Pittsylvania County, Virginia." *Rocks and Minerals*: 77(5), p. 320-325.
- Berquist, C.R., 2003, Digital representation of the 1993 geologic map of Virginia-expanded explanation. Charlottesville, VA, Virginia Department of Mines, Minerals, and Energy.
- Bethke, C.M., 2014, The Geochemist's Workbench, Release 10.0: A User's Guide to Rxn, Act2, Tact, React, and Gtplot (University of Illinois, 2002), pp. 224.
- Bouchard M.F., Sauve S., Barbeau B., Legrand M., Brodeur M.E., and Bouffard T, et al., 2011, Intellectual impairment in school-age children exposed to Manganese from drinking water. *Environ Health Perspectives*;119, p. 138–43.
- Bouchard M.F., Laforest F., Vandelac L., Bellinger D., Mergler D., 2007, Hair manganese and hyperactive behaviors: pilot study of school-age children exposed through tap water. *Environ Health Perspectives*: 115, p. 122–127.
- Brown, W.R., 1958, Geology and mineral resources of the Lynchburg Quadrangle, Virginia. Charlottesville, VA, Department of Conservation and Development. p. 71-74.
- Buhn B. and I.G. Stanistreet, 1993, Insight into the enigma of Neoproterozoic manganese and iron formations from the perspective of supercontinental break-up and glaciation. In: K. Nicholson, J.R. Hein, B. Bühn and S. Dasgupta (Editors), *Manganese Mineralisation: Geochemistry and mineralogy of Terrestrial and Marine deposits*. Special Publication of the Geological Society, 119, 81-90.
- Bullard, C.F., 1977, *Soil Survey of Campbell County and City of Lynchburg, Virginia*. Washington, D.C.: National Cooperative Soil Survey.
- Carlisle, D., 1983, Concentration of uranium and vanadium in calcretes and gypcretes. *Geological Society, London, Special Publications*, 11(1), p. 185-195.
- Chan, M. A., Parry, W. T., Petersen, E. U., & Hall, C. M., 2001, $^{40}\text{Ar}/^{39}\text{Ar}$ age and chemistry of manganese mineralization in the Moab and Lisbon fault systems, southeastern Utah. *Geology*, 29(4), 331-334.
- Chesapeake Bay Foundation, 2005, October. *Roanoke River fact sheet*. Retrieved from <http://www.cbf.org/Document.Doc?id=239>.
- Commonwealth of Virginia Department of Environmental Quality, 2014, Triennial review: Water quality standards. Richmond, VA. VADEQ.
- Conley, J. F., 1978, Geology of the Piedmont of Virginia – interpretations and problems, in *Contributions to Virginia geology - III*, Virginia Division of Mineral Resources Publication 7, p. 115-149.

- Dicken, Connie L., Nicholson, Suzanne W., Horton, John D., Kinney, Scott A., Gunther, Gregory, Foose, Michael P., and Mueller, Julia A.L., 2005, Integrated Geologic Map Databases for the United States: Delaware, Maryland, New York, Pennsylvania, and Virginia: U.S. Geological Survey Open-File Report 2005-1325, U.S. Geological Survey, Reston, VA.
- Diem, D., and W. Stumm, 1984, Is dissolved Mn^{2+} being oxidized by O_2 in absence of Mn-bacteria or surface catalysts? *Geochimica et Cosmochimica Acta*: 48, p. 1571-1573.
- Dromgoole, E. L., & Walter, L. M., 1990, Iron and manganese incorporation into calcite: Effects of growth kinetics, temperature and solution chemistry. *Chemical Geology*, 81(4), 311-336.
- Edmundson, R. S., 1938, Barite deposits of Virginia. Charlottesville, VA, Virginia Geological Survey.
- Environmental Protection Agency, 2004, Drinking water health advisory for manganese. Washington, D.C., U.S. Environmental Protection Agency Office of Water, Health and Ecological Criteria Division.
- Espenshade, G., 1954, Geology and mineral deposits of the James River-Roanoke River manganese district, Virginia. Washington, D.C., United States Government Printing Office. p. 1-155.
- ESRI, 2011. ArcGIS Desktop: Release 10.2. Redlands, CA: Environmental Systems Research Institute.
- Gilkes, R. J. and R. M. McKenzie, 1988, Geochemistry and mineralogy of manganese in soils, in R. D. Ghraham, Robert J. Hannam, Nicholas C. Uren, ed., *Manganese in soils and plants*, v. 33, Kluwer Academic Publishers, p. 23-35.
- Gooch, E. O., 1954, Iron in Virginia. Charlottesville, VA, Department of Conservation and Development.
- Gooch, E. O., 1955, Current manganese operations in Virginia: *Virginia Minerals*, v. 1, p. 1-6.
- Green, C.H., D.M. Heil, G.E. Cardon, G.L. Butters, E.F. Kelly. 2003. Solubilization of manganese and trace metals in soils affected by acid mine runoff. *Journal of Environmental Quality*. 3:1323–1334.
- Hack, J. T., 1965, Geomorphology of the Shenandoah Valley, Virginia and West Virginia and origin of the residual ore deposits. US Government Printing Office.
- Hem, J.D., 1972. Chemical factors that influence the availability of iron and manganese in aqueous systems. *Geological Society of America Bulletin* 83, 443-450.
- Henika, W. S., 1992, Stratigraphy of the Eastern Blue Ridge sequence in the Roanoke 30' x 60' quadrangle, Virginia [abs.]: *Geological Society of America Abstract with Programs*, v. 24, n. 2, p. 21.

- Henika, W.S., 1997, Virginia Division of Mineral Resources Publication 148, Geologic map of the Roanoke 30 x 60 minute quadrangle.
- Henry, D. K., J. R. Craig, and M. C. Gilbert, 1979, Ore mineralogy of the Great Gossan Lead, Virginia. *Economic Geology* 74:645–56.
- JMP®, Version 11. SAS Institute Inc., Cary, NC, 1989-2007
- Khan, K., G. A. Wasserman, X. Liu, E. Ahmed, F. Parvez, V. Slavkovich, D. Levy, J. Mey, A. van Geen, J.H. Graziano, P. Factor-Litvak , 2012, Manganese exposure from drinking water and children's academic achievement: *NeuroToxicology*, 33(1), p. 91-97.
- Kim, S. J. (1984). Syngenetic and epigenetic textures of manganese oxide ores in the supergene weathering zone. *Syngeneses and Epigenesis in the Formation of Mineral Deposits*. A. Wauschkuhn, C. Kluth and R. Zimmermann, Springer Berlin Heidelberg. p 12-17.
- Liu, L., and Lowell, R. P., 2009, Models of hydrothermal heat output from a convecting, crystallizing, replenished magma chamber beneath an oceanic spreading center. *Journal of Geophysical Research: Solid Earth (1978–2012)*, 114(B2).
- Martin, S. T., 2005, Precipitation and dissolution of iron and manganese oxides. In: V. Grassian, editor, *Environmental Catalysis*. Boca Raton, FL: Taylor & Francis Group, LLC. p 61-78.
- Markewich, H. W., Pavich, M. J., & Buell, G. R., 1990, Contrasting soils and landscapes of the Piedmont and Coastal Plain, eastern United States. *Geomorphology*, 3(3), 417-447.
- McKenzie R. M., 1980, The manganese oxides in soils. In: Varentsov I. M. & Grasselly G. eds. *Geology and Geochemistry of Manganese, Volume I: Mineralogy, Geochemistry, Methods*, pp. 259–269. Schweizerbart'sche-Verlagsbuchhandlung, Stuttgart.
- Muller, G., 1971, *Contributions to mineralogy and petrology: Chemistry and genesis of garnets in metamorphic rocks* Springer. doi:10.1007/BF00399650
- Nadaska, G., Lesny, J., & Michalik, I., 2010, Environmental aspect of manganese chemistry. *Hungarian Journal of Sciences*, ENV-100702-A, 1–16.
- Nelms, D. L. and George E. Harlow, Jr., 2003, Aquifer Susceptibility in Virginia: Data on Chemical and Isotopic Composition, Recharge Temperature, and Apparent Age of Water from Wells and Springs, 1998-2000. Richmond, VA, United States Geological Survey.
- Nicholson, K., 1992. Contrasting mineralogical–geochemical signatures of manganese oxides: guides to metallogenesis. *Econ. Geol.* 87, 1253–1264.
- Prince, P.S., J.A. Spotila, and W.S. Henika, 2010, New physical evidence of the role of stream capture in active retreat of the Blue Ridge escarpment, southern Appalachians. *Geomorphology*.: 123, p. 305-319.

- R Core Team (2012). R: A language and environment for statistical computing. R Foundation for Statistical Computing, Vienna, Austria. ISBN 3-900051-07-0, URL <http://www.R-project.org/>.
- Reimann, C., P. Filzmoser, R.G. Garrett, R.Dutter, 2008, *Statistical Data Analysis Explained: Applied Environmental Statistics with R*. Chinchester, West Sussex: John Wiley & Sons Ltd.
- Rowley, D. B., Forte, A. M., Moucha, R., Mitrovica, J. X., Simmons, N. A., and Grand, S. P. ,2013, Dynamic topography change of the eastern United States since 3 million years ago. *Science*, 340 (6140), p. 1560-1563.
- Schumann, W.,1993, Handbook of rocks, minerals, and gemstones. New York, Houghton Mifflon Company. p. 106-109.
- Severs, M., J. Beard, L. Fedele, J.M. Hanchar, S.R. Mutchler, R.J. Bodnar, 2009, Partitioning behavior of trace elements between dacitic melt and plagioclase, orthopyroxene, and clinopyroxene based on laser ablation ICPMS analysis of silicate melt inclusions: *Geochimica et Cosmochimica Acta*: 73, p. 2123-2141.
- Soil Survey Staff. Gridded Soil Survey Geographic (gSSURGO) Database for *Virginia*. United States Department of Agriculture, Natural Resources Conservation Service. Available online at <https://gdg.sc.egov.usda.gov/>. (FY2014 official release).
- U.S. Department of Agriculture, 2014, Geospatial Data Gateway. Retrieved November 2014, from <https://gdg.sc.egov.usda.gov/>
- U.S. Environmental Protection Agency, 2014, STORET. USEPA. <http://www.epa.gov/storet/> (accessed Sept. 2014).
- U.S. Geological Survey, 2003, Digital Representation of the 1993 Geologic Map of Virginia", CD ROM (ISO-9660) contains image file, expanded explanation in pdf, and ESRI shapefiles, viewing software not included. This is a digital version of "Geologic Map of Virginia" published in 1993. Available from: <https://www.dmme.virginia.gov/commerce/>.
- U.S. Geological Survey, 2004, National Uranium Resource Evaluation (NURE) Hydrogeochemical and Stream Sediment Reconnaissance data: U.S. Geological Survey, Denver, CO.
- Violante, A., V. Cozzolino, L. Perelomov, A.G. Caporale, and M. Pigna., 2010, Mobility and bioavailability of heavy metals and metalloids in soil environments. *Journal of Plant Nutrition and Soil Science*: 10, p. 268–292.
- Williams, P.A., 1990, *Oxide Zone Geochemistry*. Chinchester, West Sussex: Ellis Horwood Limited.

APPENDIX A

Groundwater data from both National Uranium Resource Evaluation (NURE) and USGS (Chapman, 2013, Nelms & Harlow) used to create Figure 1 Mn data reflect filtered samples.

County/City	Latitude	Longitude	pH	Mn	Source
Appomattox	37.27	-78.7067	6.2	50.00	Chapman (2013)
Appomattox	37.2384	-78.781	6.2	6.00	Chapman (2013)
Appomattox	37.3329	-78.8317	7.7	60.00	Chapman (2013)
Appomattox	37.2215	-78.8315	6.2	11.00	Chapman (2013)
Appomattox	37.285	-78.7744	5.9	9.00	Chapman (2013)
Bedford	37.44417	-79.6092	6.3	20.00	Chapman (2013)
Bedford	37.4196	-79.4207	6.5	70.00	Nelms & Harlow (2003)
Bedford	37.4965	-79.4443	5.7	58.00	Nelms & Harlow (2003)
Bedford	37.3734	-79.7504	7.7	49.00	Nelms & Harlow (2003)
Bedford	37.2725	-79.8168	5.4	47.00	Nelms & Harlow (2003)
Bedford	37.2725	-79.8168	5.4	47.00	Nelms & Harlow (2003)
Bedford	37.4179	-79.3526	8.6	43.00	Nelms & Harlow (2003)
Bedford	37.2775	-79.5886	6.1	30.00	NURE
Bedford	37.2779	-79.7146	6.8	21.00	NURE
Bedford	37.2801	-79.5194	7.3	17.00	NURE
Bedford	37.2854	-79.6566	5.6	16.00	NURE
Bedford	37.3701	-79.5907	6.5	14.00	NURE
Bedford	37.3825	-79.3546	6.9	14.00	NURE
Bedford	37.3257	-79.7603	7	14.00	NURE
Bedford	37.4213	-79.5196	6.8	12.00	NURE
Bedford	37.1951	-79.6921	6.7	12.00	NURE
Bedford	37.2429	-79.7011	6.5	11.00	NURE
Bedford	37.3291	-79.5804	5.9	11.00	NURE
Bedford	37.2406	-79.6385	5.3	11.00	NURE
Bedford	37.4656	-79.4075	6.2	10.00	NURE
Bedford	37.4259	-79.4764	6.5	9.00	NURE
Bedford	37.2344	-79.5831	5.8	9.00	NURE
Bedford	37.4637	-79.359	7.4	9.00	NURE
Bedford	37.2344	-79.7535	6.8	8.00	NURE
Bedford	37.2366	-79.8209	6.1	6.00	NURE
Bedford	37.3137	-79.7987	5.5	5.00	NURE
Bedford	37.2709	-79.7648	5.8	4.00	NURE
Bedford	37.3251	-79.7073	5.5	4.00	NURE
Bedford	37.3729	-79.4722	6.7	4.00	NURE
Bedford	37.3151	-79.515	6.4	3.00	NURE
Bedford	37.4621	-79.5211	6.8	3.00	NURE
Bedford	37.4848	-79.5645	6.8	1.00	NURE
Bedford	37.12639	-79.64361	6.1	1300.00	Nelms & Harlow (2003)

County/City	Latitude	Longitude	pH	Mn	Source
Bedford	37.1337	-79.4104	6.8	454.00	NURE
Bedford	37.1376	-79.5278	8.2	265.00	NURE
Bedford	37.0524	-79.496	7.4	195.00	NURE
Bedford	37.2019	-79.5159	6.6	179.00	NURE
Bedford	37.1885	-79.4709	6.3	51.00	NURE
Bedford	37.1422	-79.6374	6.6	40.00	NURE
Bedford	37.1798	-79.6529	6.8	38.00	NURE
Bedford	37.0951	-79.4436	5.9	18.00	NURE
Bedford	37.3268	-79.3042	6.1	18.00	NURE
Bedford	37.2347	-79.4652	6.9	18.00	NURE
Bedford	37.2431	-79.4097	6.2	16.00	NURE
Bedford	37.2843	-79.4736	6.5	15.00	NURE
Bedford	37.0491	-79.585	6.9	11.00	NURE
Bedford	37.2898	-79.3531	7.5	8.00	NURE
Bedford	37.1844	-79.4156	6	8.00	NURE
Bedford	37.1798	-79.6529	6	3.00	NURE
Bedford	37.2469	-79.345	6.2	2.00	NURE
Bedford	37.1962	-79.5808	6.6	2.00	NURE
Bedford	37.3375	-79.3969	6.4	1.00	NURE
Bedford	37.3769	-79.7026	7.4	149.00	NURE
Brunswick	36.5588	-77.8724	6.1	118.00	NURE
Brunswick	36.5998	-78.0379	6.3	37.80	NURE
Brunswick	36.6041	-78.003	6.3	16.30	NURE
Brunswick	36.5679	-77.9425	6.8	13.00	NURE
Brunswick	36.6016	-77.882	5.7	12.00	NURE
Brunswick	36.5625	-77.813	6	9.00	NURE
Brunswick	36.5535	-78.044	7.8	3.50	NURE
Campbell	37.0646	-78.9855	6.2	81.00	NURE
Campbell	37.1574	-78.8652	6	92.00	NURE
Campbell	37.0643	-78.927	6.2	74.00	NURE
Campbell	37.2512	-78.9248	6.9	118.00	NURE
Campbell	37.1057	-79.039	6.9	87.00	NURE
Campbell	37.1645	-78.9792	5.9	83.00	NURE
Campbell	37.1029	-79.3976	6.4	1406.00	NURE
Campbell	37.3884	-79.0475	6.2	102.00	NURE
Campbell	37.2031	-79.321	6.3	100.00	NURE
Campbell	37.3001	-79.1637	6.1	96.00	NURE
Campbell	37.2925	-79.2811	6.3	94.00	NURE
Campbell	37.3009	-79.2079	5.8	86.00	NURE
Campbell	37.2112	-79.2718	6.7	81.00	NURE
Campbell	37.2482	-79.2824	6.7	79.00	NURE
Campbell	37.3461	-79.246	6	70.00	NURE

County/City	Latitude	Longitude	pH	Mn	Source
Campbell	37.1635	-79.0544	7	1.00	NURE
Campbell	37.0717	-79.0455	6.6	140.00	NURE
Campbell	37.1604	-79.1651	7	117.00	NURE
Campbell	37.2014	-79.15	6.3	115.00	NURE
Campbell	37.1113	-79.0997	6.2	112.00	NURE
Campbell	37.261	-78.991	6.5	107.00	NURE
Campbell	37.2496	-79.1664	6.6	101.00	NURE
Campbell	37.2535	-79.0988	6.6	101.00	NURE
Campbell	37.2053	-79.2164	5.8	100.00	NURE
Campbell	37.2002	-79.088	6.5	96.00	NURE
Campbell	37.1577	-79.0373	6.2	92.00	NURE
Campbell	37.2998	-79.0956	5.7	87.00	NURE
Campbell	37.2986	-78.9892	6	85.00	NURE
Campbell	37.2517	-79.0463	6.6	85.00	NURE
Campbell	37.207	-79.0455	6.6	85.00	NURE
Campbell	37.1082	-78.9197	6	84.00	NURE
Campbell	37.1501	-79.1011	6.4	81.00	NURE
Campbell	37.1153	-79.1677	6.5	79.00	NURE
Campbell	37.1604	-79.226	6	79.00	NURE
Campbell	37.1545	-79.2665	5.9	70.00	NURE
Campbell	37.2953	-79.0468	6.3	68.00	NURE
Campbell	37.2077	-78.9267	7.4	100.00	NURE
Campbell	37.1606	-78.9332	6	99.00	NURE
Campbell	37.2028	-78.885	6.7	94.00	NURE
Campbell	37.1047	-78.9843	6.3	82.00	NURE
Campbell	37.2482	-79.2824	6.7	79.00	NURE
Campbell	37.2424	-78.871	6.3	8.00	NURE
Charlotte	37.02	-78.6122	7.5	60.00	NURE
Charlotte	36.9789	-78.6756	7.4	22.80	NURE
Charlotte	37.1119	-78.5047	6.8	17.00	NURE
Charlotte	37.05389	-78.489722	6.1	26.30	NURE
Charlotte	36.9264	-78.5071	8.1	172.30	NURE
Charlotte	36.9277	-78.5681	7.6	61.90	NURE
Charlotte	36.8881	-78.5624	7.9	57.60	NURE
Charlotte	36.8359	-78.5637	7.6	38.30	NURE
Charlotte	37.0206	-78.5047	9.2	34.00	NURE
Charlotte	36.9274	-78.6266	7.6	28.70	NURE
Charlotte	36.8797	-78.6321	7.5	24.30	NURE
Charlotte	36.9753	-78.5142	8.2	17.20	NURE
Charlotte	36.7445	-78.637	7.3	16.80	NURE
Charlotte	37.03361	-78.697222	6.8	133.00	NURE
Charlotte	37.07389	-78.843611	5.9	0.28	NURE

County/City	Latitude	Longitude	pH	Mn	Source
Charlotte	37.05083	-78.640556	5.2	7.00	NURE
Charlotte	37.05325	-78.650556	5.8	1.00	NURE
Charlotte	37.0661	-78.7385	7.4	68.00	NURE
Charlotte	37.0726	-78.79	7.4	55.00	NURE
Charlotte	37.1168	-78.5611	7.6	49.00	NURE
Charlotte	37.071	-78.8584	7.2	48.00	NURE
Charlotte	37.1098	-78.8027	6.8	39.00	NURE
Charlotte	37.2053	-78.7456	6.4	33.00	NURE
Charlotte	37.1121	-78.6825	7.4	27.00	NURE
Charlotte	37.0673	-78.6865	7.4	25.00	NURE
Charlotte	37.1209	-78.8608	7.7	25.00	NURE
Charlotte	37.0233	-78.8535	7.4	17.00	NURE
Charlotte	37.2168	-78.779	6	14.00	NURE
Charlotte	37.068	-78.6274	5.9	11.00	NURE
Charlotte	37.0223	-78.7414	6.9	10.00	NURE
Charlotte	37.1642	-78.7936	5.4	5.00	NURE
Floyd	37.04694	-80.202222	5.1	33.00	NURE
Floyd	37.0962	-80.2153	6.3	18.00	NURE
Floyd	37.0939	-80.1434	6.2	16.00	NURE
Floyd	37.0438	-80.2634	6.1	14.00	NURE
Franklin	37.1536	-79.8899	5.8	51.00	NURE
Franklin	37.1288	-79.9598	6.2	32.00	NURE
Franklin	37.0696	-80.0184	6.2	11.00	NURE
Franklin	37.1789	-79.7803	6.3	10.00	NURE
Franklin	37.2115	-79.8455	5.9	9.00	NURE
Franklin	36.92911	-80.001364	6.4	195.00	NURE
Franklin	36.991	-79.6634	7.4	208.20	NURE
Franklin	37.0721	-79.8276	7.2	160.00	NURE
Franklin	37.0751	-79.7894	6.8	136.00	NURE
Franklin	36.9716	-79.8804	7.3	98.30	NURE
Franklin	37.1216	-79.6578	6.6	95.00	NURE
Franklin	37.0092	-79.6214	6.9	81.00	NURE
Franklin	36.9966	-79.8272	6.5	80.70	NURE
Franklin	36.9949	-79.7155	6.7	71.70	NURE
Franklin	36.972	-79.9569	5.7	46.40	NURE
Franklin	37.0195	-79.6651	6.2	30.00	NURE
Franklin	37.0052	-79.7783	6.6	29.00	NURE
Franklin	37.0719	-79.7051	6.6	16.00	NURE
Franklin	36.888	-79.9427	6.3	15.60	NURE
Franklin	37.0681	-79.8725	6.1	15.00	NURE
Franklin	37.16	-79.7193	6.7	14.00	NURE
Franklin	36.945	-79.9476	7.2	12.90	NURE

County/City	Latitude	Longitude	pH	Mn	Source
Franklin	36.8465	-79.8992	6.7	11.80	NURE
Franklin	36.8446	-79.9503	6.5	9.90	NURE
Franklin	37.0245	-79.9386	5.8	9.00	NURE
Franklin	36.9332	-79.8941	6.2	7.40	NURE
Franklin	37.0192	-79.8382	6.5	7.00	NURE
Franklin	37.0728	-79.9489	7.2	2.00	NURE
Franklin	36.8016	-79.6598	6.4	61.00	NURE
Franklin	36.9007	-79.6517	6.4	41.30	NURE
Franklin	36.903	-79.7071	6.2	6.90	NURE
Franklin	36.8036	-79.8428	6.3	6.10	NURE
Halifax	37.029	-79.03	5.8	4.00	NURE
Halifax	36.7055	-78.744	7	220.10	NURE
Halifax	36.5782	-78.742	7.1	192.30	NURE
Halifax	36.7037	-78.6874	6.7	44.20	NURE
Halifax	36.8207	-78.71	6.1	38.90	NURE
Halifax	36.6712	-78.7983	6.8	36.00	NURE
Halifax	36.7686	-78.7051	7.2	27.10	NURE
Halifax	36.5696	-78.8537	7.4	23.40	NURE
Halifax	36.7168	-78.7954	7.5	21.60	NURE
Halifax	36.6208	-78.739	7.1	14.60	NURE
Halifax	36.8515	-78.6852	6.6	1.80	NURE
Halifax	36.82756	-79.0926111	5.9	0.65	NURE
Halifax	36.67531	-78.8474444	6.4	0.20	NURE
Halifax	36.82569	-78.967	6.2	0.17	NURE
Halifax	36.8275	-79.0925	5.9	0.65	NURE
Halifax	36.75306	-78.149722	5.8	0.33	NURE
Halifax	36.82556	-78.966944	6.2	0.17	NURE
Halifax	36.944	-79.024	6.7	164.90	NURE
Halifax	36.7945	-78.782	6.8	115.70	NURE
Halifax	36.6232	-78.918	6.8	88.40	NURE
Halifax	36.7175	-79.0832	6.7	81.00	NURE
Halifax	36.5788	-79.0932	6.6	70.50	NURE
Halifax	36.7179	-78.8584	7.2	60.80	NURE
Halifax	36.7578	-79.036	6	58.90	NURE
Halifax	36.8515	-78.7994	5.9	51.60	NURE
Halifax	36.7816	-78.8719	7.1	46.40	NURE
Halifax	36.7227	-79.0354	7	44.10	NURE
Halifax	36.6766	-79.1442	6.4	42.20	NURE
Halifax	36.6703	-78.9671	6.5	39.80	NURE
Halifax	36.8982	-78.756	6.4	39.20	NURE
Halifax	36.9692	-78.7522	6.6	35.50	NURE
Halifax	36.946	-79.0776	6.8	29.90	NURE

County/City	Latitude	Longitude	pH	Mn	Source
Halifax	36.8067	-78.9106	6.1	29.10	NURE
Halifax	36.8929	-78.7947	7.2	28.70	NURE
Halifax	36.8603	-78.8392	6.3	28.50	NURE
Halifax	36.8979	-78.9057	6.6	28.50	NURE
Halifax	36.6621	-78.9137	7	27.40	NURE
Halifax	36.7626	-78.9481	6.2	25.70	NURE
Halifax	36.8058	-79.0684	6.4	24.90	NURE
Halifax	36.716	-78.9658	6.3	18.90	NURE
Halifax	36.7547	-79.1387	6.8	18.90	NURE
Halifax	36.942	-78.8077	6.4	18.80	NURE
Halifax	36.9479	-78.862	6.2	14.80	NURE
Halifax	36.9055	-79.0879	6.2	12.50	NURE
Halifax	36.8528	-78.9081	6.1	11.50	NURE
Halifax	36.5789	-78.9658	6.4	11.40	NURE
Halifax	36.9487	-78.9658	6.2	10.50	NURE
Halifax	37.039	-78.9765	6.4	9.00	NURE
Halifax	36.5784	-78.9168	6.4	8.90	NURE
Halifax	36.6651	-78.864	5.8	8.80	NURE
Halifax	36.847	-79.0866	6.4	8.60	NURE
Halifax	36.9862	-78.9593	5.4	8.10	NURE
Halifax	36.9896	-79.0792	6.8	6.60	NURE
Halifax	36.9962	-78.9206	5.2	6.30	NURE
Halifax	36.9048	-79.0184	6.1	4.30	NURE
Halifax	36.5697	-79.1407	6.5	3.70	NURE
Halifax	36.8522	-79.0278	6.8	3.20	NURE
Halifax	36.8081	-79.0235	6	3.10	NURE
Halifax	36.8086	-79.1434	6.9	2.90	NURE
Halifax	36.7238	-79.1507	6.8	0.40	NURE
Halifax	36.8172	-78.9663	6.7	0.20	NURE
Halifax	36.75639	-78.798333	7.8	7.00	NURE
Halifax	36.75	-78.8046	6.9	140.70	NURE
Halifax	37.0434	-79.0823	5.8	6.00	NURE
Halifax	36.6221	-79.0894	6.5	50.90	NURE
Henry	36.7008	-79.9969	5.9	8.50	NURE
Henry	36.618	-79.7745	6.7	61.90	NURE
Henry	36.6577	-79.7213	5	61.10	NURE
Henry	36.6508	-79.7719	6.1	27.00	NURE
Henry	36.6053	-79.8271	6.3	17.10	NURE
Henry	36.70111	-80.018111	6.7	0.05	NURE
Henry	36.7569	-79.8804	6.4	88.60	NURE
Henry	36.8016	-79.6598	6.4	61.00	NURE
Henry	36.7934	-79.9991	5.6	50.30	NURE

County/City	Latitude	Longitude	pH	Mn	Source
Henry	36.7557	-80.0533	5.5	46.10	NURE
Henry	36.7798	-79.7266	6.8	46.00	NURE
Henry	36.5661	-79.8737	5.7	40.90	NURE
Henry	36.7074	-80.0626	5.7	33.30	NURE
Henry	36.5636	-79.9372	5.7	27.10	NURE
Henry	36.659	-79.8267	6	21.40	NURE
Henry	36.6586	-79.9931	6.3	17.80	NURE
Henry	36.6583	-79.8819	6.1	12.00	NURE
Henry	36.6075	-79.8888	6.5	11.00	NURE
Henry	36.7449	-79.9882	6.2	9.00	NURE
Henry	36.6827	-79.9888	6.4	8.30	NURE
Henry	36.6147	-80.0018	6.6	7.60	NURE
Henry	36.7532	-79.936	6	5.90	NURE
Henry	36.7086	-79.926	5.8	5.80	NURE
Henry	36.7471	-79.7616	6.7	4.90	NURE
Henry	36.7104	-79.8177	6	3.20	NURE
Henry	36.7449	-79.713	6.5	0.30	NURE
Henry	36.5654	-79.7794	6.9	605.00	NURE
Henry	36.6167	-79.715	6.2	253.50	NURE
Henry	36.5651	-79.7213	5.9	94.00	NURE
Mecklenburg	36.6882	-78.217	8	64.10	NURE
Mecklenburg	36.5639	-78.2758	6.7	29.80	NURE
Mecklenburg	36.6356	-78.3231	8.5	19.00	NURE
Mecklenburg	36.7867	-78.2282	8.6	15.30	NURE
Mecklenburg	36.6316	-78.2352	8.9	2.30	NURE
Mecklenburg	36.66019	-78.3781666	7.4	407.80	NURE
Mecklenburg	36.66167	-78.386947	7.1	136.00	NURE
Mecklenburg	36.6016	-78.6872	7.5	227.70	NURE
Mecklenburg	36.7012	-78.4077	6.3	148.10	NURE
Mecklenburg	36.7346	-78.2776	5.4	122.50	NURE
Mecklenburg	36.7504	-78.4623	7	115.90	NURE
Mecklenburg	36.7478	-78.5586	6.2	96.80	NURE
Mecklenburg	36.6977	-78.3454	6.9	95.70	NURE
Mecklenburg	36.6889	-78.4456	5.9	78.90	NURE
Mecklenburg	36.6032	-78.5729	5.8	49.40	NURE
Mecklenburg	36.8387	-78.5137	7.5	49.30	NURE
Mecklenburg	36.6246	-78.4211	7.1	29.80	NURE
Mecklenburg	36.6966	-78.6273	6.4	27.70	NURE
Mecklenburg	36.6932	-78.5125	5.8	26.00	NURE
Mecklenburg	36.6493	-78.5176	5.4	22.80	NURE
Mecklenburg	36.7325	-78.3227	6.7	21.00	NURE
Mecklenburg	36.5526	-78.6267	6.7	20.50	NURE

County/City	Latitude	Longitude	pH	Mn	Source
Mecklenburg	36.7799	-78.456	6.2	19.10	NURE
Mecklenburg	36.6502	-78.3982	8	17.10	NURE
Mecklenburg	36.7754	-78.5844	6.3	16.40	NURE
Mecklenburg	36.7521	-78.4139	6.5	13.60	NURE
Mecklenburg	36.5531	-78.5813	6.5	13.30	NURE
Mecklenburg	36.7818	-78.2776	6.3	12.90	NURE
Mecklenburg	36.6156	-78.4592	7.6	10.00	NURE
Mecklenburg	36.8356	-78.3994	6.1	5.40	NURE
Mecklenburg	36.7895	-78.341	6	33.10	NURE
Mecklenburg	36.5606	-78.4458	8.4	31.50	NURE
Mecklenburg	36.5506	-78.1667	6.8	10.70	NURE
Mecklenburg	36.69031	-78.1488055	5.6	0.34	Chapman (2013)
Mecklenburg	36.702	-78.2826	7	28.50	NURE
Mecklenburg	36.597	-78.2769	7.1	24.10	NURE
Mecklenburg	36.6486	-78.2841	7.6	14.00	NURE
Mecklenburg	36.7377	-78.2165	8.2	13.90	NURE
Mecklenburg	36.5865	-78.217	7.5	10.00	NURE
Mecklenburg	36.7846	-78.1136	8.8	85.50	NURE
Mecklenburg	36.6483	-78.1777	7.5	31.60	NURE
Mecklenburg	36.5469	-78.2203	6.5	20.70	NURE
Mecklenburg	36.7521	-78.0434	7.8	13.90	NURE
Mecklenburg	36.6978	-78.0513	7	12.40	NURE
Mecklenburg	36.6963	-78.1676	6.7	11.70	NURE
Mecklenburg	36.6481	-78.1108	7.4	11.10	NURE
Mecklenburg	36.6427	-78.0538	6.4	8.80	NURE
Mecklenburg	36.6014	-78.1602	8.3	7.70	NURE
Mecklenburg	36.7451	-78.1643	8.1	6.70	NURE
Montgomery	37.143	-80.1834	6.2	23.00	NURE
Montgomery	37.1974	-80.2384	6.8	792.00	NURE
Montgomery	37.286	-80.2395	7.1	68.00	NURE
Montgomery	37.2104	-80.2843	6	27.00	NURE
Montgomery	37.1144	-80.2836	7.3	17.00	NURE
Montgomery	37.2386	-80.3112	5.8	16.00	NURE
Montgomery	37.312	-80.3053	7.2	9.00	NURE
Patrick	36.7175	-80.3239	6.4	133.20	NURE
Patrick	36.8297	-80.0964	7.1	115.70	NURE
Patrick	36.8113	-80.1446	7	58.80	NURE
Patrick	36.8087	-80.3226	6.6	46.60	NURE
Patrick	36.7167	-80.245	6.7	40.60	NURE
Patrick	36.7665	-80.265	6.1	34.40	NURE
Patrick	36.7188	-80.3691	5.9	33.90	NURE
Patrick	36.7213	-80.4333	6.5	21.10	NURE

County/City	Latitude	Longitude	pH	Mn	Source
Patrick	36.772	-80.1424	6.6	20.70	NURE
Patrick	36.5764	-80.4864	5.4	19.40	NURE
Patrick	36.7619	-80.1974	6.9	18.10	NURE
Patrick	36.7681	-80.3103	6.2	17.50	NURE
Patrick	36.8417	-80.257	6.2	14.10	NURE
Patrick	36.6111	-80.4362	5.6	12.60	NURE
Patrick	36.8069	-80.252	6.8	11.30	NURE
Patrick	36.6922	-80.4104	6.7	9.50	NURE
Patrick	36.6836	-80.3629	6.4	9.00	NURE
Patrick	36.6241	-80.5449	6	8.60	NURE
Patrick	36.5793	-80.5427	5.9	6.60	NURE
Patrick	36.7342	-80.2177	6.8	5.90	NURE
Patrick	36.5832	-80.5955	7.2	5.30	NURE
Patrick	36.5745	-80.3028	7.2	107.20	NURE
Patrick	36.6299	-80.1441	5.7	66.80	NURE
Patrick	36.6233	-80.2575	6.5	60.20	NURE
Patrick	36.5762	-80.3728	6.3	45.10	NURE
Patrick	36.678	-80.0878	6.6	29.90	NURE
Patrick	36.5858	-80.188	6.1	23.40	NURE
Patrick	36.681	-80.1323	6.1	21.60	NURE
Patrick	36.6736	-80.1864	6.1	18.10	NURE
Patrick	36.5862	-80.0861	6.1	14.40	NURE
Patrick	36.5797	-80.254	6.2	14.00	NURE
Patrick	36.7197	-80.1395	6.6	13.00	NURE
Patrick	36.5811	-80.4265	6	12.00	NURE
Pittsylvania	36.5759	-79.6122	6.5	14.40	NURE
Pittsylvania	36.67794	-79.3888055	5.9	215.80	NURE
Pittsylvania	36.6707	-79.2603	6.1	17.80	NURE
Pittsylvania	36.7863	-79.189	6.4	17.70	NURE
Pittsylvania	36.8914	-79.146	6.7	15.20	NURE
Pittsylvania	36.5708	-79.2474	7	14.90	NURE
Pittsylvania	36.7078	-79.1943	6.3	12.40	NURE
Pittsylvania	36.7088	-79.3739	7.1	10.00	NURE
Pittsylvania	36.5595	-79.3017	6.1	7.10	NURE
Pittsylvania	36.6159	-79.4288	6.2	5.80	NURE
Pittsylvania	36.7837	-79.3077	6.9	5.20	NURE
Pittsylvania	37.0232	-79.1378	6.8	131.00	NURE
Pittsylvania	36.9419	-79.1453	6.9	60.90	NURE
Pittsylvania	36.8926	-79.1989	7.1	59.20	NURE
Pittsylvania	36.9416	-79.1921	6.4	13.90	NURE
Pittsylvania	36.6633	-79.4864	5.7	6.30	NURE
Pittsylvania	37.0865	-79.3254	6.4	19.00	NURE

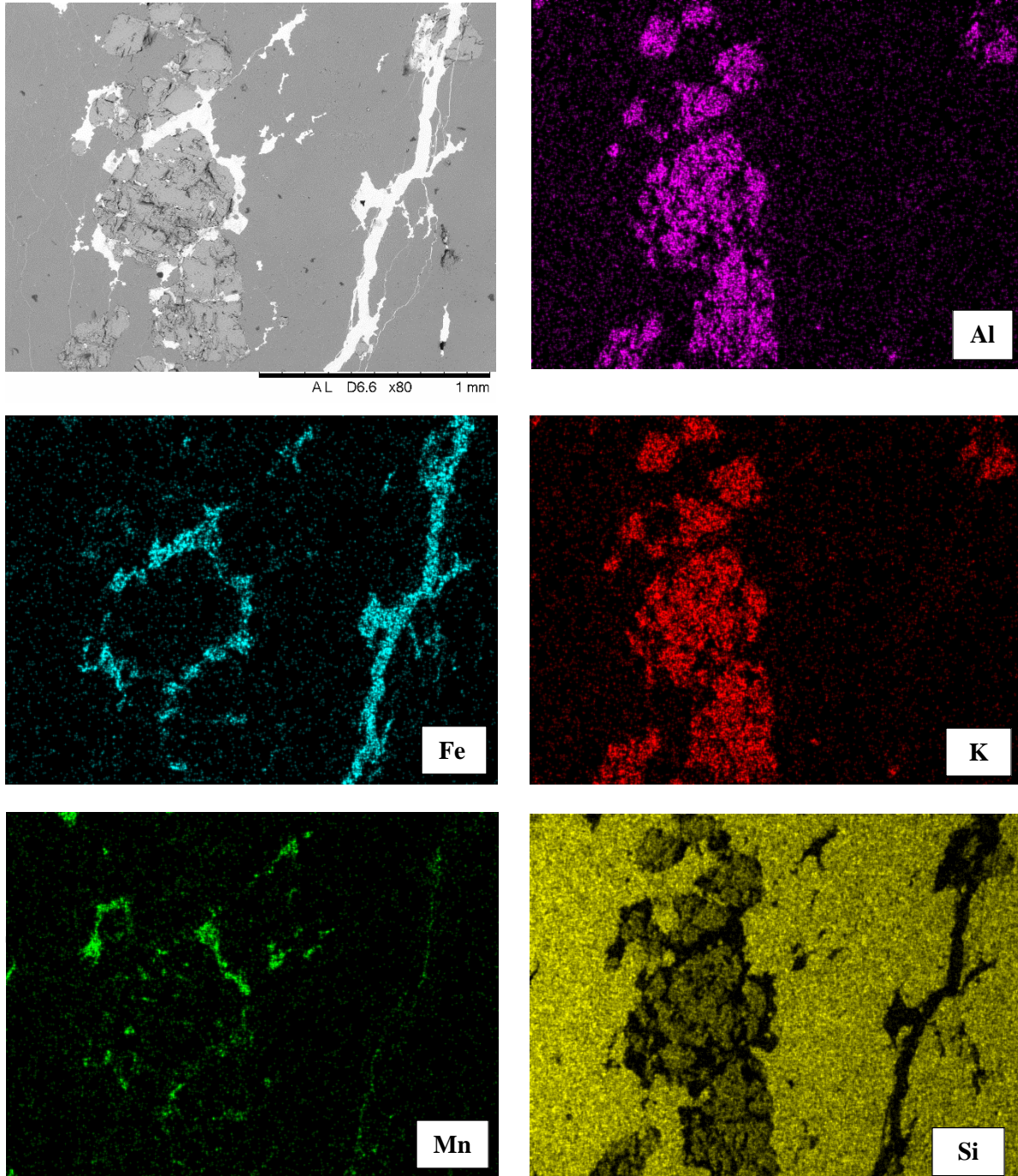
County/City	Latitude	Longitude	pH	Mn	Source
Pittsylvania	36.944	-79.597	6.5	13.40	NURE
Pittsylvania	36.6146	-79.5983	6.2	0.30	NURE
Pittsylvania	36.85028	-79.378611	6.4	144.00	Nelms & Harlow (2003)
Pittsylvania	36.7926	-79.3797	6.3	199.00	NURE
Pittsylvania	37.0347	-79.3238	5.7	123.00	NURE
Pittsylvania	36.9877	-79.2113	6.7	90.80	NURE
Pittsylvania	37.0849	-79.3772	5.8	85.00	NURE
Pittsylvania	36.9404	-79.4917	6.4	78.70	NURE
Pittsylvania	36.9794	-79.593	6.4	73.90	NURE
Pittsylvania	36.7912	-79.599	6.4	63.40	NURE
Pittsylvania	36.9444	-79.4426	6	58.00	NURE
Pittsylvania	36.9807	-79.4321	5.6	45.00	NURE
Pittsylvania	36.8342	-79.4377	6.3	44.00	NURE
Pittsylvania	36.9361	-79.2572	6	38.80	NURE
Pittsylvania	36.7566	-79.4833	6.6	34.40	NURE
Pittsylvania	36.805	-79.5092	5.9	25.70	NURE
Pittsylvania	36.9758	-79.558	6.3	23.40	NURE
Pittsylvania	36.9508	-79.5363	7.8	20.20	NURE
Pittsylvania	36.8943	-79.3693	6.1	15.90	NURE
Pittsylvania	36.8344	-79.3688	6.4	15.70	NURE
Pittsylvania	36.8381	-79.5414	6.8	15.50	NURE
Pittsylvania	36.8427	-79.5979	5.8	15.30	NURE
Pittsylvania	36.7512	-79.5544	6.7	12.10	NURE
Pittsylvania	36.7491	-79.6505	7.2	10.60	NURE
Pittsylvania	36.9926	-79.2578	6.1	9.90	NURE
Pittsylvania	36.703	-79.5857	5.9	9.20	NURE
Pittsylvania	36.9384	-79.3641	5.8	8.90	NURE
Pittsylvania	36.7503	-79.5846	6.8	8.70	NURE
Pittsylvania	37.0387	-79.2567	5.6	8.00	NURE
Pittsylvania	36.6961	-79.5425	8	7.80	NURE
Pittsylvania	36.711	-79.649	6.5	7.40	NURE
Pittsylvania	36.989	-79.3292	5.6	6.00	NURE
Pittsylvania	36.6562	-79.5908	6.6	5.60	NURE
Pittsylvania	36.9012	-79.321	5.9	4.70	NURE
Pittsylvania	36.858	-79.4769	6	4.40	NURE
Pittsylvania	36.8936	-79.4248	6.6	4.00	NURE
Pittsylvania	36.6192	-79.6501	6.4	79.70	NURE
Pittsylvania	36.5679	-79.6587	6.4	8.70	NURE
Roanoke	37.26972	-79.897778	7.5	38.00	Nelms & Harlow (2003)
Roanoke	37.1987	-80.1633	6	67.00	NURE
Roanoke	37.1921	-80.1447	7.5	51.00	NURE
Roanoke	37.127	-80.128	6.4	48.00	NURE

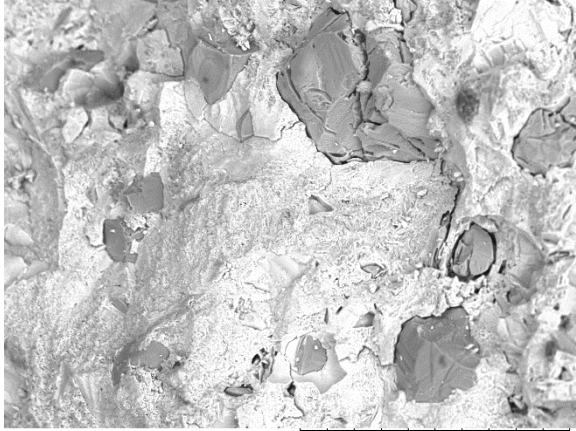
County/City	Latitude	Longitude	pH	Mn	Source
Roanoke	37.2466	-79.9049	6.8	29.00	NURE
Roanoke	37.1692	-79.9428	6	17.00	NURE
Roanoke	37.2142	-79.8853	7.5	14.00	NURE
Roanoke	37.1591	-79.9747	7.4	9.00	NURE
Roanoke	37.2399	-79.8682	6.9	7.00	NURE
Roanoke	37.3137	-80.2087	7	319.00	NURE
Roanoke	37.3407	-80.0136	6.8	227.00	NURE
Roanoke	37.3529	-79.9845	7.5	188.00	NURE
Roanoke	37.3816	-79.9953	7.1	170.00	NURE
Roanoke	37.3311	-80.1614	7.5	96.00	NURE
Roanoke	37.3666	-80.0445	7.2	70.00	NURE
Roanoke	37.3623	-80.1015	7.7	56.00	NURE
Roanoke	37.2905	-80.2389	7.3	56.00	NURE
Roanoke	37.3495	-80.1253	7.6	37.00	NURE
Roanoke	37.3107	-80.0929	8.2	36.00	NURE
Roanoke	37.2192	-80.1879	7.3	29.00	NURE
Roanoke	37.2514	-80.038	7.3	18.00	NURE
Roanoke	37.2645	-80.0791	8	17.00	NURE
Roanoke	37.3943	-80.0646	7.4	15.00	NURE
Roanoke	37.3181	-80.0086	7.6	14.00	NURE
Roanoke	37.2953	-80.1417	5.8	13.00	NURE
Roanoke	37.3407	-79.9497	7.4	100.00	NURE

APPENDIX B

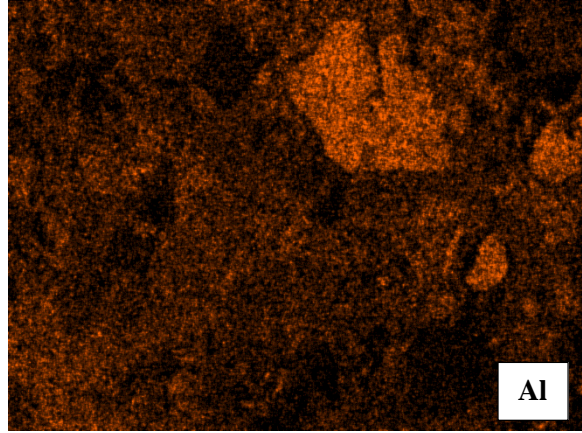
Photomicrographs of selected samples using scanning electron microscopy (SEM) and energy dispersive spectroscopy (EDS). The upper-left image for each sample is a back-scattered electron (BSE) photomicrograph. Colored images are element maps generated through EDS of the same area represented in the BSE image. Each element map is labeled to designate which element is represented.

Sample Number: LVL-100

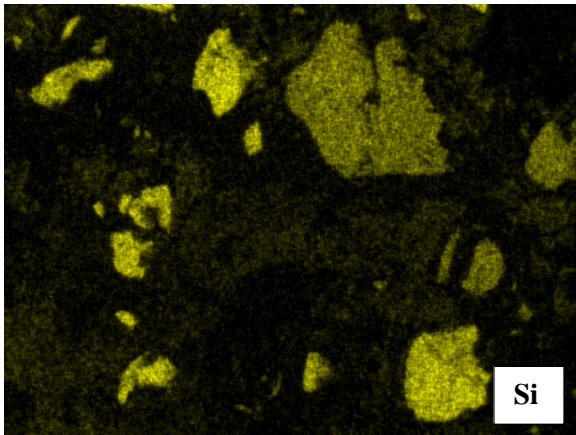




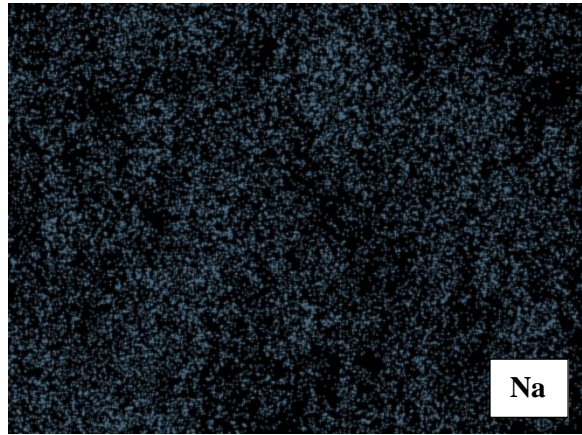
AL D6.7 x400 200 um



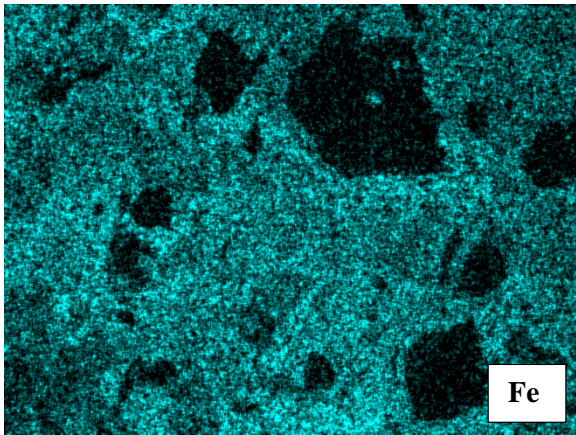
Al



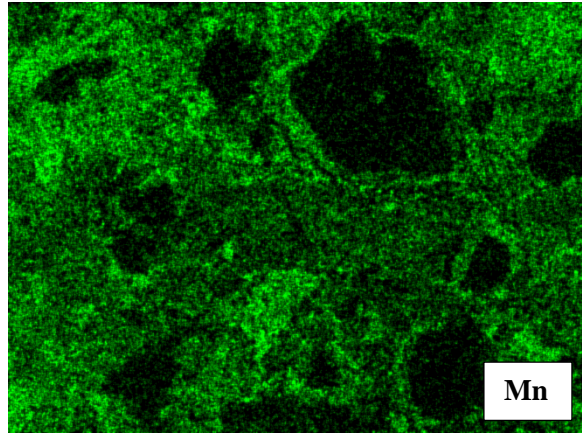
Si



Na

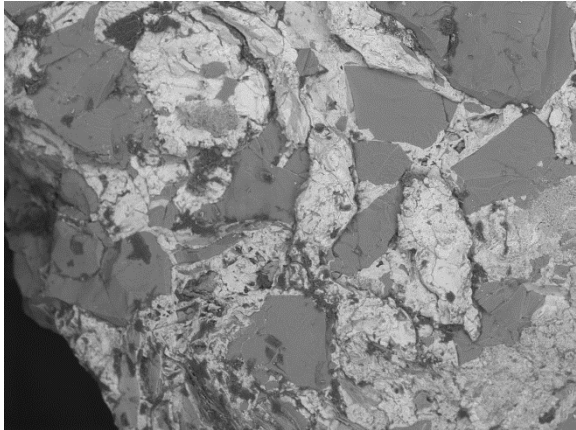


Fe

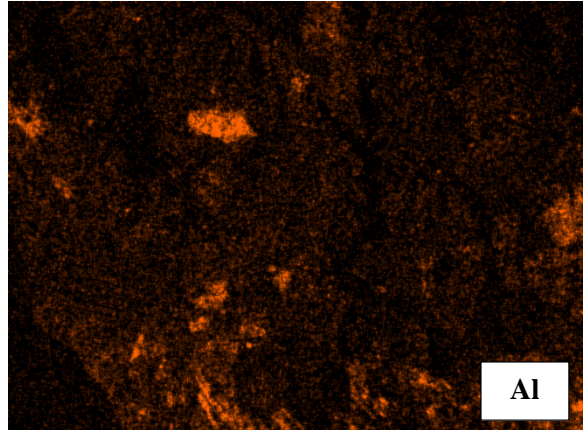


Mn

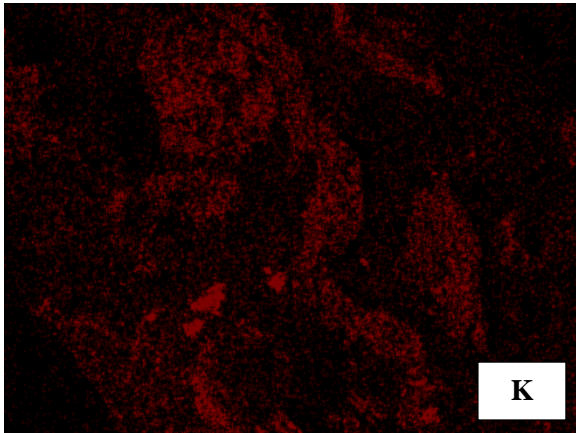
Sample Number: LVL-102



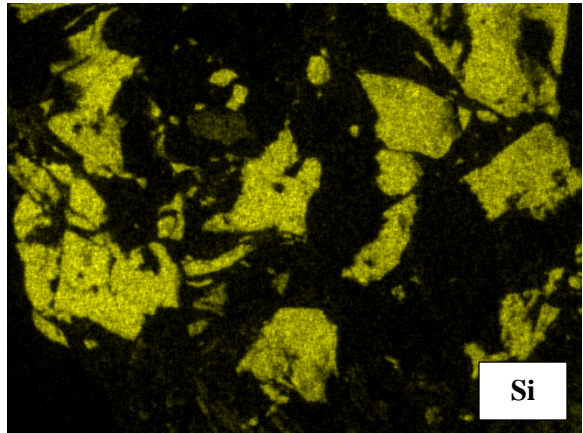
AL D7.5 x150 500 um



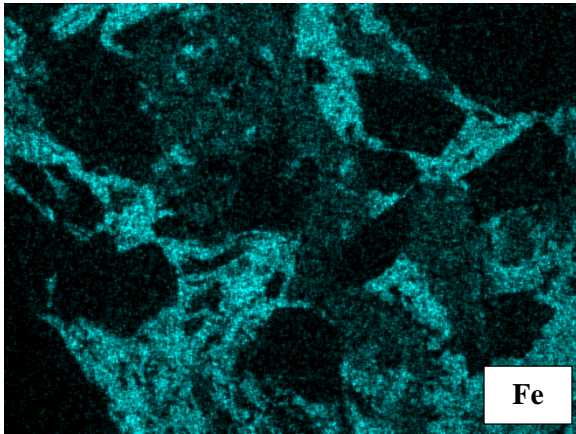
Al



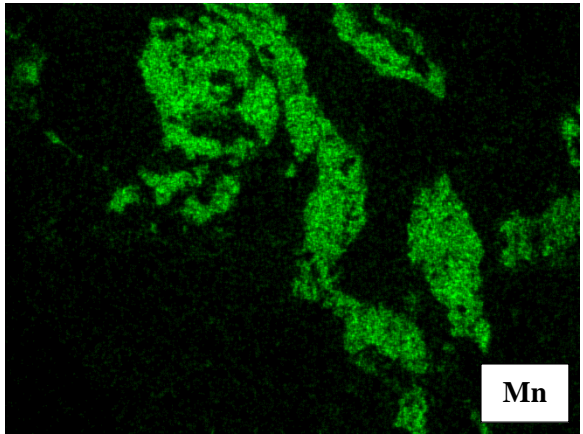
K



Si

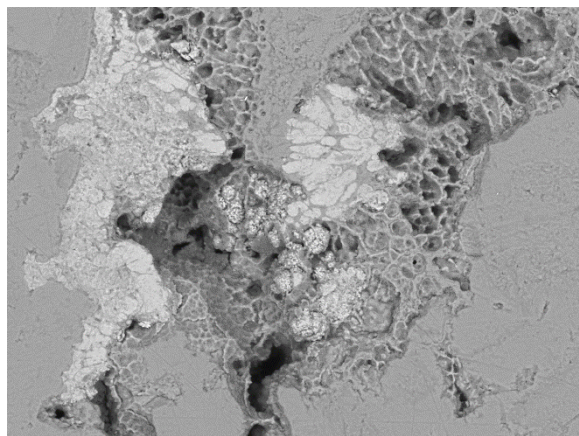


Fe

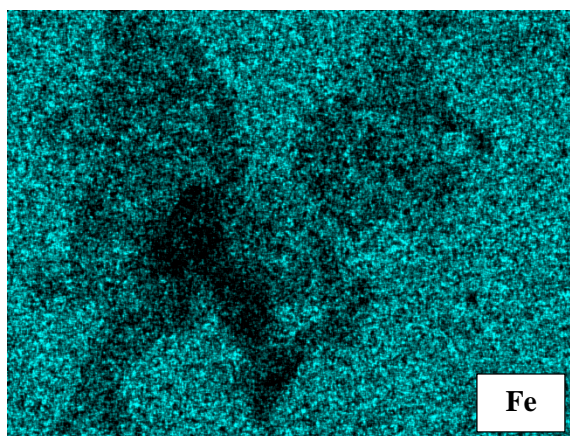


Mn

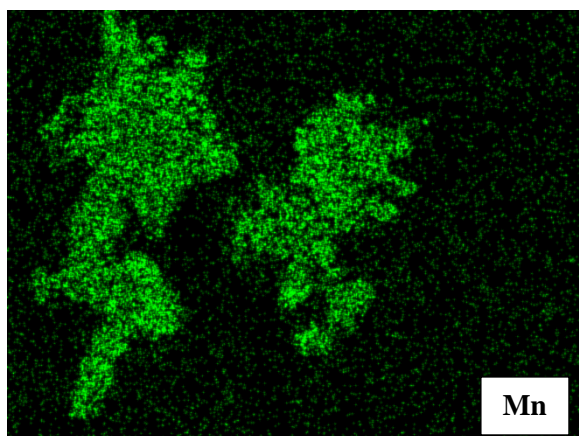
Sample Number: RBG01-BH



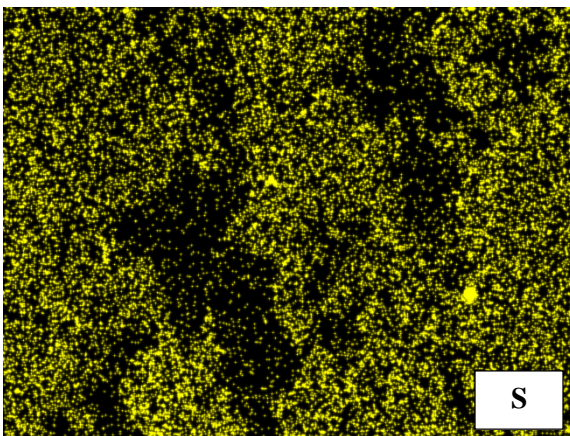
AL D6.1 x800 100 um



Fe

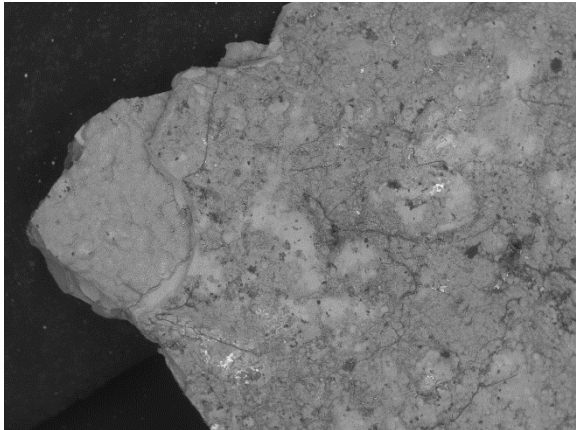


Mn

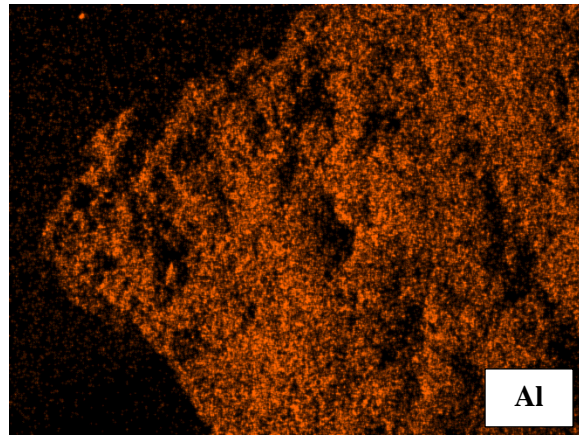


S

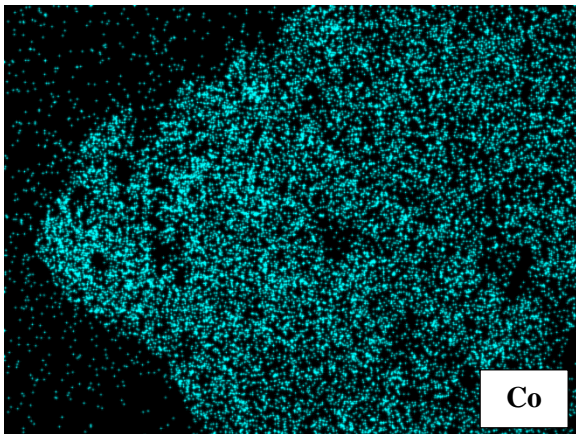
Sample Number: RBG-110



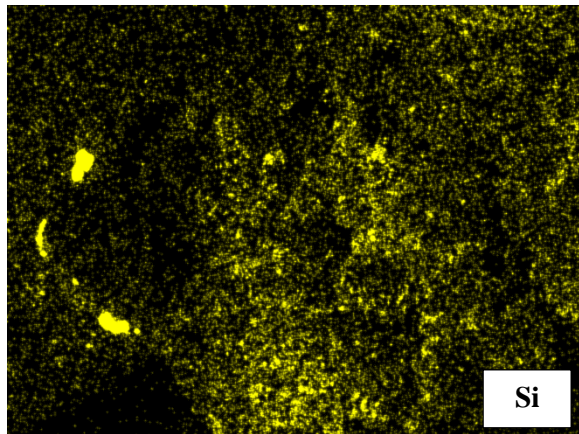
AL D7.0 x40 2mm



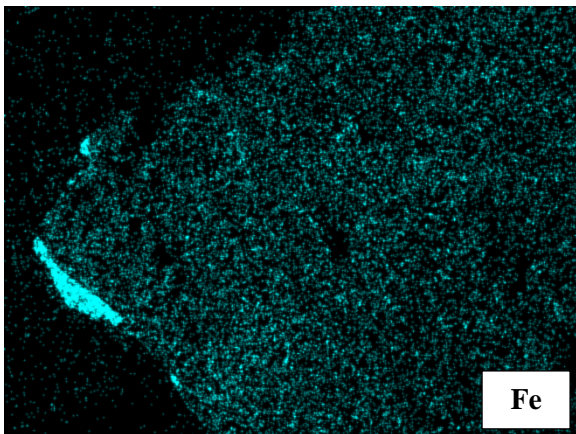
Al



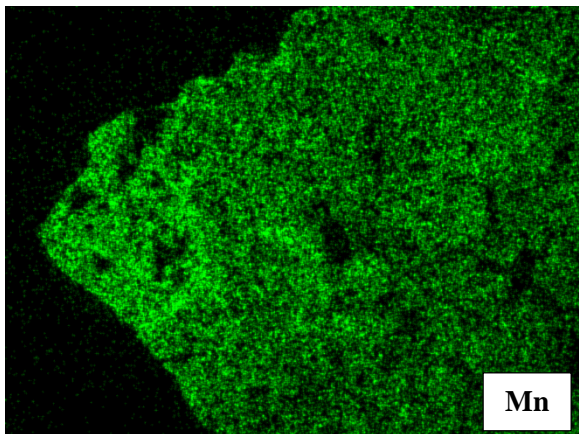
Co



Si

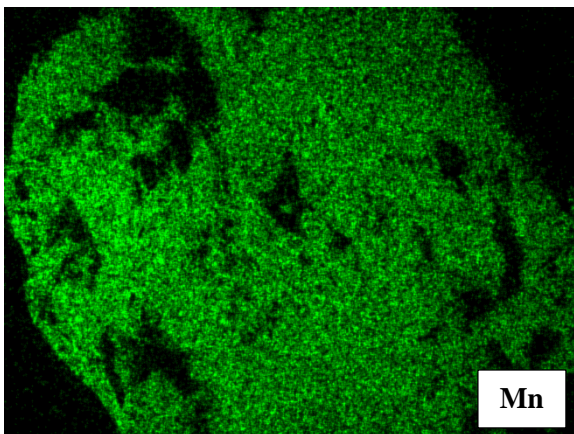
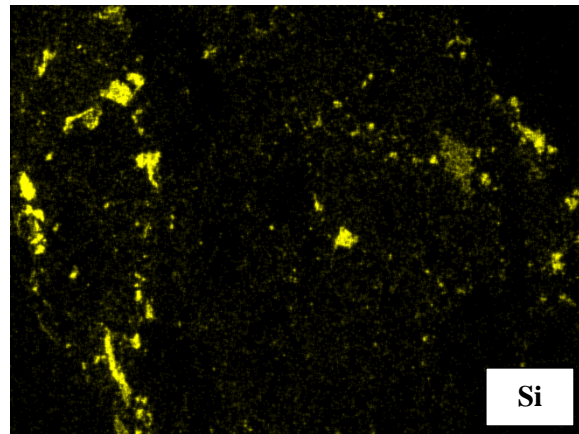
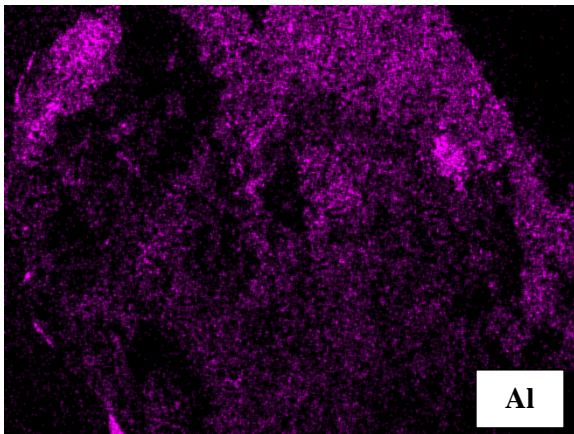
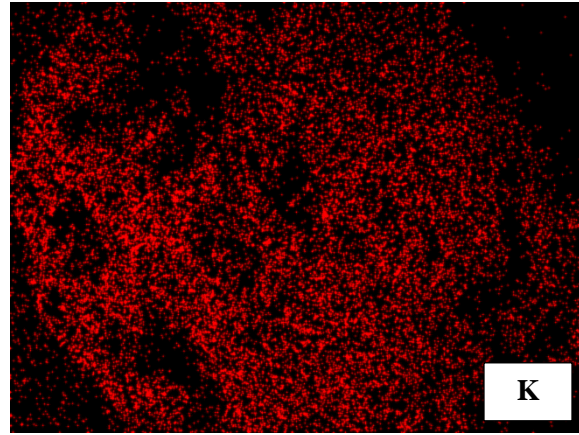
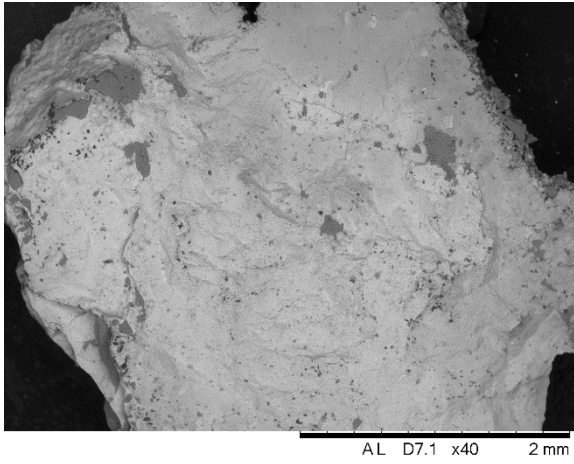


Fe

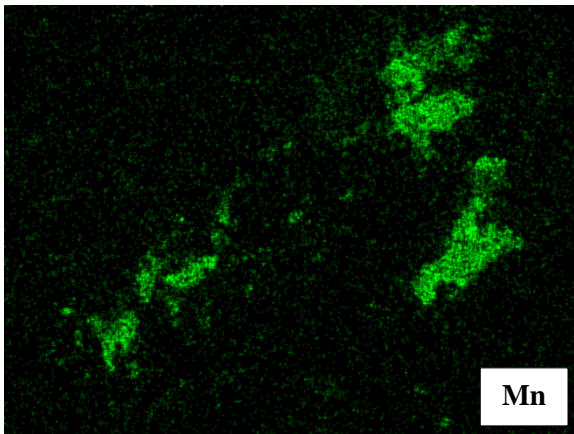
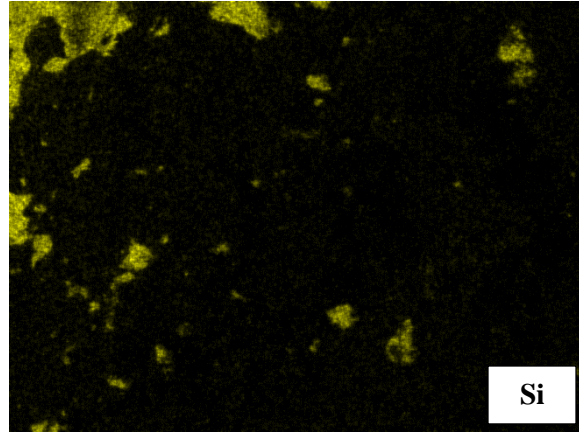
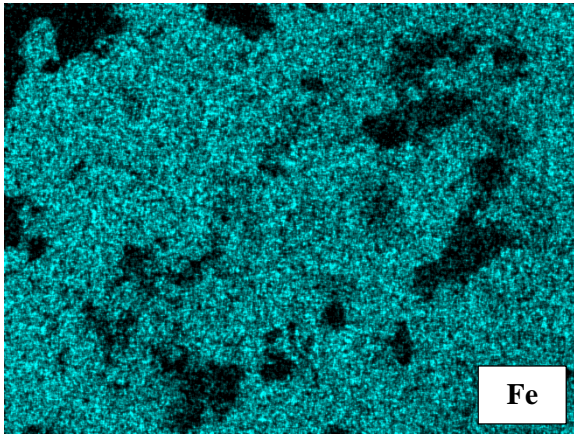
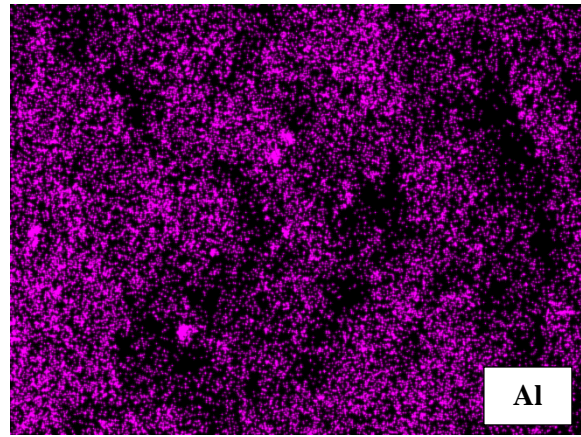
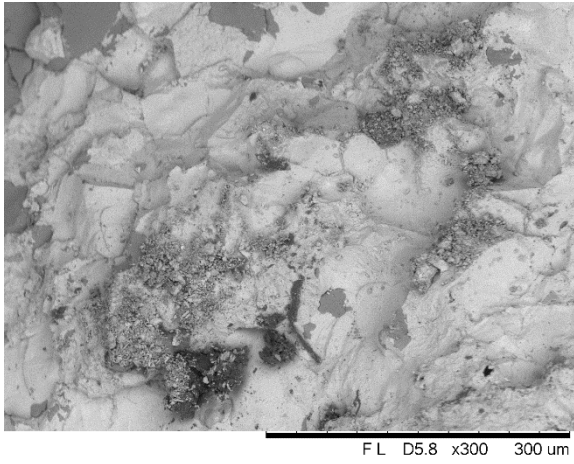


Mn

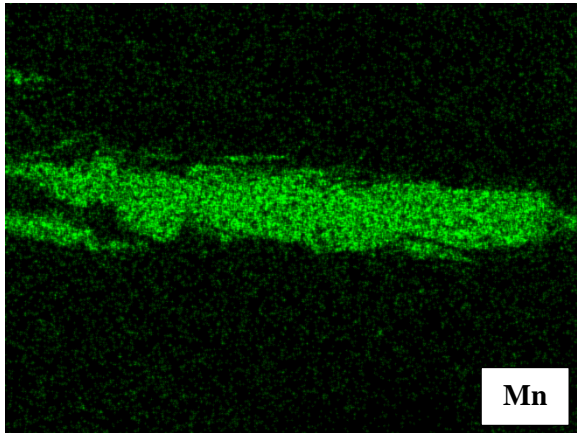
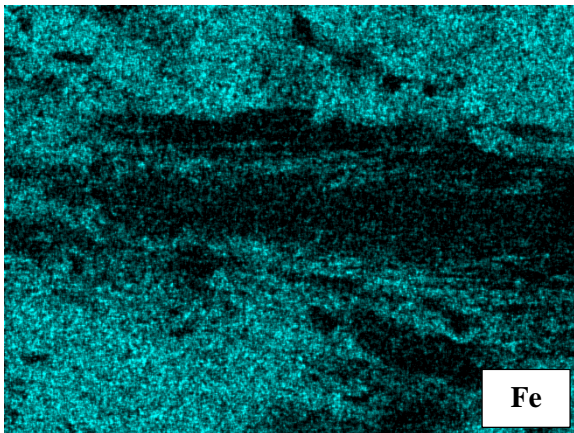
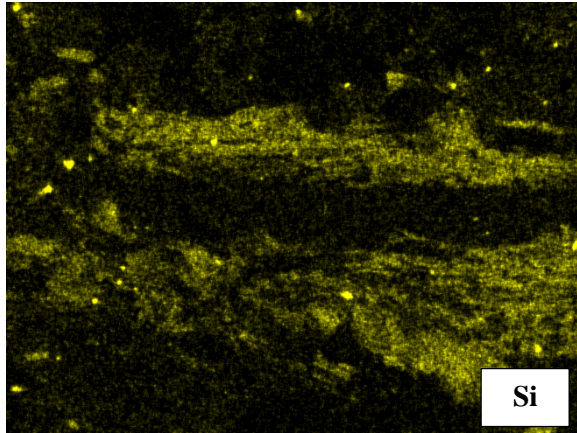
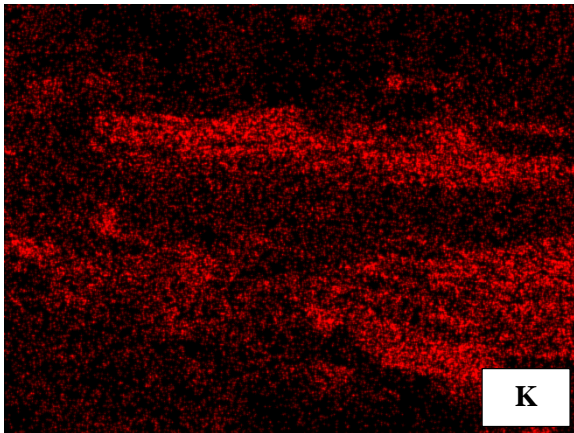
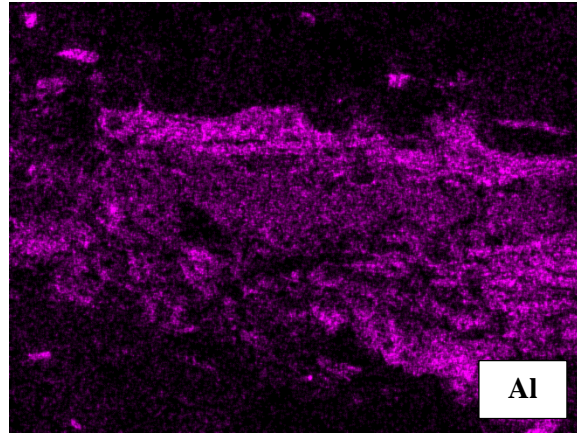
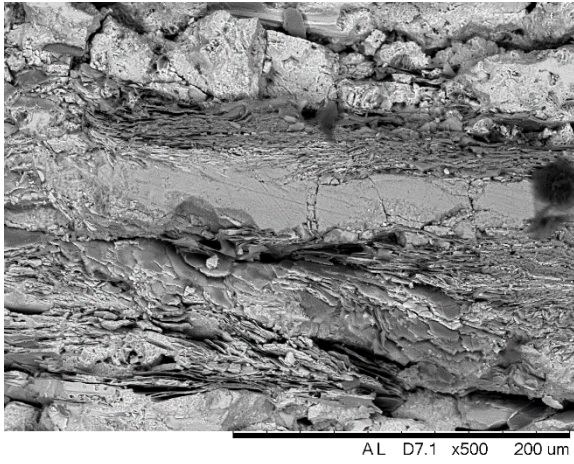
Sample Number: RBG-111



Sample Number: RBG-112A

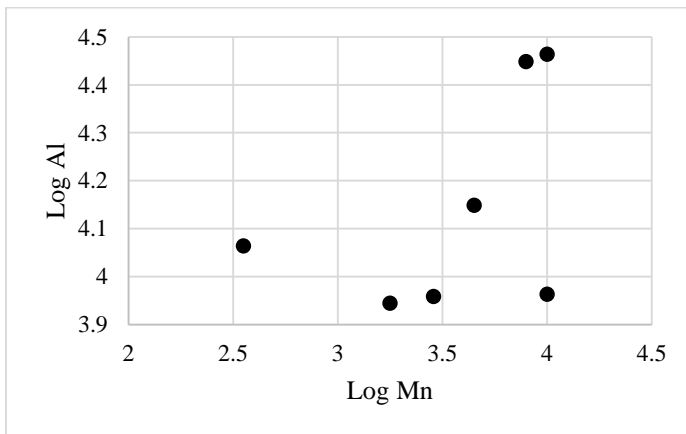
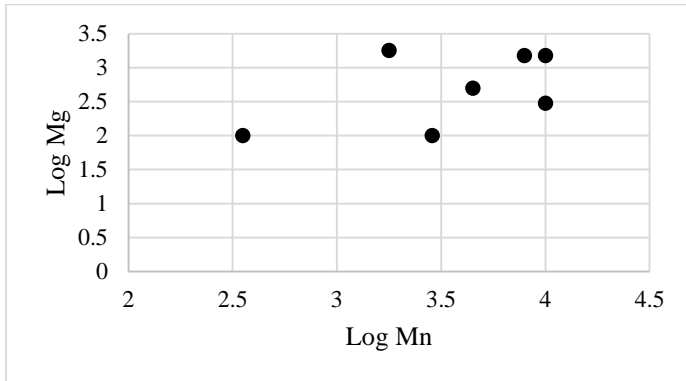
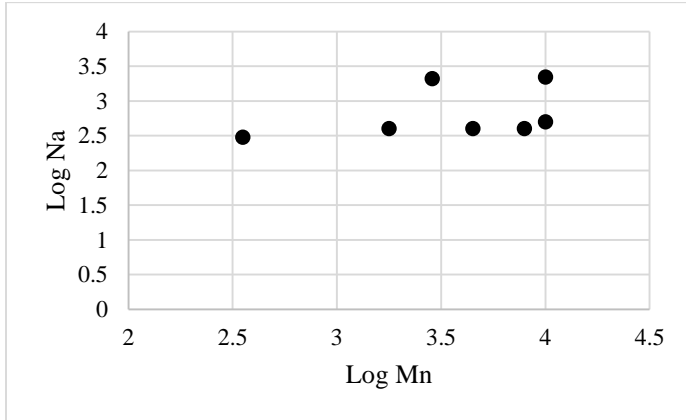


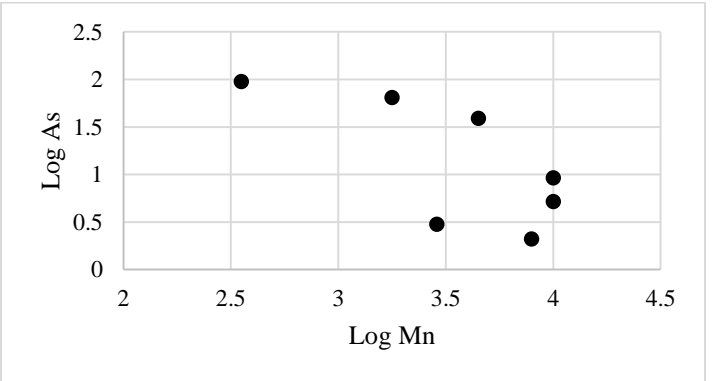
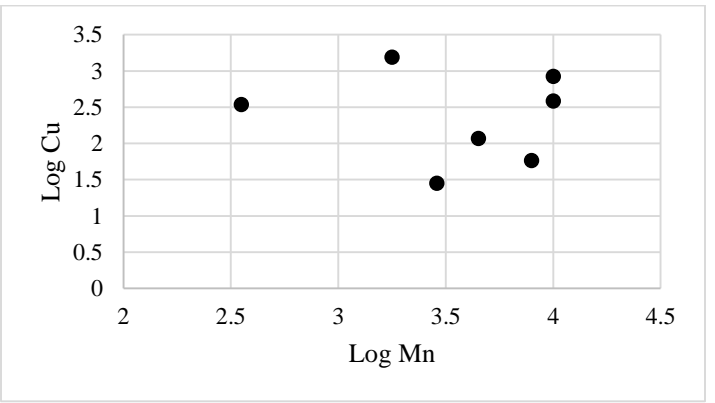
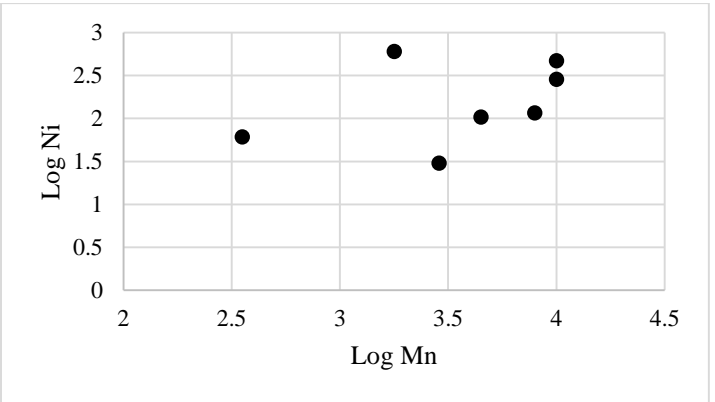
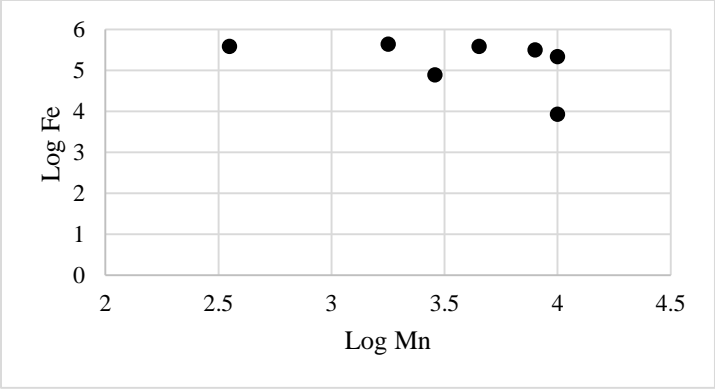
Sample Number: RBG-114

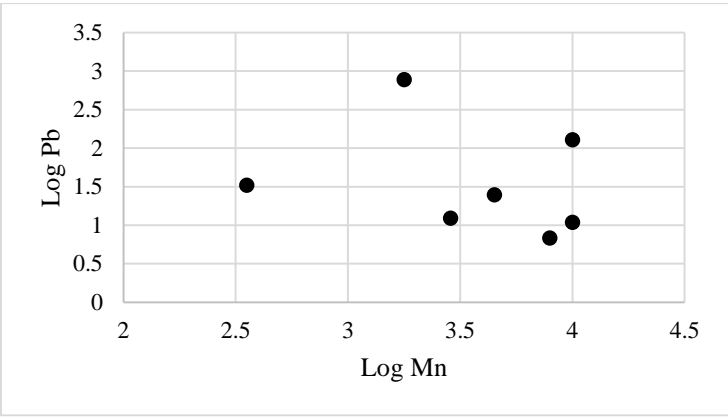
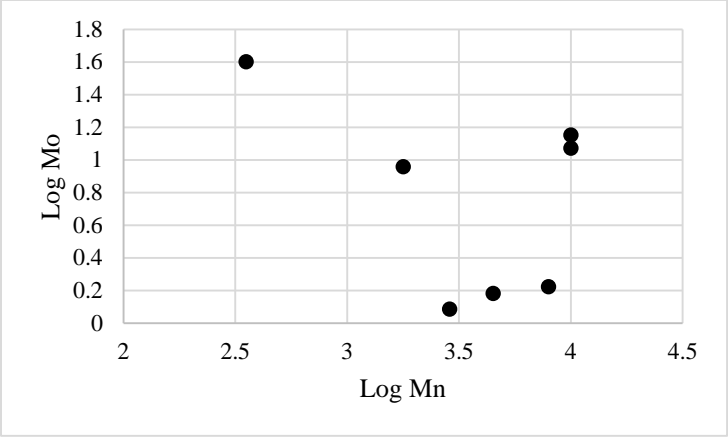


APPENDIX C

Additional plots of analytes in relation to Mn from ore samples analyzed by near-total acid digestions and ICPMS. All data are log transformed from original concentrations.







APPENDIX D

Compilation of total Mn groundwater data in the Roanoke River watershed. Data are grouped by county.

County or City	Latitude	Longitude	pH	Mn (ppb)	Source
Appomattox	37.347077	-78.907205	6.1	30	STORET
Appomattox	37.311521	-78.902206	6.4	10	STORET
Appomattox	37.268463	-78.714715	6.5	10	STORET
Appomattox	37.292631	-78.785823	---	200	STORET
Appomattox	37.331243	-78.86693	---	10	STORET
Appomattox	37.349692	-78.823696	7.24	50	STORET
Appomattox	37.346723	-78.854491	6.3	10	STORET
Bedford	37.046244	-79.576081	6.5	30	STORET
Bedford	37.408192	-79.403025	7.6	170	STORET
Bedford	37.444584	-79.610519	6.6	50	STORET
Bedford	37.282357	-79.551635	6.3	10	STORET
Bedford	37.373469	-79.344138	7.2	50	STORET
Bedford	37.268472	-79.84663	6.1	10	STORET
Bedford	37.16569	-79.635802	7.7	50	STORET
Bedford	37.35069	-79.283029	---	50	STORET
Bedford	37.254577	-79.398306	6.8	10	STORET
Bedford	37.290413	-79.498579	7.4	60	STORET
Bedford	37.0818	-79.575248	6	10	STORET
Bedford	37.136524	-79.649135	7.8	10	STORET
Bedford	37.240135	-79.596912	8	80	STORET
Bedford	37.065966	-79.550248	7.3	410	STORET
Bedford	37.142355	-79.500248	5.8	10	STORET
Bedford	37.446529	-79.608019	6.28	50	STORET
Bedford	37.156801	-79.643857	6.5	20	STORET
Bedford	37.384304	-79.58691	6.3	20	STORET
Bedford	37.389687	-79.553706	7.55	220	STORET
Bedford	37.232082	-79.805798	6	10	STORET
Bedford	37.283749	-79.749409	6.5	100	STORET
Bedford	37.267917	-79.847463	5.8	10	STORET
Bedford	37.251249	-79.807186	6.4	10	STORET
Bedford	37.259582	-79.739686	6.4	80	STORET
Bedford	37.398751	-79.700796	6.5	10	STORET
Bedford	37.382361	-79.623298	6.8	60	STORET
Bedford	37.294305	-79.782185	6.5	30	STORET
Bedford	37.225134	-79.556357	6.5	10	STORET
Bedford	37.28875	-79.786908	6.2	10	STORET
Bedford	37.146246	-79.66469	6.7	90	STORET
Bedford	37.287914	-79.604133	6	10	STORET
Bedford	37.269859	-79.718299	5.8	10	STORET

Bedford	37.297918	-79.82024	6.2	10	STORET
Bedford	37.142913	-79.65719	6.6	140	STORET
Bedford	37.28125	-79.844963	5.7	10	STORET
Bedford	37.387638	-79.553299	5.7	10	STORET
Bedford	37.477364	-79.659684	5.7	10	STORET
Bedford	37.151246	-79.662746	6.7	10	STORET
Bedford	37.402919	-79.713296	7.8	20	STORET
Bedford	37.440419	-79.678851	8.1	10	STORET
Bedford	37.319861	-79.738574	6.5	10	STORET
Bedford	37.302635	-79.462469	6.2	10	STORET
Bedford	37.087912	-79.573304	7	70	STORET
Bedford	37.116523	-79.569691	6.3	20	STORET
Bedford	37.044577	-79.551637	6.7	60	STORET
Bedford	37.044299	-79.552192	6.5	390	STORET
Bedford	37.246527	-79.805798	6.4	10	STORET
Bedford	37.248471	-79.799409	7.3	90	STORET
Bedford	37.250416	-79.798853	6.2	40	STORET
Bedford	37.246249	-79.797464	6.1	20	STORET
Bedford	37.250971	-79.787742	8	50	STORET
Bedford	37.249304	-79.783575	6.6	10	STORET
Bedford	37.24986	-79.801909	6.5	10	STORET
Bedford	37.249582	-79.802742	6.1	10	STORET
Bedford	37.248749	-79.801631	6	100	STORET
Bedford	37.246249	-79.804964	6.7	120	STORET
Bedford	37.240138	-79.80552	6	40	STORET
Bedford	37.246249	-79.804964	6.1	10	STORET
Bedford	37.248193	-79.803298	5.5	10	STORET
Bedford	37.250693	-79.798853	6.1	10	STORET
Bedford	37.249582	-79.798298	7.3	20	STORET
Bedford	37.248749	-79.794409	6	10	STORET
Bedford	37.24736	-79.793298	6.4	40	STORET
Bedford	37.244304	-79.798853	6	10	STORET
Bedford	37.246804	-79.798298	6.1	10	STORET
Bedford	37.246527	-79.798853	6.1	10	STORET
Bedford	37.246249	-79.794686	6.8	30	STORET
Bedford	37.246249	-79.796631	5.9	10	STORET
Bedford	37.372082	-79.579965	7.1	50	STORET
Bedford	37.40403	-79.710518	7.6	10	STORET
Bedford	37.442085	-79.662184	7.8	10	STORET
Bedford	37.342917	-79.713852	6.8	10	STORET
Bedford	37.1468	-79.598025	6.2	10	STORET
Bedford	37.27875	-79.810797	---	60	STORET
Bedford	37.270138	-79.732186	---	90	STORET

Bedford	37.447085	-79.679129	---	10	STORET
Bedford	37.199303	-79.734688	7.01	110	STORET
Bedford	37.305417	-79.766908	6.15	50	STORET
Botetourt	37.374586	-79.84496	8	20	STORET
Botetourt	37.415976	-79.859404	7.4	40	STORET
Botetourt	37.428199	-79.911903	7.3	90	STORET
Botetourt	37.421533	-79.887737	7.3	120	STORET
Botetourt	37.340696	-79.877461	7	40	STORET
Botetourt	37.352085	-79.840795	7.1	10	STORET
Botetourt	37.368474	-79.814128	7.1	10	STORET
Botetourt	37.367642	-79.902738	1	120	STORET
Botetourt	37.425422	-79.911903	7.5	10	STORET
Botetourt	37.425422	-79.911903	7.5	50	STORET
Botetourt	37.379864	-79.87746	7.8	10	STORET
Brunswick	36.549295	-77.889177	5.6	10	STORET
Campbell	37.160967	-79.083591	6.64	120	STORET
Campbell	37.226799	-79.226643	6.7	10	STORET
Campbell	37.078746	-78.884155	6.9	20	STORET
Campbell	37.304577	-79.049979	6.2	40	STORET
Campbell	37.268743	-78.92304	6.1	10	STORET
Campbell	37.155134	-79.228588	6.3	30	STORET
Campbell	37.192356	-79.208033	7.5	690	STORET
Campbell	37.100413	-79.113314	7.5	10	STORET
Campbell	37.228466	-79.228865	6.6	10	STORET
Campbell	37.209577	-79.207199	5.9	10	STORET
Campbell	37.222633	-79.197755	6.6	30	STORET
Campbell	37.228466	-79.234976	7.5	10	STORET
Campbell	37.254855	-79.280809	6.4	500	STORET
Campbell	37.264577	-79.169144	5.64	50	STORET
Campbell	37.269022	-79.170533	5.44	10	STORET
Campbell	37.284577	-79.080257	6.1	10	STORET
Campbell	37.1693	-79.211644	6.58	60	STORET
Campbell	37.213188	-79.187199	7	20	STORET
Campbell	37.282356	-79.296919	6.2	50	STORET
Campbell	37.307078	-79.160811	5.61	50	STORET
Campbell	37.258188	-79.032202	6.18	50	STORET
Campbell	37.190967	-79.214699	6.42	50	STORET
Charlotte	36.908743	-78.529169	6.6	10	STORET
Charlotte	37.075687	-78.699718	6.6	10	STORET
Charlotte	37.010405	-78.492227	5.6	20	STORET
Charlotte	37.05374	-78.573058	6.6	10	STORET
Charlotte	36.779304	-78.626108	6.3	40	STORET
Charlotte	36.825136	-78.608054	6.7	10	STORET

Charlotte	36.992633	-78.701385	6.4	10	STORET
Charlotte	36.82708	-78.646108	5.9	10	STORET
Charlotte	36.820691	-78.596388	6	10	STORET
Charlotte	37.049851	-78.574724	6.4	10	STORET
Charlotte	37.060129	-78.612222	5.9	10	STORET
Charlotte	37.099019	-78.664164	6.6	10	STORET
Charlotte	36.917634	-78.653054	7.2	60	STORET
Floyd	37.108198	-80.157181	6.2	10	STORET
Floyd	37.110421	-80.154681	6.3	10	STORET
Floyd	37.099032	-80.178847	6.83	10	STORET
Floyd	37.120142	-80.136348	7.13	10	STORET
Floyd	37.101532	-80.180792	6.46	50	STORET
Franklin	37.016529	-80.059129	6.92	100	STORET
Franklin	37.080054	-79.934881	6.8	110	STORET
Franklin	37.100416	-79.889132	6.2	10	STORET
Franklin	37.178747	-79.718855	7	320	STORET
Franklin	37.217916	-79.811909	7.7	80	STORET
Franklin	37.210138	-79.804964	5.6	10	STORET
Franklin	37.194304	-79.82552	7	120	STORET
Franklin	37.158193	-79.83691	7.3	50	STORET
Franklin	37.158193	-79.839687	6	10	STORET
Franklin	37.094306	-80.050518	6.2	30	STORET
Franklin	36.837362	-79.940517	6	20	STORET
Franklin	36.875138	-79.758023	6	20	STORET
Franklin	37.087357	-79.690524	7.3	30	STORET
Franklin	37.102636	-79.700802	6.8	170	STORET
Franklin	37.035412	-79.651915	6.8	10	STORET
Franklin	37.147084	-80.01274	6.3	30	STORET
Franklin	37.034859	-79.829412	---	320	STORET
Franklin	37.039304	-79.9058	7.83	320	STORET
Franklin	36.91736	-79.889686	6.79	50	STORET
Franklin	37.109859	-79.844411	6.46	50	STORET
Halifax	36.779028	-78.764715	6.1	10	STORET
Halifax	36.875415	-78.788326	6.8	10	STORET
Halifax	36.598471	-79.073874	5.8	100	STORET
Halifax	36.752918	-78.960544	6.4	10	STORET
Henry	36.741751	-79.879683	7.1	10	STORET
Henry	36.827362	-79.991626	---	2000	STORET
Henry	36.655751	-79.868767	7.9	10	STORET
Henry	36.776446	-80.029207	7.2	1260	STORET
Henry	36.742084	-79.893294	7.6	20	STORET
Henry	36.632473	-79.851989	6.7	70	STORET
Henry	36.712834	-79.974875	5.9	30	STORET

Henry	36.723335	-80.034789	7.1	10	STORET
Henry	36.715696	-80.053011	6.24	50	STORET
Henry	36.74903	-79.95107	7.33	50	STORET
Henry	36.754306	-79.934404	6.2	20	STORET
Henry	36.743473	-79.694688	6.4	30	STORET
Henry	36.779862	-79.839963	6	30	STORET
Henry	36.792918	-79.895795	6.6	30	STORET
Henry	36.623473	-79.847461	6.4	60	STORET
Henry	36.623204	-80.944643	7.1	10	STORET
Henry	36.648473	-80.022455	6.6	20	STORET
Henry	36.749585	-80.037455	6.4	20	STORET
Henry	36.710141	-80.048844	6.9	20	STORET
Henry	36.687918	-79.965236	6.4	10	STORET
Henry	36.630973	-80.016067	6.8	20	STORET
Henry	36.592337	-79.89003	7.16	90	STORET
Mecklenburg	36.594857	-78.402502	6.5	50	STORET
Mecklenburg	36.596522	-78.142504	7.3	90	STORET
Mecklenburg	36.680414	-78.347224	6.4	80	STORET
Mecklenburg	36.575412	-78.218615	6.4	10	STORET
Mecklenburg	36.672358	-78.415835	6.4	10	STORET
Mecklenburg	36.573192	-78.666385	6.4	10	STORET
Mecklenburg	36.748193	-78.53861	6.4	10	STORET
Montgomery	37.176534	-80.238456	7.3	10	STORET
Montgomery	37.212869	-80.358646	7.5	30	STORET
Montgomery	37.1957	-80.239678	7.5	60	STORET
Montgomery	37.238506	-80.225985	---	430	STORET
Montgomery	37.090425	-80.389395	7.4	20	STORET
Montgomery	37.103479	-80.330231	7.4	10	STORET
Montgomery	37.110617	-80.255456	7.4	30	STORET
Montgomery	37.10181	-80.219929	6.3	610	STORET
Montgomery	37.170648	-80.405144	7.5	20	STORET
Montgomery	37.169314	-80.391339	7.3	20	STORET
Montgomery	37.16787	-80.408171	7.3	10	STORET
Montgomery	37.170176	-80.401534	7.4	10	STORET
Montgomery	37.166953	-80.413977	7.3	580	STORET
Montgomery	37.169176	-80.394478	7.4	10	STORET
Montgomery	37.162089	-80.254956	6.9	50	STORET
Montgomery	37.229037	-80.379395	7.2	10	STORET
Montgomery	37.23487	-80.362451	7.2	200	STORET
Montgomery	37.225703	-80.373007	7	40	STORET
Montgomery	37.199314	-80.39495	7.5	40	STORET
Montgomery	37.200981	-80.388006	7.3	60	STORET
Montgomery	37.192092	-80.38245	7.2	40	STORET

Montgomery	37.191259	-80.380228	7.3	40	STORET
Montgomery	37.190981	-80.374951	7.2	60	STORET
Montgomery	37.190981	-80.370507	7	140	STORET
Montgomery	37.184869	-80.352174	7.7	60	STORET
Montgomery	37.1457	-80.264122	7.2	80	STORET
Montgomery	37.24487	-80.393006	7.2	60	STORET
Montgomery	37.262369	-80.326619	7.3	70	STORET
Montgomery	37.192925	-80.366618	7.2	100	STORET
Montgomery	37.139312	-80.325231	7.3	10	STORET
Montgomery	37.140701	-80.313009	7.4	100	STORET
Montgomery	37.146256	-80.264122	7.3	60	STORET
Montgomery	37.144867	-80.26329	7.2	120	STORET
Montgomery	37.1432	-80.264677	7.1	140	STORET
Montgomery	37.1282	-80.263012	7	80	STORET
Montgomery	37.125978	-80.263011	7.4	80	STORET
Montgomery	37.130145	-80.254401	7.3	60	STORET
Montgomery	37.1757	-80.257178	7.1	80	STORET
Montgomery	37.209868	-80.2869	7	270	STORET
Montgomery	37.22959	-80.2769	6.5	800	STORET
Montgomery	37.222646	-80.281344	6.3	10	STORET
Montgomery	37.113758	-80.374673	7.2	70	STORET
Montgomery	37.107369	-80.370785	7.2	60	STORET
Montgomery	37.104869	-80.370507	7.2	30	STORET
Montgomery	37.10348	-80.36884	7.1	50	STORET
Montgomery	37.104036	-80.368007	7.2	40	STORET
Montgomery	37.112369	-80.365785	7.5	40	STORET
Montgomery	37.116813	-80.353563	7.6	30	STORET
Montgomery	37.117925	-80.348008	7.1	50	STORET
Montgomery	37.094312	-80.334674	7.7	40	STORET
Montgomery	37.094868	-80.335508	7.6	40	STORET
Montgomery	37.101812	-80.329398	7.2	20	STORET
Montgomery	37.246814	-80.392172	7.5	70	STORET
Montgomery	37.258759	-80.39606	7.8	50	STORET
Montgomery	37.274871	-80.396338	7.3	40	STORET
Montgomery	37.27626	-80.392727	7.2	170	STORET
Montgomery	37.283203	-80.371061	6.9	560	STORET
Montgomery	37.293759	-80.372449	7.3	30	STORET
Montgomery	37.086259	-80.429948	7.6	40	STORET
Montgomery	37.083759	-80.41856	7.3	50	STORET
Montgomery	37.093203	-80.414116	7.4	270	STORET
Montgomery	37.281257	-80.246066	7.3	340	STORET
Montgomery	37.280148	-80.368839	7.4	10	STORET
Montgomery	37.239311	-80.207457	7.2	10	STORET

Montgomery	37.10959	-80.305788	7.54	50	STORET
Montgomery	37.123758	-80.373285	7.82	50	STORET
Montgomery	37.289314	-80.375783	7.9	50	STORET
Patrick	36.643196	-80.200782	6.95	50	STORET
Patrick	36.606418	-80.12834	5.5	70	STORET
Patrick	36.626807	-80.29189	6.27	50	STORET
Patrick	36.663752	-80.106063	6.4	20	STORET
Patrick	36.733197	-80.377995	5.46	50	STORET
Patrick	36.751807	-80.09912	6.7	110	STORET
Patrick	36.751807	-80.098564	6.3	10	STORET
Patrick	36.649863	-80.203004	7.2	10	STORET
Patrick	36.63653	-80.213559	6.4	160	STORET
Patrick	36.654029	-80.096064	6.4	10	STORET
Patrick	36.59653	-80.28439	5.7	10	STORET
Patrick	36.604029	-80.217448	6.1	20	STORET
Patrick	36.696252	-80.44688	7.05	20	STORET
Patrick	36.642084	-80.114119	6.14	10	STORET
Patrick	36.75153	-80.097175	6.91	80	STORET
Patrick	36.553751	-80.140785	6.68	10	STORET
Patrick	36.841809	-80.220507	7.87	210	STORET
Patrick	36.605974	-80.406329	7.8	50	STORET
Patrick	36.82292	-80.195229	7.88	50	STORET
Patrick	36.769587	-80.277723	7.06	50	STORET
Patrick	36.800165	-80.366319	---	50	STORET
Pittsylvania	36.765419	-79.389142	7.58	210	STORET
Pittsylvania	36.748474	-79.387753	6.82	370	STORET
Pittsylvania	36.719862	-79.562748	6.6	10	STORET
Pittsylvania	36.616528	-79.498307	---	10	STORET
Pittsylvania	36.620418	-79.604691	6.22	10	STORET
Pittsylvania	36.614583	-79.539694	7.39	710	STORET
Roanoke	37.283116	-80.121958	---	10	STORET
Roanoke	37.196029	-79.998546	7.7	80	STORET
Roanoke	37.301059	-80.032959	7.7	20	STORET
Roanoke	37.316614	-79.932516	8	10	STORET
Roanoke	37.232446	-80.008211	7.6	10	STORET
Roanoke	37.254033	-80.187735	7.9	10	STORET
Roanoke	37.222917	-79.87163	6.2	10	STORET
Roanoke	37.257922	-80.177457	7.42	50	STORET
Roanoke	37.367367	-80.049124	6.53	890	STORET
Roanoke	37.280822	-79.890267	7.2	10	STORET
Roanoke	37.276761	-79.887439	7.02	50	STORET
Roanoke	37.324865	-80.025237	8.53	20	STORET
Roanoke	37.20125	-79.948297	8.21	10	STORET

Roanoke	37.237363	-80.046628	6.5	10	STORET
Roanoke	37.220141	-80.038572	6.2	10	STORET
Roanoke	37.228196	-80.035239	7.5	10	STORET
Roanoke	37.190973	-79.996629	6.7	36	STORET
Roanoke	37.199583	-79.942741	6.7	30	STORET
Roanoke	37.204306	-79.954407	7.6	40	STORET
Roanoke	37.20625	-79.945241	7.1	40	STORET
Roanoke	37.207362	-79.956629	7	50	STORET
Roanoke	37.204306	-79.954407	6.7	50	STORET
Roanoke	37.203194	-79.94663	6.7	30	STORET
Roanoke	37.28931	-80.141068	7.2	210	STORET
Roanoke	37.273199	-80.129958	6.7	70	STORET
Roanoke	37.278755	-80.154402	7.3	50	STORET
Roanoke	37.294309	-80.07107	7	10	STORET
Roanoke	37.301255	-80.087736	6.6	10	STORET
Roanoke	37.29014	-79.855796	7.35	10	STORET
Roanoke	37.29014	-79.855796	6.71	50	STORET
Roanoke	37.288199	-80.113292	7.5	10	STORET
Roanoke	37.257361	-79.891907	5.8	20	STORET
Roanoke	37.236806	-80.000795	6.8	40	STORET
Roanoke	37.194862	-79.999684	6.1	30	STORET
Roanoke	37.200697	-80.073294	7.3	50	STORET
Roanoke	37.244863	-80.026072	7.1	30	STORET
Roanoke	37.217641	-80.02385	6.1	30	STORET
Roanoke	37.228196	-80.009961	---	40	STORET
Roanoke	37.204029	-79.952741	6.8	60	STORET
Roanoke	37.20403	-80.032183	6.5	30	STORET
Roanoke	37.310419	-79.888572	6.9	30	STORET
Roanoke	37.318474	-79.899128	6.9	40	STORET
Roanoke	37.313474	-79.888572	6.8	30	STORET
Roanoke	37.315141	-79.888295	6.8	40	STORET
Roanoke	37.357365	-79.964681	7.2	60	STORET
Roanoke	37.355698	-79.96607	7.2	60	STORET
Roanoke	37.330975	-79.918294	6.7	20	STORET
Roanoke	37.339308	-79.935794	7.2	30	STORET
Roanoke	37.358198	-79.969681	7	10	STORET
Roanoke	37.326532	-80.022459	7.1	70	STORET
Roanoke	37.324032	-80.010515	7.2	70	STORET
Roanoke	37.255694	-79.898851	6.1	10	STORET
Roanoke	37.381256	-80.060512	5.9	70	STORET
Roanoke	37.369867	-80.057735	7.4	60	STORET
Roanoke	37.346531	-79.91496	7.7	10	STORET
Roanoke	37.203753	-80.073016	8.1	10	STORET

Roanoke	37.181528	-79.953852	7.36	10	STORET
Roanoke	37.205974	-80.049128	7.43	10	STORET
Roanoke	37.263753	-80.080793	8.03	10	STORET

APPENDIX E

Compilation of total Mn data from wells within geologic formations of interest in the Roanoke River watershed.

County	Latitude	Longitude	Formation	pH	Mn (ppb)	Source
Appomattox	37.465556	-78.943333	ABF	5.6	10	STORET
Appomattox	37.513611	-78.878611	ABF	6.6	10	STORET
Appomattox	37.311667	-78.901944	BF	6.4	10	STORET
Appomattox	37.347222	-78.906944	FMF	6.1	30	STORET
Appomattox	37.325556	-78.910556	FMF	6.4	30	STORET
Appomattox	37.455278	-78.873333	FMF	5.2	20	STORET
Appomattox	37.476667	-78.838056	FMF	5.7	10	STORET
Appomattox	37.331389	-78.866667	FMF	5.15	10	STORET
Appomattox	37.36199	-78.827354	FMF	6.8	50	STORET
Appomattox	37.346577	-78.854754	FMF	6.3	10	STORET
Bedford	37.046389	-79.575833	ABF	6.5	30	STORET
Bedford	37.081944	-79.575	ABF	6	10	STORET
Bedford	37.066111	-79.55	ABF	7.3	410	STORET
Bedford	37.146389	-79.664444	ABF	6.7	90	STORET
Bedford	37.143056	-79.656944	ABF	6.6	140	STORET
Bedford	37.151389	-79.6625	ABF	6.7	10	STORET
Bedford	37.088056	-79.573056	ABF	7	70	STORET
Bedford	37.116667	-79.569444	ABF	6.3	20	STORET
Bedford	37.146944	-79.597778	ABF	6.2	10	STORET
Bedford	37.126389	-79.643611	ABF	6.1	1300	STORET
Bedford	37.165833	-79.635556	AF	7.7	50	STORET
Bedford	37.254722	-79.398056	AF	6.8	10	STORET
Bedford	37.225278	-79.556111	AF	6.5	10	STORET
Bedford	37.044722	-79.551389	CF	6.7	60	STORET
Bedford	37.044444	-79.551944	CF	6.5	390	STORET
Campbell	37.226944	-79.226389	ABF	6.7	10	STORET
Campbell	37.37	-79.109722	ABF	7	30	STORET
Campbell	37.228611	-79.228611	ABF	6.6	10	STORET
Campbell	37.228611	-79.234722	ABF	7.5	10	STORET
Campbell	37.3625	-79.099167	ABF	7.2	10	STORET
Campbell	37.307222	-79.160556	ABF	5.61	50	STORET
Campbell	37.2825	-79.296667	AF	6.2	50	STORET
Campbell	37.161111	-79.083333	BF	6.09	20	STORET
Campbell	37.161111	-79.083333	BF	6.3	30	STORET
Campbell	37.161111	-79.083333	BF	6.3	20	STORET
Campbell	37.161111	-79.083333	BF	6.75	120	STORET
Campbell	37.161111	-79.083333	BF	6.07	50	STORET
Campbell	37.161111	-79.083333	BF	6.84	50	STORET

Campbell	37.161111	-79.083333	BF	6.23	120	STORET
Campbell	37.268889	-78.922778	BF	6.1	10	STORET
Campbell	37.155278	-79.228333	BF	6.3	30	STORET
Campbell	37.1925	-79.207778	BF	7.5	690	STORET
Campbell	37.169444	-79.211389	BF	6.58	60	STORET
Campbell	37.258333	-79.031944	BF	6.18	50	STORET
Campbell	37.191111	-79.214444	BF	6.42	50	STORET
Campbell	37.255	-79.280556	CF	6.4	500	STORET
Campbell	37.273889	-79.106111	FMF	6.55	20	STORET
Campbell	37.273889	-79.106111	FMF	6.3	20	STORET
Campbell	37.357778	-79.01	FMF	5.9	10	STORET
Campbell	37.2775	-79.129167	FMF	6.8	110	STORET
Campbell	37.100556	-79.113056	FMF	7.5	10	STORET
Campbell	37.209722	-79.206944	FMF	5.9	10	STORET
Campbell	37.222778	-79.1975	FMF	6.6	30	STORET
Campbell	37.264722	-79.168889	FMF	5.64	50	STORET
Campbell	37.269167	-79.170278	FMF	5.44	10	STORET
Campbell	37.284722	-79.08	FMF	6.1	10	STORET
Campbell	37.213333	-79.186944	FMF	7	20	STORET
Pittsylvania	37.097222	-79.3125	ABF	6.7	30	STORET
Pittsylvania	36.620556	-79.604444	AF	6.22	10	STORET
Pittsylvania	36.72	-79.5625	FMF	6.6	10	STORET
Pittsylvania	36.850278	-79.378611	FMF	6.4	144	STORET

Abbreviations for geologic formations:

ABF = Alligator Back Formation

AF = Ashe Formation

BF = Bassett Formation

CF = Candler Formation

FMF = Fork Mountain Format

APPENDIX F

Complete list of geochemical data for counties in which geologic formations of interested are located, within the Roanoke River watershed. All data was extracted from STORET (2014). All samples were unfiltered. Group 1: Mn<50 ppb; Group 2 50<Mn< 300 ppb; Group 3 Mn> 300 ppb.

Group	County	Latitude	Longitude	pH	Ca	Mg	K	Na	HCO ₃ ⁻	SO ₄ ²⁻	F	As	Cu	Fe	Pb	Mn	Ni	Zn	TDS
					mg/L	mg/L	mg/L	mg/L	mg/L	mg/L	mg/L	ppb	ppb	ppb	ppb	ppb	ppb	ppb	ppb
1	Appomattox	37.31152	-78.902206	6.4	11	5.7	0.5	6	65.8	1	0.06	1	10	30	2	10	10	80	56.8
1	Appomattox	37.26846	-78.714715	6.5	13	1.4	3	5	54.9	1.1	0.08	1	10	20	7	10	10	580	51.2
1	Appomattox	37.33124	-78.86693	---	5.3	1.3	1	2.9	---	---	---	---	40	20	---	10	10	40	10.6
1	Appomattox	37.34672	-78.854491	6.3	2.01	1.11	0.91	2.32	13.4	0.5	---	3	10	30	10	10	100	1500	15.1
1	Bedford	37.28236	-79.551635	6.3	19	2.3	4.2	16	58.5	10	0.1	---	780	60	10	10	---	80	81.3
1	Bedford	37.26847	-79.84663	6.1	3.4	1.4	1.2	5	24.4	5.8	0.18	1	460	120	8	10	10	20	29.6
1	Bedford	37.25458	-79.398306	6.8	21	8.7	1.3	9	96.3	7.3	0.1	1	20	40	1	10	10	100	94.9
1	Bedford	37.0818	-79.575248	6	5	2.2	1.7	7	26.8	1	0.11	1	10	600	5	10	10	1900	32.7
1	Bedford	37.13652	-79.649135	7.8	18	6.4	5.6	11	160.9	7.9	0.1	1	10	70	1	10	10	70	128.3
1	Bedford	37.14236	-79.500248	5.8	5	1.4	1.7	7	37.8	1	0.12	1	70	30	4	10	30	100	35.1
1	Bedford	37.23208	-79.805798	6	4	1.9	2.6	5	15.8	1	0.09	---	20	60	---	10	10	30	22.5
1	Bedford	37.26792	-79.847463	5.8	2.2	1	1.1	5	19.5	1	0.09	---	120	190	---	10	10	50	20.4
1	Bedford	37.25125	-79.807186	6.4	13	3.5	2	7	63.4	1	0.66	---	40	70	---	10	20	10	58.5
1	Bedford	37.39875	-79.700796	6.5	19	7.4	1.6	9	70.7	1	0.18	---	10	290	---	10	10	40	73.3
1	Bedford	37.22513	-79.556357	6.5	9	6.5	2	6	59.7	18.06	0.08	---	10	200	---	10	10	10	71.2
1	Bedford	37.28875	-79.786908	6.2	12	2.7	3	10	73.2	1	0.48	---	220	10	---	10	10	10	65.4
1	Bedford	37.28791	-79.604133	6	13	9.2	3.3	7	47.5	1	0.06	---	180	10	---	10	10	10	57.1
1	Bedford	37.26986	-79.718299	5.8	5	2	2	8	147.5	1	0.05	---	230	20	---	10	10	10	90.9
1	Bedford	37.29792	-79.82024	6.2	18	2.2	0.75	5	37.8	1	0.22	---	10	20	---	10	20	10	45.8
1	Bedford	37.28125	-79.844963	5.7	3	1.4	1.1	2	22.1	1	0.07	---	360	10	---	10	10	130	20.0
1	Bedford	37.38764	-79.553299	5.7	6	2.2	4.3	5	18.3	1	0.06	---	1000	10	---	10	10	1100	29.7
1	Bedford	37.47736	-79.659684	5.7	3	1.5	1.3	4	36.6	1	0.07	---	920	10	---	10	10	90	29.9
1	Bedford	37.15125	-79.662746	6.7	24	9.2	5.6	7	107.3	13.76	0.14	---	30	---	---	10	---	10	112.5
1	Bedford	37.44042	-79.678851	8.1	22	21	1.8	5	173.1	10.2	0.16	1	10	500	1	10	10	40	145.8
1	Bedford	37.31986	-79.738574	6.5	4	0.7	0.01	5	25.6	1	0.14	1	40	550	8	10	---	20	24.1

1	Bedford	37.30264	-79.462469	6.2	4	0.9	1.6	3	26.8	1.4	0.06	1	40	10	1	10	10	20	24.2
1	Bedford	37.24653	-79.805798	6.4	16	0.8	4.7	7	39	1	1.01	1	20	120	5	10	10	90	49.9
1	Bedford	37.2493	-79.783575	6.6	3	0.7	0.9	4	59.7	1	0.13	1	10	80	1	10	10	120	39.3
1	Bedford	37.24986	-79.801909	6.5	9	0.8	3.2	6	36.6	1	0.97	1	10	30	1	10	10	130	39.2
1	Bedford	37.24958	-79.802742	6.1	6	1.2	3	5	43.9	1	0.4	1	20	10	3	10	10	170	38.4
1	Bedford	37.24625	-79.804964	6.1	5	0.7	2.4	5	23.2	1	0.89	1	10	40	1	10	10	140	26.6
1	Bedford	37.24819	-79.803298	5.5	6	0.8	2.3	5	11	1	0.14	1	250	20	11	10	10	150	21.1
1	Bedford	37.25069	-79.798853	6.1	3	0.8	2	3	24.4	3.1	0.12	1	10	10	2	10	10	50	24.1
1	Bedford	37.24875	-79.794409	6	3	1	1.4	5	20.7	1	0.12	1	20	320	6	10	10	30	22.1
1	Bedford	37.2443	-79.798853	6	3	1.2	2.2	5	19.5	1	0.16	1	50	690	4	10	10	80	23.0
1	Bedford	37.2468	-79.798298	6.1	3	1	1.4	4	21.9	1	0.18	1	10	550	1	10	10	30	22.0
1	Bedford	37.24653	-79.798853	6.1	3	1.6	2.5	4	26.8	1.8	0.26	1	10	60	1	10	10	30	26.5
1	Bedford	37.24625	-79.796631	5.9	3	0.6	1.4	4	18.3	1	0.14	1	10	260	1	10	10	40	19.5
1	Bedford	37.40403	-79.710518	7.6	23	15	2.7	3	1.7	5.7	0.29	---	110	400	---	10	10	10	51.1
1	Bedford	37.44209	-79.662184	7.8	35	14	1.5	6	171.9	1	0.4	---	60	20	---	10	20	10	142.5
1	Bedford	37.34292	-79.713852	6.8	3	3	---	5	37.8	1	0.24	---	70	10	---	10	---	60	31.0
1	Bedford	37.1468	-79.598025	6.2	8	1.4	2	7	48.8	1	0.14	---	90	300	---	10	20	670	44.6
1	Bedford	37.44709	-79.679129	---	26.9	11.5	2.1	1.7	---	---	---	---	20	320	---	10	10	50	42.6
1	Campbell	37.2268	-79.226643	6.7	9	5	2	6	64.6	1	0.12	2	20	700	1	10	10	30	55.7
1	Campbell	37.26874	-78.92304	6.1	3	1.7	1.8	4	29.3	1.7	0.06	1	10	90	1	10	10	90	26.9
1	Campbell	37.10041	-79.113314	7.5	27	1	1	6	85.3	1	0.06	1	10	50	3	10	10	40	78.1
1	Campbell	37.22847	-79.228865	6.6	8	4	0.4	4	53.6	1	0.11	---	10	10	---	10	---	10	43.9
1	Campbell	37.20958	-79.207199	5.9	1	0.3	0.4	2	6	1	0.07	---	180	10	---	10	10	10	7.9
1	Campbell	37.22847	-79.234976	7.5	20	8.5	2.7	11	125.6	1	1.9	---	10	10	---	10	10	10	106.9
1	Campbell	37.26902	-79.170533	5.44	1.9	2.4	0.9	4.4	3.7	4.12	0.1	---	30	10	---	10	10	20	15.7
1	Campbell	37.28458	-79.080257	6.1	2.9	1.8	0.4	2.9	25.6	1.07	---	---	880	10	---	10	10	703	23.3
1	Franklin	37.10042	-79.889132	6.2	5	0.6	1.8	6	45.1	1.4	0.1	1	120	40	6	10	10	6700	44.0
1	Franklin	37.21014	-79.804964	5.6	3	0.9	2	5	6	1	0.03	1	20	120	6	10	10	50	15.1
1	Franklin	37.15819	-79.839687	6	6	1	1.8	5	34.1	1	0.07	1	430	140	6	10	10	30	32.3
1	Franklin	37.03541	-79.651915	6.8	8.8	6.1	2.4	4.7	67.1	1.1	0.1	---	10	80	---	10	10	30	56.3
1	Henry	36.74175	-79.879683	7.1	6	3	1.2	5	43.9	2	0.1	---	20	80	4	10	---	520	39.5

1	Henry	36.65575	-79.868767	7.9	32	8	4	10	150	16	0.18	---	640	7000	478	10	---	780	152.8
1	Henry	36.72334	-80.034789	7.1	39	2.6	2.4	12	97.5	3	0.07	1	1300	30	20	10	20	90	108.5
1	Henry	36.6232	-80.944643	7.1	17	4	2.7	11	84.1	4.1	0.08	1	70	150	2	10	20	10	80.5
1	Henry	36.68792	-79.965236	6.4	5.1	1.2	1.3	3.8	28	0.7	0.07	---	50	740	---	10	10	30	26.8
1	Patrick	36.75181	-80.098564	6.3	2	1	0.7	4	17.8	2.4	0.09	1	310	120	7	10	10	1700	21.1
1	Patrick	36.64986	-80.203004	7.2	2	0.6	1.2	3	18.5	1	0.11	---	30	20	---	10	10	50	17.1
1	Patrick	36.65403	-80.096064	6.4	11	3.1	2.3	7	65.8	1.2	0.1	---	90	10	---	10	10	50	57.2
1	Patrick	36.59653	-80.28439	5.7	1	0.6	1	1	7.3	1	0.1	---	140	140	---	10	10	30	8.6
1	Patrick	36.64208	-80.114119	6.14	5.3	1.1	1.4	2.2	19.6	1.25	0.1	---	140	30	---	10	10	10	21.2
1	Patrick	36.55375	-80.140785	6.68	3.9	1.4	1.5	5.7	33.3	1.68	0.1	---	30	110	---	10	10	30	30.8
1	Pittsylvania	36.71986	-79.562748	6.6	9	1.9	2	8	46.3	1.7	0.27	1	20	40	1	10	10	50	45.8
1	Pittsylvania	36.61653	-79.498307	---	3	2.6	1.2	8	---	---	---	1	10	30	1	10	10	20	14.9
1	Pittsylvania	36.62042	-79.604691	6.22	7.8	1.7	3.7	10.5	29.3	5.02	0.1	---	280	30	---	10	10	30	43.6
1	Bedford	37.1568	-79.643857	6.5	7	3.4	0.9	4	46.3	3	---	---	---	70	2	20	---	40	41.2
1	Bedford	37.3843	-79.58691	6.3	4	1	1.7	5	24.4	---	---	---	---	1300	37	20	---	1800	26.9
1	Bedford	37.40292	-79.713296	7.8	45	25	2.3	12	208.5	28.9	0.37	1	10	250	6	20	10	40	216.4
1	Bedford	37.11652	-79.569691	6.3	7	2.8	1.4	7	45.1	3.4	0.14	1	20	950	1	20	10	40	45.0
1	Bedford	37.24625	-79.797464	6.1	4	1.3	3.7	4	21.9	3.7	0.12	1	10	10	1	20	10	160	27.8
1	Bedford	37.24958	-79.798298	7.3	16	2.6	4.6	6	64.6	11.9	0.28	1	10	470	1	20	10	30	73.7
1	Campbell	37.07875	-78.884155	6.9	25	4	3	20	120.7	6	0.71	2	10	200	1	20	10	30	118.3
1	Campbell	37.21319	-79.187199	7	15.2	3.9	2.8	5.1	76.8	3.61	0.1	---	60	540	---	20	10	60	69.2
1	Franklin	36.83736	-79.940517	6	3	1.6	1.4	4	26.8	3.9	0.1	1	230	100	2	20	10	190	27.7
1	Franklin	36.87514	-79.758023	6	5	1	2	6	34.1	1	0.06	2	120	40	7	20	10	160	32.2
1	Henry	36.74208	-79.893294	7.6	24	6	3	21	115.8	8.28	0.09	---	50	40	---	20	10	20	119.4
1	Henry	36.75431	-79.934404	6.2	22	4.1	3	20	62.2	1	0.06	---	70	20	---	20	---	30	80.9
1	Henry	36.64847	-80.022455	6.6	14	5	5.2	7	58.5	18	0.07	1	300	250	7	20	10	180	78.8
1	Henry	36.74959	-80.037455	6.4	8	2.1	1.5	6	40.2	1.2	0.09	1	10	120	7	20	30	50	38.9
1	Henry	36.71014	-80.048844	6.9	12	1.8	2.5	6	58.5	1.4	0.09	1	120	310	11	20	10	170	53.2
1	Henry	36.63097	-80.016067	6.8	10.7	7.1	0.6	4.1	71.9	0.5	0.04	---	30	20	---	20	10	550	59.0
1	Patrick	36.66375	-80.106063	6.4	6	1.5	2.2	6	36.6	2.1	0.07	1	40	50	9	20	10	70	36.1
1	Patrick	36.60403	-80.217448	6.1	9	1.6	2.1	5	56.1	1	0.1	---	30	570	---	20	10	10000	57.0

1	Patrick	36.69625	-80.44688	7.05	14.7	0.7	1.8	3.1	39.5	3.3	0.1	---	40	1680	---	20	10	120	45.0
1	Appomattox	37.34708	-78.907205	6.1	2	1.5	0.6	3	18.8	1	0.08	1	10	280	3	30	10	70	17.8
1	Bedford	37.04624	-79.576081	6.5	19	1.8	3.9	17	57.3	11	0.1	---	10	3700	3	30	10	220	84.9
1	Bedford	37.29431	-79.782185	6.5	18	5.8	5.5	10	97.5	1	0.3	---	10	160	---	30	10	50	88.8
1	Bedford	37.24625	-79.794686	6.8	15	3.7	7	7	73.2	6.8	0.14	1	10	2500	1	30	10	100	78.3
1	Campbell	37.15513	-79.228588	6.3	3	2	2.6	4	18.3	11.9	0.16	1	20	880	1	30	10	230	33.8
1	Campbell	37.22263	-79.197755	6.6	9	2	3	7	46.3	10.9	0.17	---	10	1400	---	30	10	40	56.3
1	Franklin	37.09431	-80.050518	6.2	3	1	2	4	21.5	1	0.06	1	20	1700	7	30	10	4000	27.4
1	Franklin	37.08736	-79.690524	7.3	36	3.7	3.1	16	158.5	2	0.1	1	10	40	6	30	10	30	139.0
1	Franklin	37.14708	-80.01274	6.3	7.1	1.7	6.3	5.5	37.8	1.4	0.08	---	2290	140	---	30	10	160	43.3
1	Henry	36.71283	-79.974875	5.9	6	5.5	1.6	6	6.1	1.3	0.07	1	220	680	17	30	10	130	24.6
1	Henry	36.74347	-79.694688	6.4	6	1.3	1.6	7	37.8	1	0.06	1	10	70	5	30	70	150	35.9
1	Henry	36.77986	-79.839963	6	4	0.9	2.2	7	30.5	1	0.03	1	10	80	20	30	90	30	30.4
1	Henry	36.79292	-79.895795	6.6	9	2.5	1.4	5	51.2	1	0.08	1	10	360	19	30	90	40	44.7
1	Bedford	37.25042	-79.798853	6.2	8	2	5.2	4	29.3	8.5	0.19	1	10	10	4	40	10	300	42.7
1	Bedford	37.24014	-79.80552	6	7	0.8	2.8	5	28	2.9	1.67	1	10	20	1	40	10	80	34.1
1	Bedford	37.24736	-79.793298	6.4	7	1.7	5	6	37.8	2.8	0.13	1	60	1300	1	40	10	60	42.7
1	Campbell	37.30458	-79.049979	6.2	6	1.4	0.6	4	28	1.9	0.07	1	50	100	10	40	10	70	28.0
2	Appomattox	37.34969	-78.823696	7.24	25	7.5	1.3	6.7	110.1	5.51	---	---	50	50	---	50	50	50	100.4
2	Bedford	37.44458	-79.610519	6.6	6.8	1	1.3	6	30.1	2.4	0.61	---	50	50	---	50	50	50	33.2
2	Bedford	37.37347	-79.344138	7.2	7	2.3	1.7	4.7	---	1.2	0.1	---	70	50	---	50	50	110	17.3
2	Bedford	37.16569	-79.635802	7.7	16	4	6	8	241.4	14.2	0.06	1	20	1800	7	50	10	50	168.9
2	Bedford	37.35069	-79.283029	---	6	4.6	1.4	5.6	---	---	---	---	250	290	---	50	50	60	18.3
2	Bedford	37.44653	-79.608019	6.28	5.3	0.9	1.4	8.4	16.5	1.05	0.24	---	50	50	---	50	50	50	25.7
2	Bedford	37.25097	-79.787742	8	10	1.9	3.3	6	182.9	9.6	0.29	1	10	270	10	50	10	50	121.4
2	Bedford	37.37208	-79.579965	7.1	11	1.3	5.5	5	62.2	1.6	0.26	---	30	10	---	50	10	80	55.4
2	Bedford	37.30542	-79.766908	6.15	2.9	0.7	1.1	4.2	21.8	0.31	0.1	---	50	50	---	50	50	110	20.3
2	Campbell	37.26458	-79.169144	5.64	1.7	0.9	0.9	1.3	8.4	1.75	0.1	---	1650	70	---	50	10	340	12.9
2	Campbell	37.28236	-79.296919	6.2	2.3	1.1	1.2	3.2	24	1.3	0.1	---	70	50	---	50	50	50	21.3
2	Campbell	37.30708	-79.160811	5.61	0.7	0.6	0.7	0.7	9.1	1	0.1	---	50	50	---	50	50	50	8.5
2	Campbell	37.25819	-79.032202	6.18	2.9	1.6	1.2	2.8	23.5	1.3	0.1	---	50	50	---	50	50	50	21.7

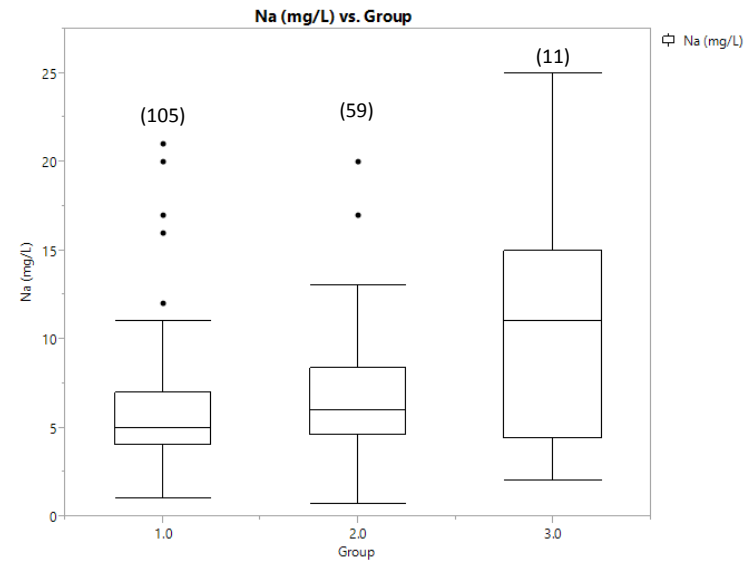
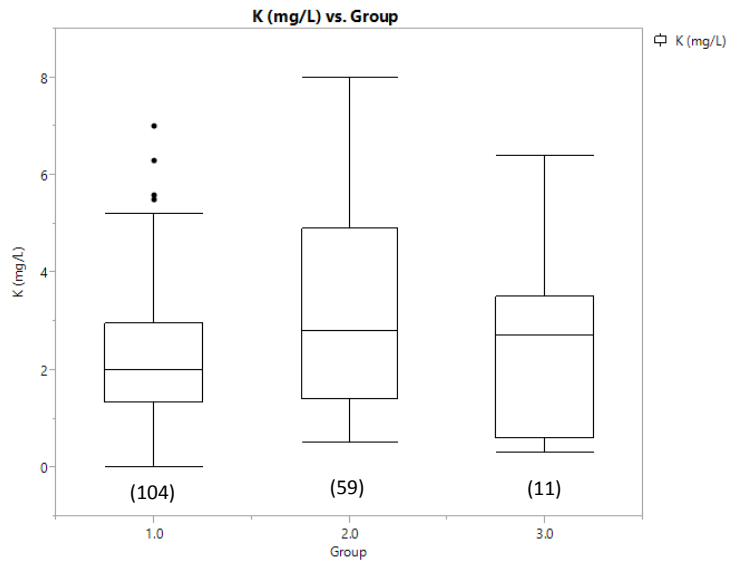
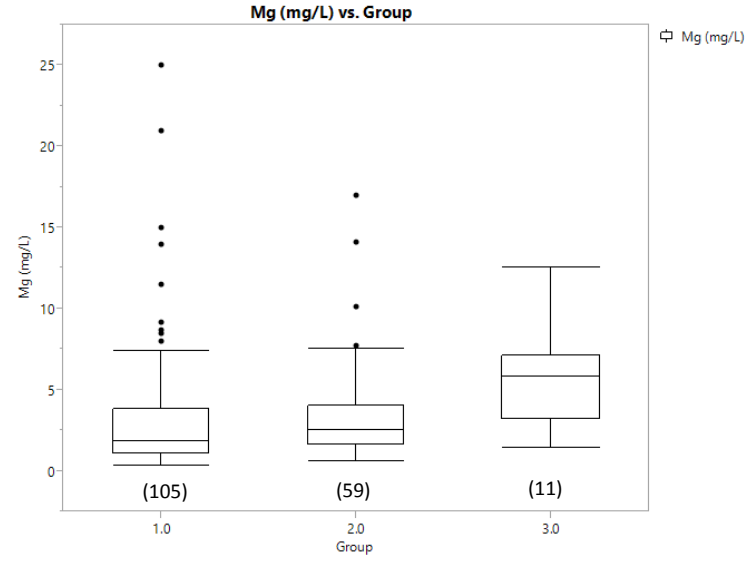
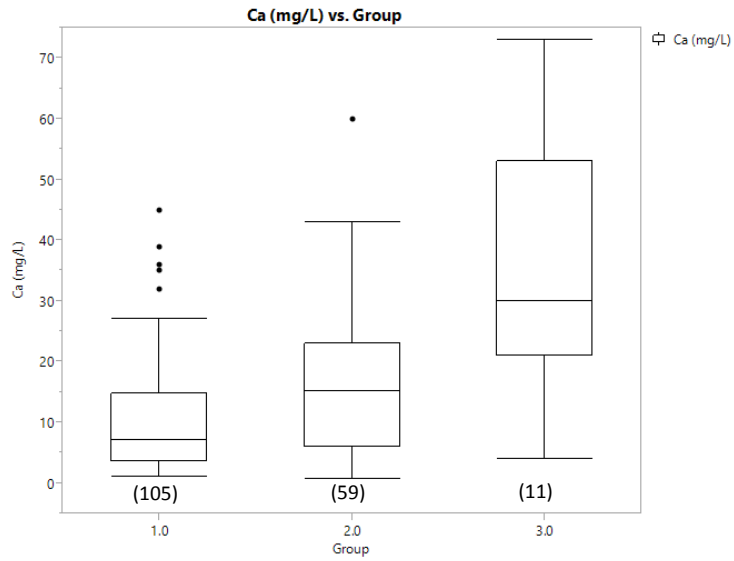
2	Campbell	37.19097	-79.214699	6.42	6.2	2.5	1.7	5.2	42.7	---	0.1	---	50	50	---	50	50	50	36.9
2	Franklin	37.15819	-79.83691	7.3	18	1.4	5.1	6	78	5.2	0.15	1	10	30	1	50	10	30	74.3
2	Franklin	36.91736	-79.889686	6.79	6	3.8	1.3	3.8	45.4	1.35	0.1	---	50	50	---	50	50	70	38.9
2	Franklin	37.10986	-79.844411	6.46	4.3	0.8	1.5	5.3	21.6	0.71	1.17	---	50	50	---	50	50	50	24.7
2	Henry	36.7157	-80.053011	6.24	6.2	2.9	0.8	3.5	37.8	0.4	0.12	---	50	60	---	50	50	330	33.0
2	Henry	36.74903	-79.95107	7.33	34	14.1	2.7	11.7	150.9	22.7	0.1	---	260	530	---	50	50	50	160.4
2	Patrick	36.6432	-80.200782	6.95	27.8	1.6	2.8	3.7	87.5	11.2	0.1	---	50	50	---	50	50	50	90.5
2	Patrick	36.62681	-80.29189	6.27	3.3	1.5	0.5	1.9	25.4	1.1	0.1	---	50	3900	---	50	50	2740	27.7
2	Patrick	36.7332	-80.377995	5.46	4.8	1.6	1.1	1.3	23.5	0.39	0.1	---	50	120	---	50	50	310	21.4
2	Patrick	36.60597	-80.406329	7.8	15.2	2.1	1.8	4.7	59.3	---	0.12	---	50	90	---	50	50	500	53.8
2	Patrick	36.82292	-80.195229	7.88	25.2	1.9	3.2	5.5	95.2	8.32	0.1	---	50	180	10	50	50	50	91.4
2	Patrick	36.76959	-80.277723	7.06	8.7	4.6	2.3	3	59	1.35	0.1	---	50	120	10	50	50	60	49.4
2	Patrick	36.80017	-80.366319	---	---	---	---	---	---	---	---	---	---	---	---	50	---	---	0.1
2	Bedford	37.29041	-79.498579	7.4	17	3.7	3	12	90.2	5.8	0.26	1	10	180	1	60	10	40	86.4
2	Bedford	37.38236	-79.623298	6.8	28	6.7	4.2	7	132.9	1	1.58	---	10	610	---	60	10	120	114.6
2	Bedford	37.04458	-79.551637	6.7	20	2.8	2	8	84.1	2.8	0.15	1	30	70	1	60	10	90	77.4
2	Bedford	37.27875	-79.810797	---	21.8	1.8	3.5	8.8	---	---	---	---	80	60	---	60	10	120	36.2
2	Campbell	37.1693	-79.211644	6.58	5.3	4.8	3.6	6.2	54.1	5.53	0.1	---	50	620	---	60	10	120	53.0
2	Henry	36.62347	-79.847461	6.4	23	2.7	2	11	78	11.5	0.15	1	10	180	55	60	20	10	89.0
2	Bedford	37.08791	-79.573304	7	15	3.3	4.5	7	74.4	3.2	0.21	1	10	260	2	70	10	40	70.2
2	Henry	36.63247	-79.851989	6.7	60	6.7	4.6	20	145.1	68.3	0.19	---	10	130	---	70	10	90	231.4
2	Patrick	36.60642	-80.12834	5.5	6	1.5	2.8	1	25.6	1	0.1	1	100	50	---	70	10	290	25.5
2	Bedford	37.24014	-79.596912	8	15	2.7	5.2	7	165.8	8.2	0.1	1	20	250	1	80	10	30	120.1
2	Bedford	37.25958	-79.739686	6.4	19	5.2	5.6	10	74.4	1	0.12	---	30	970	---	80	10	530	79.1
2	Franklin	37.21792	-79.811909	7.7	20	3.9	8	9	75.6	10	0.3	---	10	650	---	80	10	160	89.3
2	Patrick	36.75153	-80.097175	6.91	9.9	2.9	0.6	6.5	49.9	8.4	0.18	---	10	560	---	80	10	1340	55.0
2	Bedford	37.14625	-79.66469	6.7	19	6.4	5	6	95.1	7.76	0.06	---	10	1300	---	90	10	10	92.4
2	Bedford	37.24847	-79.799409	7.3	27	1.8	3.9	13	95.1	4.3	2.8	2	10	170	4	90	20	30	99.9
2	Bedford	37.27014	-79.732186	---	21.5	4.6	5.8	8.4	---	---	---	---	50	190	---	90	10	40	40.7
2	Henry	36.59234	-79.89003	7.16	7.2	3.5	2.5	5.3	48.4	6.5	0.13	---	10	1820	---	90	10	300	51.2
2	Bedford	37.28375	-79.749409	6.5	13	3.7	5.5	5	69.5	1.93	0.22	---	20	700	---	100	10	40	64.4

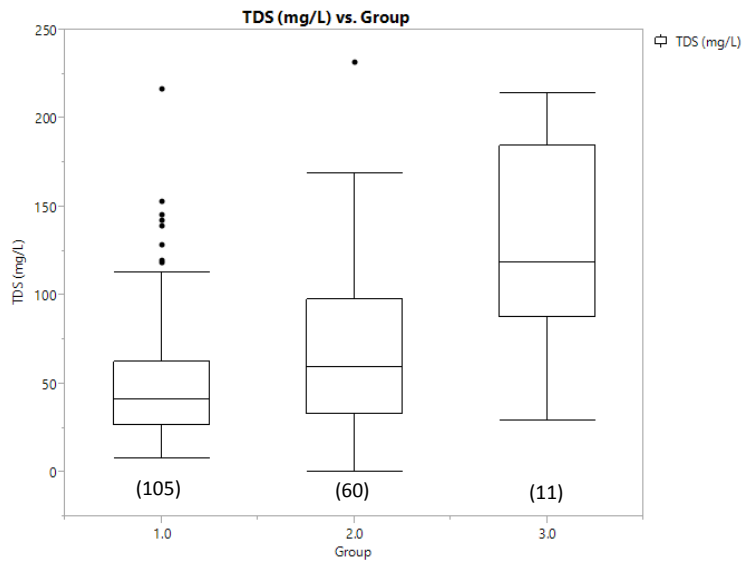
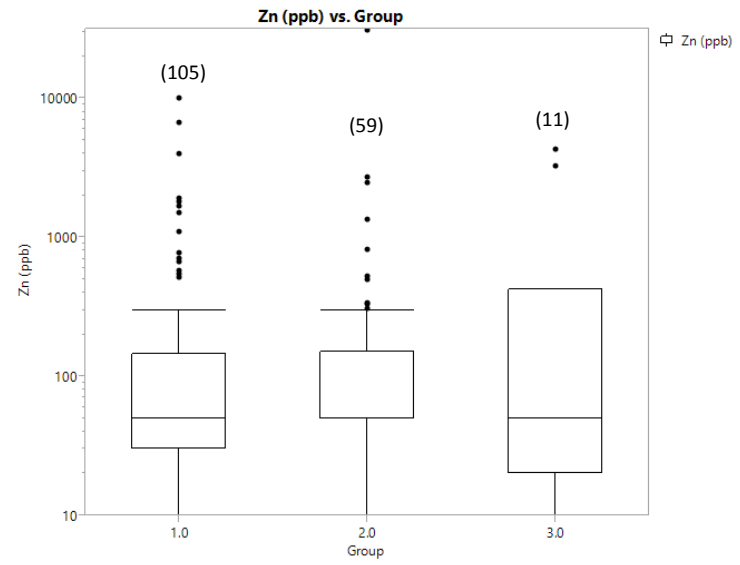
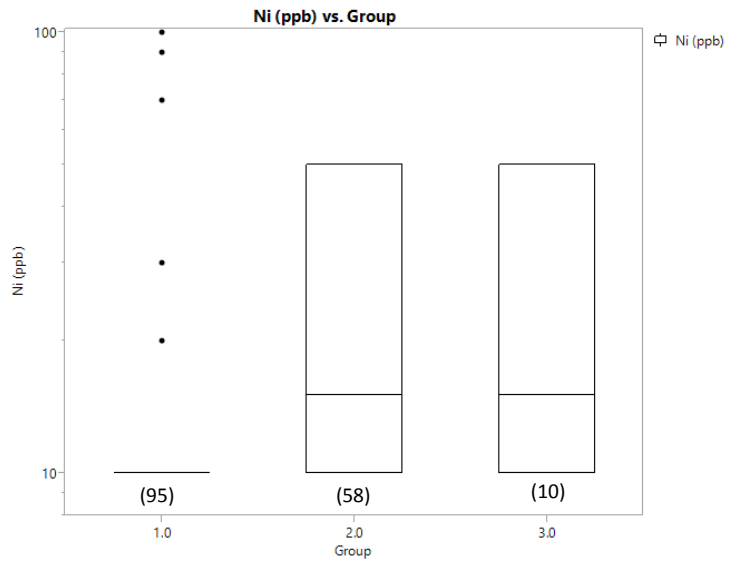
2	Bedford	37.24875	-79.801631	6	18	2.4	5.8	8	37.8	1.9	1.55	1	10	30	2	100	10	90	56.5
2	Franklin	37.01653	-80.059129	6.92	13	1.5	3	4.1	41.3	17	0.26	---	10	390	---	100	10	2470	62.1
2	Bedford	37.1993	-79.734688	7.01	24.4	4	7.2	7.9	100.6	4.97	0.1	---	10	1840	---	110	10	10	100.0
2	Franklin	37.08005	-79.934881	6.8	43	17	4.9	13	89	1	0.1	---	20	300	18	110	20	31000	154.2
2	Patrick	36.75181	-80.09912	6.7	5	2.6	1.7	9	41.5	7.1	0.21	---	10	1300	1	110	10	820	48.3
2	Bedford	37.24625	-79.804964	6.7	18	1.3	4.9	8	64.6	3.2	3.14	2	10	220	1	120	10	30	70.7
2	Campbell	37.16097	-79.083591	6.64	5.9	2.5	2.6	4.6	36.6	5.1	0.1	---	200	1230	---	120	50	50	40.4
2	Franklin	37.1943	-79.82552	7	32	1.6	2.6	5	63.4	9	0.2	---	20	80	---	120	40	20	81.9
2	Bedford	37.14291	-79.65719	6.6	25	10.1	5.6	17	143.9	7.9	0.08	---	10	7000	---	140	20	10	143.6
2	Patrick	36.63653	-80.213559	6.4	17	1.5	1.4	8	19.4	12.1	0.14	---	60	4600	---	160	10	290	54.8
2	Bedford	37.40819	-79.403025	7.6	28	2	5.5	4	112.2	7	0.1	---	90	180	2	170	---	20	102.2
2	Franklin	37.10264	-79.700802	6.8	21	5	3.9	9	104.9	11.9	0.15	1	10	2600	4	170	10	80	105.4
2	Appomattox	37.29263	-78.785823	---	13	2	0.7	5	---	---	---	1	10	7000	15	200	10	150	28.1
2	Patrick	36.84181	-80.220507	7.87	22.6	2.5	3.8	6.9	88.9	---	0.13	---	50	670	---	210	50	50	80.7
2	Pittsylvania	36.76542	-79.389142	7.58	29.7	7.7	0.9	8.4	141.4	6.1	0.19	---	50	2490	---	210	50	50	125.4
2	Bedford	37.38969	-79.553706	7.55	31.6	2.7	7.3	8.8	115.3	13.2	0.47	---	50	420	---	220	50	50	121.6
3	Franklin	37.17875	-79.718855	7	68	5.8	6.4	17	213.4	10.9	0.23	---	60	540	---	320	20	10	214.2
3	Franklin	37.03486	-79.829412	---	22.3	12.5	2	2.3	---	---	---	---	40	3600	---	320	10	50	43.1
3	Franklin	37.0393	-79.9058	7.83	39.4	2.3	3.5	4.4	129.1	8.88	0.13	---	50	1010	---	320	50	300	123.8
3	Pittsylvania	36.74847	-79.387753	6.82	3.88	9.2	0.5	14	185.6	6.1	0.19	---	50	320	---	370	50	50	126.0
3	Bedford	37.0443	-79.552192	6.5	22	3.9	2.7	10	96.3	2.2	0.12	1	20	390	11	390	50	3300	92.4
3	Bedford	37.06597	-79.550248	7.3	30	4.7	2.7	11	121.9	8.4	0.27	1	10	800	1	410	10	30	118.3
3	Campbell	37.25486	-79.280809	6.4	4	3.2	0.3	2	30.5	3.2	0.12	---	10	500	---	500	10	60	28.9
3	Campbell	37.19236	-79.208033	7.5	53	6	5.3	15	207.3	1	0.31	1	10	1300	4	690	30	20	184.6
3	Pittsylvania	36.61458	-79.539694	7.39	52.9	7.1	0.6	14.6	209.7	13.2	0.3	---	10	290	---	710	10	10	192.8
3	Henry	36.77645	-80.029207	7.2	21	1.4	1.2	5	85.3	11	0.1	---	20	350	4	1260	---	4300	87.6
3	Henry	36.82736	-79.991626	---	73	6.9	3	25	---	---	---	---	10	5100	---	2000	10	420	115.4

Note: Total dissolved solids (TDS) was calculated by summing together the concentrations of all available analytes. Data points with a “---” entry represent analytes where data is unavailable. Group 1: Total Mn concentrations <50 ppb; Group 2: Total Mn concentrations >50 ppb and <300 ppb; Group 3: Total Mn concentrations >300 ppb.

APPENDIX G

Additional boxplots and statistical tests performed using data from Appendix F





P-values for group comparisons

		Group (Ca)		
		1	2	3
Group (Ca)	1	----	0.000337	0.000322
	2	0.000337	----	0.000337
	3	0.000322	0.0103	-----

		Group (Zn)		
		1	2	3
Group (Zn)	1	----	0.209	0.810
	2	0.209	----	0.819
	3	0.810	0.819	-----

		Group (Mg)		
		1	2	3
Group (Mg)	1	----	0.469	0.390
	2	0.469	----	0.198
	3	0.390	0.198	-----

		Group (TDS)		
		1	2	3
Group (TDS)	1	----	0.00653	0.000167
	2	0.00653	----	0.00468
	3	0.000167	0.00468	-----

		Group (K)		
		1	2	3
Group (K)	1	----	0.0132	0.743
	2	0.0132	----	0.325
	3	0.743	0.325	-----

		Group (Na)		
		1	2	3
Group (Na)	1	----	0.175	0.0631
	2	0.175	----	0.0757
	3	0.0631	0.0757	-----

		Group (Ni)		
		1	2	3
Group (Ni)	1	----	2.378 x 10 ⁻⁷	0.00200
	2	2.378 x 10 ⁻⁷	----	0.766
	3	0.00200	0.766	-----

Appendix H

Groundwater data from Chapman (2013) from samples within the Piedmont and Blue Ridge crystalline aquifers in Virginia. Data are grouped based on their Mn concentrations. Group 1: Mn <50 ppb; Group 2: Mn >50 ppb and <300 ppb; Group 3: Mn >300 ppb.

Group	County	Latitude	Longitude	DO (mg/L)	pH	Mn (ppb)
1	PRINCE	38.630667	-77.38666667	7.2	5.9	<0.2
1	PRINCE	38.6945	-77.30133333	6.4	6.2	<0.2
1	AMELIA	37.421389	-78.06988889	7.4	5.8	<1
1	GRAYSO	36.691111	-81.27	1.02	6.9	<1
1	CARROL	36.796389	-80.85166667	7.2	6.2	<1
1	LOUDOU	39.142397	-77.7163958	3.9	6.1	<1
1	FAIRFA	38.886333	-77.36388333	1.8	6.2	<1
1	STAFFO	38.468	-77.43271667	7.2	5.8	<1
1	PRINCE	38.614806	-77.34361111	8.2	6.2	<1
1	PRINCE	38.659525	-77.37393889	8.1	6	<1
1	PRINCE	38.662269	-77.313625	9.4	6	<1
1	PRINCE	38.670067	-77.32255	8.3	5.7	<1
1	FAIRFA	38.814983	-77.42163333	8	5.84	<1
1	STAFFO	38.45165	-77.48165067	7.9	6.2	<1
1	LOUDOU	39.258025	-77.630475	7.5	6.6	<1
1	PRINCE	38.693747	-77.53623056	8.6	5.3	<1
1	MECKLE	36.660194	-78.37816667	5.5	5.4	2
1	HALIFA	36.825694	-78.967	7.3	5.3	2
1	FAIRFA	38.884767	-77.27246667	3.5	6.3	2
1	FAUQUI	38.509847	-77.60387639	8.3	5.6	3
1	FLOYD	36.831389	-80.44666667	8.3	6.1	3
1	CARROL	36.780556	-80.55444444	3.9	5.6	3
1	FAIRFA	38.73165	-77.23283333	6.9	5.9	3
1	LOUDOU	39.162892	-77.76908333	2.6	7.2	4
1	CARROL	36.703056	-80.51	3.1	5.5	4
1	CARROL	36.781389	-81.01805556	4.8	5	4
1	PITTSY	36.677944	-79.38880556	2.5	5.4	7
1	LOUDOU	39.050256	-77.49325556	0.8	7.3	7
1	LOUDOU	39.12455	-77.77943863	0.11	7.6	8
1	GRAYSO	36.6275	-81.47888889	6.5	5.6	8
1	GRAYSO	36.680833	-81.07055556	0.12	6.2	9
1	PRINCE	38.619353	-77.37301111	1.2	6.2	10
1	CHARLO	37.053778	-78.48972222	6.5	5.3	10
1	LOUDOU	39.066731	-77.46764167	4.2	6	10
1	CHARLO	37.073972	-78.84366667	6.8	5.7	12
1	APPOMA	37.390722	-78.64222222	3	6	14
1	CARROL	36.653889	-80.78666667	5.6	4.8	14

1	GRAYSO	36.608889	-81.1575	9.4	4.9	15
1	PRINCE	38.716158	-77.48853889	2.8	7.1	16
1	FAIRFA	38.991717	-77.36626667	5.85	5.08	17
1	PRINCE	37.194917	-78.24719444	6	4.8	18
1	BRUNSW	36.832056	-77.9575	4.2	5.4	18
1	LOUDOU	39.135383	-77.69665935	1.3	7.4	22
1	CUMBER	37.446667	-78.20888889	0.7	5.1	22
1	LOUDOU	38.981025	-77.651425	0.1	7.3	25
1	MECKLE	36.690306	-78.14880556	0.2	5.9	30
1	POWHAT	37.484333	-77.86655556	4.1	5.8	30
1	MONTGO	37.001944	-80.52277778	4.2	6.2	31
1	FLOYD	36.936111	-80.31555556	2.4	5.3	36
1	CUMBER	37.628806	-78.11466667	1.5	5.1	42
1	PRINCE	38.618333	-77.35216667	0.4	7.1	49
2	LOUDOU	38.95645	-77.50770556	4.7	4.8	51
2	FAIRFA	38.769972	-77.33913889	0.5	6.1	62
2	HALIFA	36.753028	-79.14977778	6.6	6	66
2	LOUISA	37.91875	-78.07813889	2.4	5.5	70
2	PRINCE	38.673017	-77.39945	0.5	6.9	88
2	MONTGO	37.022778	-80.44333333	1	5.9	91
2	HALIFA	36.675306	-78.84744444	8.6	7.1	98
2	POWHAT	37.508722	-77.97075	1.5	5.8	101
2	DINWID	37.11575	-77.80966667	0.6	5.1	103
2	LOUDOU	38.989342	-77.57297778	3.9	6.2	107
2	PRINCE	38.790947	-77.61050278	0.64	6.6	109
2	SPOTSY	38.059389	-77.76438889	8.7	5.6	127
2	HENRIC	37.638201	-77.47331731	6	5.5	138
2	FAIRFA	38.850056	-77.24631944	0.3	6.5	191
2	CARROL	36.641944	-80.86138889	3.3	5.2	196
2	FAUQUI	38.594314	-77.61531944	0.15	6.8	244
3	FLOYD	36.913889	-80.31111111	0.14	6.6	584
3	FLOYD	36.870278	-80.43083333	1.4	6.7	621
3	BRUNSW	36.588944	-77.9815	3.6	4.9	722
3	BUCKIN	37.643889	-78.29369444	1.1	5.9	1000
3	PRINCE	38.751853	-77.56401944	0.22	6.4	1490

Note: For concentrations below detection limits (" $<$ "), a concentration one-half of the detection limit was used in statistical tests.

APPENDIX I

Well data obtained from STORET (2014) used for the production of a regional potentiometric surface map in the Roanoke River watershed.

County/City	Latitude	Longitude	Elevation (famsl)	Static Water Level (ft)	Hydraulic head (ft)
Appomattox	37.348922	-78.826513	780	6	774
Appomattox	37.375	-78.838	830	9	821
Appomattox	37.35275	-78.814733	790	11	779
Appomattox	37.406799	-78.815541	835	20	815
Appomattox	37.365552	-78.829857	859	25	834
Appomattox	37.393466	-78.889705	675	25	650
Appomattox	37.332673	-78.77751	835	25	810
Appomattox	37.349692	-78.823696	795	27	768
Appomattox	37.309854	-78.901095	640	30	610
Appomattox	37.297353	-78.741658	690	30	660
Appomattox	37.455134	-78.873593	815	30	785
Appomattox	37.34245	-78.816901	880	31	849
Appomattox	37.408188	-78.817207	855	35	820
Appomattox	37.362495	-78.829798	855	37	818
Appomattox	37.311521	-78.902206	680	38	642
Appomattox	37.268463	-78.714715	715	40	675
Appomattox	37.247629	-78.683884	690	40	650
Appomattox	37.346723	-78.854491	770	45	725
Appomattox	37.331243	-78.86693	640	45	595
Appomattox	37.346723	-78.854714	783	45	738
Appomattox	37.513468	-78.87887	710	46	664
Appomattox	37.395686	-78.640272	493	48	445
Appomattox	37.355687	-78.723879	665	49	616
Appomattox	37.359022	-78.827208	760	50	710
Appomattox	37.325411	-78.910817	760	50	710
Appomattox	37.476523	-78.838317	700	50	650
Appomattox	37.364298	-78.764988	725	50	675
Appomattox	37.322908	-78.659716	620	50	570
Appomattox	37.362888	-78.823013	846	52	794
Appomattox	37.350443	-78.810718	814	60	754
Appomattox	37.377633	-78.793598	765	80	685
Appomattox	37.362135	-78.82709	850	85	765
Appomattox	37.346798	-78.804709	765	110	655
Appomattox	37.347077	-78.907205	880	165	715
Appomattox	37.292631	-78.785823	690	250	440
Bedford	37.448751	-79.606352	2510	8	2502

Bedford	37.391527	-79.555799	875	9	866
Bedford	37.373445	-79.709963	925	11	914
Bedford	37.533195	-79.361634	820	12	808
Bedford	37.358746	-79.286918	840	15	825
Bedford	37.42857	-79.498363	940	18	922
Bedford	37.540695	-79.392466	800	20	780
Bedford	37.407637	-79.403858	930	20	910
Bedford	37.408192	-79.403025	930	20	910
Bedford	37.532918	-79.414133	1000	20	980
Bedford	37.150413	-79.644413	890	20	870
Bedford	37.105412	-79.598025	820	20	800
Bedford	37.116523	-79.569691	1000	20	980
Bedford	37.372082	-79.579965	1025	20	1005
Bedford	37.442085	-79.662184	1080	20	1060
Bedford	37.556763	-79.412444	1079	21	1058
Bedford	37.201525	-79.699411	970	25	945
Bedford	37.260137	-79.73191	1000	25	975
Bedford	37.259581	-79.732187	1000	25	975
Bedford	37.422638	-79.505522	920	25	895
Bedford	37.40403	-79.710518	1065	25	1040
Bedford	37.1468	-79.598025	1055	25	1030
Bedford	37.305967	-79.305807	900	30	870
Bedford	37.398191	-79.259695	730	30	700
Bedford	37.500416	-79.266081	660	30	630
Bedford	37.338747	-79.453025	870	30	840
Bedford	37.422916	-79.4933	860	30	830
Bedford	37.21847	-79.741632	960	30	930
Bedford	37.30625	-79.779408	1280	30	1250
Bedford	37.536806	-79.403855	1040	30	1010
Bedford	37.457359	-79.275527	920	30	890
Bedford	36.980776	-79.283366	900	30	870
Bedford	37.319856	-79.29414	900	30	870
Bedford	37.472637	-79.266082	925	30	895
Bedford	37.16569	-79.635802	989	30	959
Bedford	37.35069	-79.283029	940	30	910
Bedford	37.254577	-79.398306	785	30	755
Bedford	37.076244	-79.55997	800	30	770
Bedford	37.342917	-79.713852	2080	30	2050
Bedford	37.305417	-79.766908	1130	30	1100
Bedford	37.481249	-79.277471	1220	31	1189
Bedford	37.302635	-79.462469	780	32	748

Bedford	37.199303	-79.734688	880	32	848
Bedford	36.978025	-79.30681	890	33	857
Bedford	37.38653	-79.736434	990	35	955
Bedford	37.087912	-79.573304	840	35	805
Bedford	37.318467	-79.284696	890	35	855
Bedford	37.452637	-79.261917	920	37	883
Bedford	37.251249	-79.801075	1030	37	993
Bedford	37.305967	-79.306362	910	40	870
Bedford	37.305134	-79.251364	900	40	860
Bedford	37.203744	-79.411639	940	40	900
Bedford	37.046244	-79.576081	810	40	770
Bedford	37.500416	-79.26497	660	40	620
Bedford	36.986942	-79.218895	820	40	780
Bedford	37.365414	-79.426914	800	40	760
Bedford	37.312914	-79.567745	970	40	930
Bedford	37.215415	-79.747743	920	40	880
Bedford	37.063744	-79.462193	640	40	600
Bedford	37.329026	-79.583577	970	40	930
Bedford	37.251522	-79.406917	830	40	790
Bedford	37.343471	-79.663298	1000	40	960
Bedford	37.526529	-79.412744	1040	40	1000
Bedford	37.330136	-79.517467	1100	40	1060
Bedford	37.418747	-79.281917	880	40	840
Bedford	37.21569	-79.566079	890	40	850
Bedford	37.414306	-79.635241	1160	40	1120
Bedford	36.980358	-79.333697	820	40	780
Bedford	37.069578	-79.595526	830	40	790
Bedford	36.979942	-79.289338	920	40	880
Bedford	37.533195	-79.361912	820	40	780
Bedford	37.065966	-79.550248	820	40	780
Bedford	37.304858	-79.563578	1010	40	970
Bedford	37.230968	-79.614967	947	40	907
Bedford	37.314858	-79.568301	970	43	927
Bedford	37.425974	-79.714129	1120	45	1075
Bedford	36.990387	-79.209868	820	47	773
Bedford	37.246249	-79.804964	910	47	863
Bedford	37.363838	-79.706359	1070	47	1023
Bedford	37.418748	-79.336359	900	48	852
Bedford	37.249582	-79.798298	985	48	937
Bedford	37.147635	-79.660246	840	50	790
Bedford	37.193746	-79.600246	890	50	840

Bedford	37.098189	-79.628025	820	50	770
Bedford	37.400136	-79.323305	920	50	870
Bedford	37.211524	-79.588857	840	50	790
Bedford	37.314302	-79.568023	970	50	920
Bedford	37.313747	-79.567745	970	50	920
Bedford	37.379025	-79.403303	870	50	820
Bedford	37.419302	-79.283306	880	50	830
Bedford	37.330968	-79.294695	900	50	850
Bedford	37.386803	-79.406636	860	50	810
Bedford	37.384581	-79.404414	920	50	870
Bedford	36.982691	-79.330975	840	50	790
Bedford	37.351802	-79.460524	910	50	860
Bedford	37.044577	-79.551637	800	50	750
Bedford	37.249304	-79.783575	980	50	930
Bedford	37.065689	-79.58497	840	52	788
Bedford	36.99047	-79.225089	800	54	746
Bedford	37.09705	-79.623525	840	55	785
Bedford	37.097912	-79.627191	840	55	785
Bedford	37.466526	-79.276638	890	55	835
Bedford	36.970996	-79.687553	980	55	925
Bedford	37.267356	-79.49608	820	55	765
Bedford	37.249582	-79.802742	1000	55	945
Bedford	37.246527	-79.805798	920	56	864
Bedford	37.443748	-79.328581	1020	57	963
Bedford	37.242592	-79.622643	1020	59	961
Bedford	37.0518	-79.580804	840	60	780
Bedford	37.453192	-79.252194	850	60	790
Bedford	37.126801	-79.64469	960	60	900
Bedford	37.193746	-79.600246	890	60	830
Bedford	37.126524	-79.643857	940	60	880
Bedford	37.474581	-79.257749	900	60	840
Bedford	37.141524	-79.614135	950	60	890
Bedford	37.14819	-79.660802	860	60	800
Bedford	37.337914	-79.451358	870	60	810
Bedford	37.09705	-79.623525	840	60	780
Bedford	37.09705	-79.623525	840	60	780
Bedford	37.103468	-79.625803	850	60	790
Bedford	37.111523	-79.589969	890	60	830
Bedford	37.329026	-79.583577	970	60	910
Bedford	37.449581	-79.24525	850	60	790
Bedford	37.378468	-79.273584	860	60	800

Bedford	37.474026	-79.231917	820	60	760
Bedford	37.46347	-79.25886	840	60	780
Bedford	37.373469	-79.344138	850	60	790
Bedford	36.996802	-79.297476	640	60	580
Bedford	36.986663	-79.688998	1030	60	970
Bedford	37.383747	-79.396914	980	60	920
Bedford	37.261801	-79.548857	980	60	920
Bedford	36.986469	-79.329753	960	60	900
Bedford	37.274389	-79.830658	1030	60	970
Bedford	37.358747	-79.439969	900	60	840
Bedford	37.457359	-79.275527	920	60	860
Bedford	37.382358	-79.408858	920	60	860
Bedford	37.384581	-79.409414	940	60	880
Bedford	37.524584	-79.385523	825	60	765
Bedford	37.0818	-79.575248	890	60	830
Bedford	37.36458	-79.393026	890	60	830
Bedford	37.240135	-79.596912	810	60	750
Bedford	37.240967	-79.541358	970	60	910
Bedford	37.301802	-79.547189	970	60	910
Bedford	37.142355	-79.500248	885	60	825
Bedford	37.044299	-79.552192	810	60	750
Bedford	37.240138	-79.80552	860	60	800
Bedford	37.337636	-79.439691	900	65	835
Bedford	37.329026	-79.583577	970	65	905
Bedford	37.330968	-79.293029	900	65	835
Bedford	37.050966	-79.580526	840	70	770
Bedford	37.354583	-79.65302	978	70	908
Bedford	37.070688	-79.53497	850	70	780
Bedford	37.383469	-79.399414	980	70	910
Bedford	37.469859	-79.23775	880	70	810
Bedford	37.290413	-79.498579	885	70	815
Bedford	37.136524	-79.649135	810	70	740
Bedford	37.319861	-79.738574	1080	70	1010
Bedford	37.250416	-79.798853	1020	70	950
Bedford	37.248749	-79.801631	940	70	870
Bedford	37.248749	-79.794409	980	70	910
Bedford	37.250971	-79.787742	1000	71	929
Bedford	37.250693	-79.798853	1010	72	938
Bedford	37.337358	-79.451636	870	73	797
Bedford	37.398752	-79.744962	1140	75	1065
Bedford	37.244304	-79.798853	940	77	863

Bedford	37.251249	-79.796075	1010	78	932
Bedford	37.432359	-79.277749	920	80	840
Bedford	37.085689	-79.576915	880	80	800
Bedford	37.428471	-79.403579	960	80	880
Bedford	37.161802	-79.694967	800	80	720
Bedford	37.207357	-79.624689	900	80	820
Bedford	37.248471	-79.799409	980	86	894
Bedford	37.246249	-79.804964	910	87	823
Bedford	37.25569	-79.558302	1000	90	910
Bedford	37.366248	-79.516078	910	90	820
Bedford	37.38458	-79.401636	960	90	870
Bedford	37.402919	-79.713296	1040	90	950
Bedford	37.24986	-79.801909	1000	109	891
Bedford	37.246804	-79.798298	960	110	850
Bedford	37.24736	-79.793298	950	116	834
Bedford	37.246527	-79.798853	980	116	864
Bedford	37.533195	-79.361634	820	120	700
Bedford	37.141801	-79.649413	970	122	848
Bedford	37.434028	-79.534687	1550	122	1428
Bedford	37.246249	-79.796631	990	125	865
Bedford	37.141524	-79.650246	920	128	792
Bedford	37.110142	-79.618231	940	130	810
Bedford	37.246249	-79.797464	990	145	845
Bedford	37.428472	-79.53191	1450	154	1296
Bedford	37.248193	-79.803298	980	158	822
Bedford	37.248471	-79.832185	1100	160	940
Bedford	37.389782	-79.554649	865	7	858
Bedford	37.39132	-79.555255	865	9	856
Bedford	37.389687	-79.553706	865	13	852
Bedford	37.390512	-79.555565	875	13	862
Bedford	37.096111	-79.579166	840	10	830
Bedford	37.338728	-79.452234	870	20	850
Bedford	37.094156	-79.570633	921	28	893
Bedford	0	0	680	30	650
Bedford	37.296995	-79.354145	919	30	889
Bedford	37.29743	-79.354237	900	35	865
Bedford	37.535696	-79.360754	715	40	675
Bedford	37.069731	-79.594962	837	40	797
Bedford	37.298576	-79.354935	860	40	820
Bedford	37.0975	-79.5775	855	40	815
Bedford	37.535533	-79.360592	715	42	673

Bedford	37.062525	-79.546893	845	42	803
Bedford	37.096111	-79.58	835	44	791
Bedford	37.096666	-79.411666	800	44	756
Bedford	37.063878	-79.546333	830	46	784
Bedford	37.066081	-79.585004	840	48	792
Bedford	37.535352	-79.360485	718	50	668
Bedford	37.297838	-79.35552	874	55	819
Bedford	37.33515	-79.578804	1004	60	944
Bedford	37.104129	-79.597971	854	60	794
Bedford	37.099694	-79.625748	860	70	790
Bedford	37.385411	-79.720867	1030	70	960
Bedford	37.195331	-79.684997	1090	88	1002
Bedford	37.533383	-79.361375	825	90	735
Bedford	37.533176	-79.361348	820	90	730
Bedford	37.14172	-79.649185	934	122	812
Bedford	37.141586	-79.649556	930	128	802
Campbell	37.32816	-78.978184	850	10	840
Campbell	37.192356	-79.208033	785	15	770
Campbell	37.209794	-79.049086	706	20	686
Campbell	37.30217	-79.149478	912	20	892
Campbell	37.259022	-79.181644	890	20	870
Campbell	37.196824	-79.197792	855	25	830
Campbell	37.112333	-79.012083	665	25	640
Campbell	37.247911	-79.246921	710	25	685
Campbell	37.228466	-79.228865	730	29	701
Campbell	37.385023	-79.06588	531	30	501
Campbell	37.331628	-78.983481	876	30	846
Campbell	37.160967	-79.083591	725	30	695
Campbell	37.357633	-79.010257	775	30	745
Campbell	37.329856	-79.119977	760	30	730
Campbell	37.132356	-79.29942	680	30	650
Campbell	37.209577	-79.207199	830	31	799
Campbell	37.362356	-79.099422	690	31	659
Campbell	37.227355	-79.237476	800	32	768
Campbell	37.1693	-79.211644	845	34	811
Campbell	37.102397	-78.995028	657	35	622
Campbell	37.268743	-78.92304	710	35	675
Campbell	37.213188	-79.187199	885	35	850
Campbell	37.301944	-79.148333	892	37	855
Campbell	37.273744	-79.106367	882	40	842
Campbell	37.222633	-79.197755	895	40	855

Campbell	37.254855	-79.280809	890	40	850
Campbell	37.302634	-79.236364	910	40	870
Campbell	37.280411	-79.060535	840	45	795
Campbell	37.254022	-79.185811	940	45	895
Campbell	37.264577	-79.169144	1000	48	952
Campbell	37.324743	-79.145204	1064	50	1014
Campbell	37.047747	-79.144452	980	50	930
Campbell	37.347412	-79.14356	815	50	765
Campbell	37.197716	-78.969261	528	50	478
Campbell	37.226799	-79.226643	825	50	775
Campbell	37.155134	-79.228588	825	50	775
Campbell	37.243466	-79.1272	860	50	810
Campbell	37.344153	-78.98832	860	60	800
Campbell	37.196439	-79.198564	878	60	818
Campbell	37.328031	-78.978679	849	60	789
Campbell	37.3293	-79.119422	745	60	685
Campbell	37.307078	-79.160811	1000	60	940
Campbell	37.258188	-79.032202	730	60	670
Campbell	37.265133	-79.169144	1010	60	950
Campbell	37.195134	-79.237754	705	60	645
Campbell	37.173467	-79.336641	900	60	840
Campbell	37.282356	-79.296919	840	68	772
Campbell	37.100413	-79.113314	645	70	575
Campbell	37.190967	-79.214699	795	70	725
Campbell	37.280966	-79.05859	860	80	780
Campbell	37.08958	-79.04776	595	82	513
Campbell	37.272911	-79.106923	905	100	805
Campbell	37.277355	-79.129423	900	105	795
Campbell	37.304577	-79.049979	850	110	740
Campbell	37.228466	-79.234976	810	110	700
Campbell	37.369856	-79.109977	800	175	625
Campbell	37.164578	-79.066369	745	230	515
Campbell	37.284577	-79.080257	960	250	710
Campbell	37.078746	-78.884155	525	290	235
Campbell	37.388189	-79.059144	520	290	230
Campbell	37.250411	-79.017202	750	300	450
Franklin	36.927043	-80.014605	1280	8	1272
Franklin	36.929252	-79.871126	1060	12	1048
Franklin	37.123585	-79.675067	872	12	860
Franklin	37.139783	-79.711453	930	15	915
Franklin	37.087792	-79.629291	825	15	810

Franklin	37.107539	-79.977388	1464	15	1449
Franklin	36.850331	-80.065596	995	16	979
Franklin	36.928759	-80.013443	1289	17	1272
Franklin	36.926397	-80.012411	1260	18	1242
Franklin	37.104461	-79.816833	1135	20	1115
Franklin	37.08555	-79.63165	827	20	807
Franklin	37.084964	-79.630836	830	20	810
Franklin	37.086067	-79.631308	834	20	814
Franklin	37.116747	-79.714175	1028	20	1008
Franklin	36.9308	-80.185775	2485	21	2464
Franklin	37.140058	-79.710939	892	25	867
Franklin	37.114222	-79.72	964	26	938
Franklin	36.781648	-80.025528	861	30	831
Franklin	36.994569	-79.687156	999	30	969
Franklin	37.061096	-79.635381	905	30	875
Franklin	37.138783	-79.712931	915	30	885
Franklin	37.139197	-79.712698	936	30	906
Franklin	37.083211	-79.751044	1084	30	1054
Franklin	37.070267	-79.675228	947	32	915
Franklin	37.133532	-79.672342	868	35	833
Franklin	37.05925	-79.637473	866	35	831
Franklin	37.160194	-79.716361	962	35	927
Franklin	37.029488	-79.64507	850	38	812
Franklin	37.146575	-79.706472	821	38	783
Franklin	37.13454	-79.715759	865	38	827
Franklin	37.055838	-79.608467	838	40	798
Franklin	37.138458	-79.712724	931	40	891
Franklin	36.833893	-79.755439	990	40	950
Franklin	37.101909	-79.817466	1146	40	1106
Franklin	37.071424	-79.670645	970	40	930
Franklin	37.160528	-79.716833	953	40	913
Franklin	37.047056	-79.681833	842	40	802
Franklin	37.006488	-79.622175	867	40	827
Franklin	36.928583	-79.878944	1132	41	1091
Franklin	37.149376	-79.676999	854	42	812
Franklin	37.056797	-79.621594	887	42	845
Franklin	37.056936	-79.620867	880	42	838
Franklin	37.018256	-79.817203	1169	43	1126
Franklin	37.03745	-79.643734	898	45	853
Franklin	36.849616	-79.927817	1185	46	1139
Franklin	37.134709	-79.673161	889	46	843

Franklin	36.987189	-79.749787	1030	48	982
Franklin	37.111872	-79.716904	1000	50	950
Franklin	37.03505	-79.728961	835	50	785
Franklin	37.08643	-79.632928	867	53	814
Franklin	37.013191	-79.610307	890	55	835
Franklin	37.115	-79.718694	980	55	925
Franklin	37.070632	-79.647553	853	60	793
Franklin	37.138214	-79.713042	926	60	866
Franklin	37.046768	-79.706061	880	60	820
Franklin	36.994569	-79.687156	997	60	937
Franklin	37.097722	-79.652583	860	60	800
Franklin	37.063628	-79.629617	860	61	799
Franklin	37.064389	-79.628083	885	62	823
Franklin	37.099358	-79.65162	920	63	857
Franklin	37.086404	-79.633345	867	64	803
Franklin	37.13525	-79.673394	895	65	830
Franklin	37.032778	-79.711389	841	65	776
Franklin	37.161425	-79.715733	863	65	798
Franklin	37.062916	-79.932326	1168	69	1099
Franklin	36.997117	-79.690058	1025	70	955
Franklin	37.115025	-79.718694	980	72	908
Franklin	37.010584	-79.614863	838	80	758
Franklin	37.160978	-79.716247	915	80	835
Franklin	37.117946	-79.659071	876	82	794
Franklin	37.037881	-79.64292	917	84	833
Franklin	37.185889	-79.722778	947	90	857
Franklin	37.163722	-79.722055	976	90	886
Franklin	37.162954	-79.84744	1191	95	1096
Franklin	37.018938	-79.612398	910	119	791
Franklin	36.925527	-79.884187	1200	125	1075
Franklin	37.036111	-79.63	904	125	779
Franklin	37.106126	-79.661396	858	127	731
Franklin	37.098472	-79.653056	880	142	738
Franklin	37.037381	-79.643262	912	147	765
Franklin	37.107685	-79.659451	878	148	730
Franklin	36.9295	-79.882472	1156	149	1007
Franklin	37.108426	-79.659276	868	153	715
Franklin	37.092615	-79.645729	939	153	786
Franklin	37.064008	-79.62484	871	155	716
Franklin	37.099043	-79.655974	982	170	812
Franklin	37.184615	-79.887723	1685	226	1459

Franklin	37.134642	-79.717007	959	304	655
Franklin	37.187133	-79.763098	939	315	624
Franklin	37.187037	-79.763221	932	386	546
Franklin	37.183841	-79.888074	1668	400	1268
Pittsylvania	36.91449538	-79.539851	695	7.89	687.11
Pittsylvania	36.614583	-79.539694	710	20	690
Pittsylvania	37.097079	-79.312753	640	24	616
Pittsylvania	36.765419	-79.389142	660	30	630
Pittsylvania	37.179045	-80.759929	1942	31	1911
Pittsylvania	36.672084	-79.410809	660	38	622
Pittsylvania	37.010413	-79.336642	840	40	800
Pittsylvania	37.052358	-79.239699	660	40	620
Pittsylvania	36.979578	-79.413862	943	40	903
Pittsylvania	36.719862	-79.562748	770	42	728
Pittsylvania	37.078453	-79.354807	872	44	828
Pittsylvania	37.089758	-79.35398	800	50	750
Pittsylvania	36.620418	-79.604691	890	61	829
Pittsylvania	36.744056	-79.505638	865	65	800
Pittsylvania	36.622639	-79.415253	600	65	535
Pittsylvania	36.940968	-79.562192	822	67	755
Pittsylvania	37.025691	-79.258033	890	75	815
Pittsylvania	37.078815	-79.368199	850	80	770
Pittsylvania	37.086531	-79.355904	840	80	760
Pittsylvania	36.616528	-79.498307	620	90	530
Pittsylvania	36.601687	-79.497605	616	90	526
Pittsylvania	36.72557	-82.766449	1600	110	1490
Pittsylvania	36.640095	-79.563878	766	115	651